The Expedition ARKTIS XVIII/1 a, b of the Research Vessel „Polarstern“ in 2002

Edited by
Peter Lemke
with contributions of the participants

Ber. Polarforsch. Meeresforsch. 446 (2003)
ISSN 1618 - 3193

ARK XVIII/ 1 a, b

25.06.2002 – 24.08.2002

Bremerhaven - Tromsø

Fahrtleiter / Chief Scientist

Peter Lemke

KOORDINATOR /COORDINATOR

Eberhard Fahrbach

Contents

Contents

1. ZUSAMMENFASSUNG UND FAHRTVERLAUF

POLARSTERN lief am 25.6.2002 mittags in Bremerhaven zur Fahrt ARK XVIII/1 aus mit dem Ziel, im Ostgrönlandstrom und in der nördlichen Grönlandsee geologische, biologische und ozeanographische Untersuchungen durchzuführen (Fig. 1.1). Zunächst wurden im südlichen Bereich der Ostküste Grönlands (südlich und nördlich der Dänemarkstraße) Sedimentkerne gezogen, mit deren Hilfe die Variabilität der thermohalinen Zirkulation im Ozean der letzten 150 000 Jahre mit multidekadischer Zeitauflösung aufgeklärt werden soll. Gleichzeitig wurden Multicorer eingesetzt, um lee- und luvseitig der Dänemark-Straße die rezenten Verteilungsmuster der Faunen, der Geochemie und einiger stabiler Isotope mit Oberflächenproben gezielt zu dokumentieren. Anschließend wurden nördlich der Dänemarkstraße geo-biologische Untersuchung an Schwammgemeinschaften auf Vesterisbanken und Jan Mayen Sporn durchgeführt

Ziel der Untersuchungen im multidisziplinären BMBF-Verbundvorhaben ARKTIEF-II war es, die Bedeutung von Rinnensystemen für die Wassermassenerneuerung und die Umwelt-bedingungen in der arktischen Tiefsee zu erforschen. Dazu erfolgten neben hydrographischen Messungen biologische und biochemische Arbeiten, um großskalige Besiedlungsmuster im Bereich eines hangnormalen Rinnensystems am ostgrönländischen Kontinentalhang und in der tiefen Grönlandsee zu erfassen und biologische Umsatzprozesse in ihrer Bedeutung für das Ökosystem "Arktische Tiefsee" abzuschätzen. Durch die geologischen Arbeiten dieses Verbund-vorhabens wurde der Einfluss von Resuspensions- und Transportvorgängen auf die vertikalen Flüsse biogener und terrigener Partikel im Grönlandbecken untersucht, um die langfristige Bedeutung dieser Sedimentationsprozesse auf geologischen Zeitskalen abschätzen zu können.

Die anschließenden ozeanographischen Untersuchungen betrafen einen hydrographischen Schnitt entlang 75N, der jährlich wiederholt wird, um Veränderungen der Wassermassen, insbesondere die Erneuerung der Tiefen- und Bodenwassermassen der Grönlandsee langfristig zu erfassen. Dieser hydrographische Schnitt konnte wegen der leichten Eisbedingungen zum erstenmal direkt an der Küste Grönlands begonnen werden. Ein weiterer Höhepunkt bestand in der intensiven Untersuchung eines Tiefseewirbels, der in der Nähe des Greenwich Meridians entdeckt wurde.

Nach Abschluss dieser Arbeiten wurde Ende Juli ein Teil der wissenschaftlichen Fahrt-teilnehmer in Longyearbyen ausgetauscht. Im zweiten Teil des Fahrtabschnittes wurden zunächst interdisziplinäre Arbeiten an einer Tiefsee-Langzeitstation im benthologischen Hausgarten durchgeführt, um Effekte physikalischer, chemischer und biologischer Gradienten in der Tiefsee zu untersuchen und damit die Dynamik benthischer Bakteriengemeinschaften zu verstehen.

Es schlossen sich ozeanographische Arbeiten an, um den Wassermassenaustausch zwischen Nordpolarmeer und Atlantik und die Zirkulation in der Fram-Straße zu untersuchen. Dafür wurden Messungen mit Temperatur- und Salzgehaltssonden entlang eines Schnittes bei 79N ausgeführt sowie Wasserproben genommen, um Spurenstoffe zu messen. Ferner wurden zehn ozeanographische Verankerungen aufgenommen und zwölf ausgelegt, um kontinuierliche mehrjährige Messreihen aus dem Untersuchungsgebiet zu erhalten.

Während der gesamten Fahrtroute wurden an verschiedenen Orten umfassende Studien zur Ökologie sogenannter oligotropher, an niedrige Nährstoffkonzentrationen angepasster Bakterien, und einzelliger Organismen, sogenannter mixotropher

Protisten, die sowohl Photosynthese betreiben als auch organisches Material als Nahrung aufnehmen können, durchgeführt.
Den Abschluss der Fahrt bilden geochemische Untersuchungen am Håkon Mosby Schlammvulkan. Diese Untersuchungen zielten primär darauf ab, die Gesamtmenge des freigesetzten Methans abzuschätzen sowie sein weiteres Schicksal in der Wassersäule zu verfolgen. Nach Beendigung dieser Arbeiten lief Polarstern planmäßig am 24. August 2002 um 7:00 Uhr in Tromsø ein.

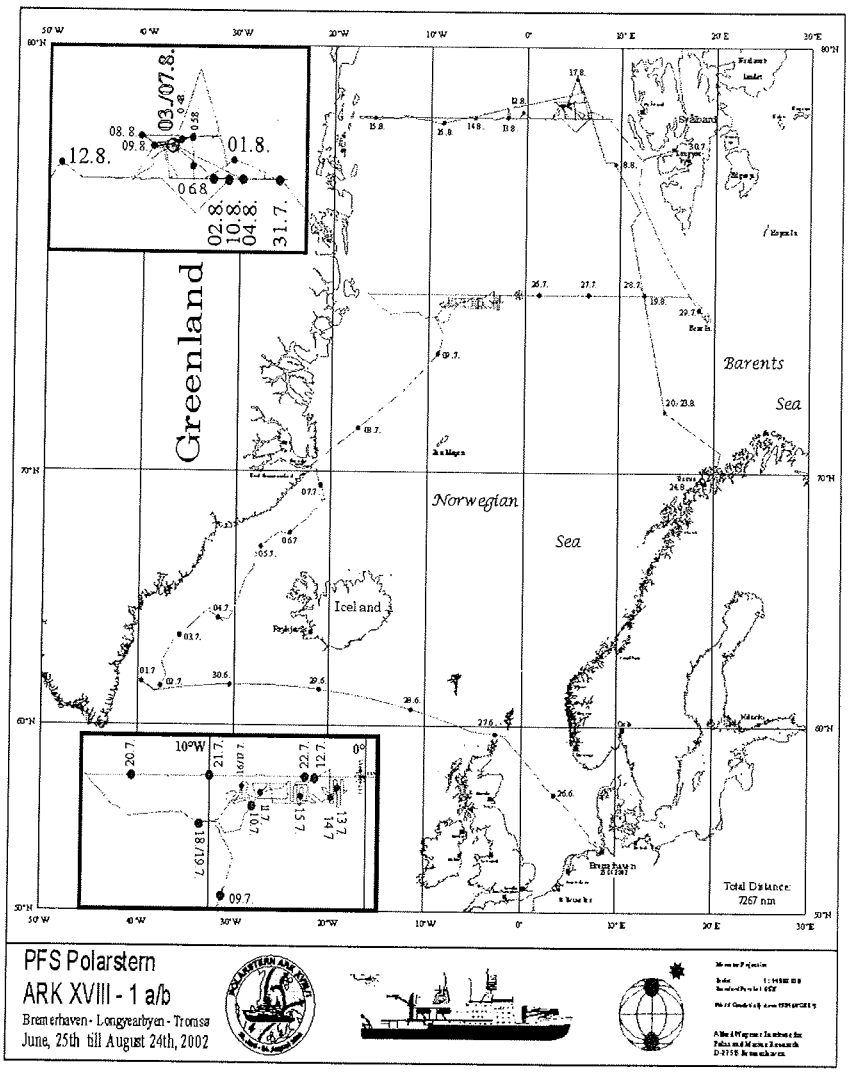

Fig. 1.1: Cruise track during ARK XVIII/1.

2. SUMMARY AND ITINERARY

Polarstern left the port of Bremerhaven for cruise ARK XVIII/1 on 25 June 2002 to perform oceanographic, geological and biological investigations in the East Greenland Current and the northern Greenland Sea (see figure). In the beginning long sediment cores were taken on several transects across the lower East Greenland continental margin to the south and north of Denmark Strait, which will help to uncover the variability of thermohaline surface and deepwater circulation at multidecadal resolution over the last 150,000 years from glacial to interglacial and stadial to inter-stadial times. At the same time a multicorer was employed on several transects for sampling the modern faunal, geo-chemical, and isotopic distribution patterns on the lee and luff side of the Denmark Strait Overflow. Continuing north of Denmark Strait sponge communities on arctic spiculite mats of Vesterisbanken and Jan Mayen Sporn were investigated. Autochthonous spiculites are mats of sponge silicate spicules which host a rich endofauna of sponge species.

The goal of biological and biochemical work performed on Polarstern during the BMBF project ARKTIEF-II was to assess large-scale distribution patterns of benthic organisms in and around channel systems crossing the eastern Greenland continental margin and the deep central Greenland Sea, and to estimate benthic processes within these areas and their relevance for the Arctic Ocean ecosystem. The geological work of ARKTIEF-II aimed at characterizing the influence of resuspension and transport processes on the vertical fluxes of biogenic and terrigenous particles in the Greenland basin in order to estimate the influence of these sedimentation processes on geological time-scales.

The following oceanographic work included a hydrographic section along 75N, which is repeated each year in order to investigate long-term changes in water masses and especially in the renewal of deep and bottom water in the Greenland Sea. Due to light ice conditions this section started for the first time in immediate vicinity of the coast of Greenland. Another highlight were the extensive measurements of a deep sea eddy. During the course of the section and the eddy work, velocity profiles were taken with a new ADCP (Acoustic Doppler Current Profiler) to obtain estimates of vertical mixing rates. Furthermore, the existing time-series of CFC measurements were continued.

After completion of this work, several members of the scientific community were exchanged at Longyearbyen. In the beginning of the second part of this cruise leg, interdisciplinary work at a deep-sea long-term station in the benthic 'Hausgarten' was performed to investigate the effects of physical, chemical and biological gradients in the deep sea on the dynamics of benthic bacterial communities.

Oceanographic work, which followed was dedicated to investigate the water mass exchange between the Arctic and the North Atlantic and the circulation in Fram Strait. A hydrographic section along 79N was taken, and water samples for tracer determination were collected. In total, on both sections (75N and 79N) eighteen moorings were recovered, and sixteen were re-deployed, to enlarge the existing time-series for the investigation of long-term variability.

During the entire cruise studies of protists in the food web of the Greenland Sea were undertaken, especially concerning the role of mixotrophic protists in the water column, the trophic function of heterotrophic and mixotrophic protists of the sea ice and the relative importance of grazing and nutrient control within the pelagic microbial food web, with special reference to species-specific differences. In addition the quantitative distribution and diversity of oligotrophic, low-nutrient bacteria was investigated by means of classical and molecular biological methods.

The final research component of this cruise was concerned with geo-chemical investigations at the Håkon Mosby Mud Volcano. These investigations aimed at the assessment of the total methane release and of the fate of methane within the water column. After the conclusion of this work Polarstern steamed towards Tromsø and reached port on 24. August 2002.

3. METEOROLOGY

3.1 The meteorological conditions
(Behr, Buldt)

R/V Polarstern left Bremerhaven harbour with moderate westerly winds heading to the Pentlands. After passing the northern tip of Scotland she crossed an area of strong westerly winds and rough sea caused by an intense gale centre lying in the Norwegian Sea. After two days of bad weather R/V Polarstern steamed westwards to her first working area at 62° N/38° W. A second gale centre originating over Newfoundland crossed the course of R/V Polarstern in the meantime. It produced southeasterly winds with 7 to 8 Bft., a wind sea of 4 m and a 3 m swell coming from the Southwest.

At the start of scientific work the wind was light and moderate. As the next lows starting at Newfoundland passed along the western coast of Greenland R/V Polarstern remained in a weather situation with moderate winds. Due to the origin of the air masses reaching our working area there were days with good visibility and others with longer lasting fog. After crossing the polar circle R/V Polarstern met the first ice floes surrounded by a large field of fog.

Four persons were disembarked at Scoresbysund by helicopter in good flying conditions. R/V Polarstern worked northward along the coast of East-Greenland up to 75° N and into the ARKTIEF-Area between fields of ice floes and fog patches. After leaving the coast of East-Greenland on 19. July horizontal visibility improved due to the formation of an intense gale centre over northern Siberia transporting cold and dry air southward into our working area. At the end of the working-period along 75° N a gale centre moved from Iceland towards Svalbard causing strong easterly winds (17 m/s) on 27. and 29. July. Later on this low crossed the track of R/V Polarstern and went eastwards towards the Kara Sea. After a circular tour around Bjørnøya, R/V Polarstern sailed towards Longyearbyen roads which were reached at 30 July, 09:30 UTC. After disembarking and embarking scientific personnel, she left at 22:30 UTC.

During the first week of working in the "AWI-Hausgarten" the weather-situation was influenced by a flat trough of a stationary Siberian low transporting cold and clear air from the north into the working area. A high-pressure area moved from Greenland to the Barents Sea. At the end of its 3-days-passage an intense low transported warm and humid air masses from Iceland northwards into our working area. R/V Polarstern worked again in a widespread area of fog. This period with poor visibility lasted up to the end of the working-period in the AWI-Hausgarten. Horizontal visibility improved as soon as R/V Polarstern reached colder water-masses on her course towards Northeast-Greenland. The period was characterized by a flat pressure gradient with light and variable winds.

At the beginning of the transect from Northeast-Greenland back towards Svalbard an intense low approached our working area from Iceland, causing north-easterly winds up to 6 to 7 Bft. Horizontal visibility was very poor in front of this low due to an extended field of rain. The winds shifted to the south and decreased slowly after the passage of this gale centre. Therefore, the work planned to be carried out at **H**åkon **M**osby **M**ud **V**olcano (HMMV) could be performed without any restrictions due to the weather situation.

R/V Polarstern left her final working area on 23. August and steamed towards Tromsø, which was reached in the morning of 24. August.

Finally some statistics: The daily cycles of air pressure (p), wind speed (ff), and air- and sea-temperature (T_A, T_S) are given in separate figures. Their numbers are listed in this table:

Time-interval	Working area		p	ff	T_A/T_S
25.06.-30.06.	A	Approaching the first working area	1.1	1.2	1.3
01.07.-07.07.	B	Up to Scroresby Sund	1.4	1.5	1.6
08.07.-19.07.	C	East-Greenland, ARKTIEF	1.7	1.8	1.9
20.07.-30.07.	D	along 75° N	1.10	1.11	1.12
31.07.-16.08.	E	AWI-Hausgarten & along 79° N	1.13	1.14	1.15
17.08.-23.08.	F	Svalbard – HMMV – Tromsø	1.16	1.17	1.18

Tab. 1.1: Figure numbers presented in this chapter.

Concerning horizontal visibility, there are two ranks worth mentioning:

visibility	ARK XVIII/1a	ARK XVIII/1b
< 1.5 km	28 %	24 %
> 9 km	58 %	57 %

Tab. 1.2: Frequencies of horizontal visibility during ARK XVIII/1a+b.

The daily duration of sunshine for the entire curise is shown in Fig. 1.19

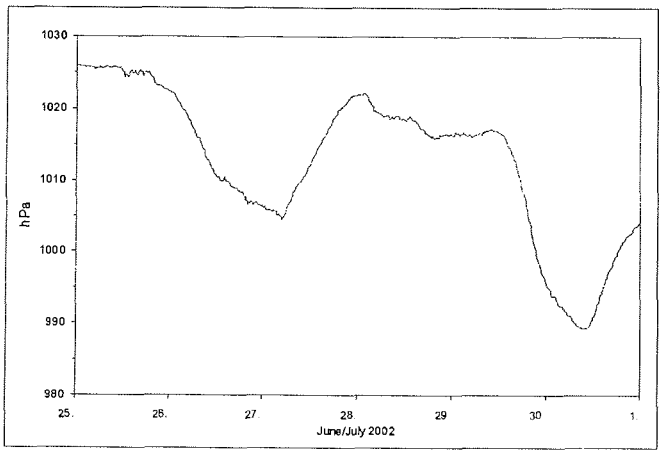

Fig. 1.1: Air pressure

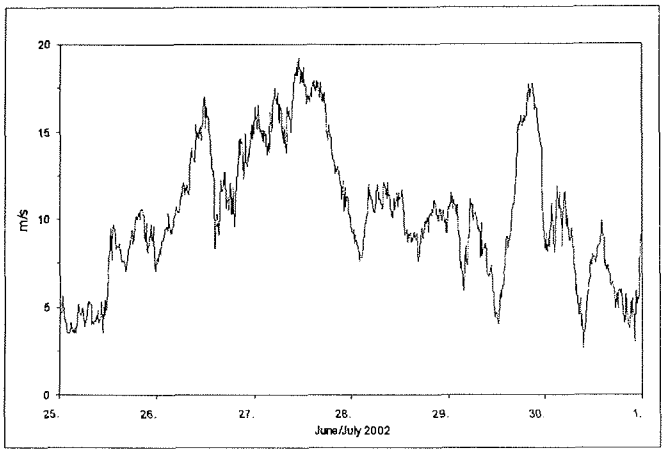

Fig. 1.2: Wind speed

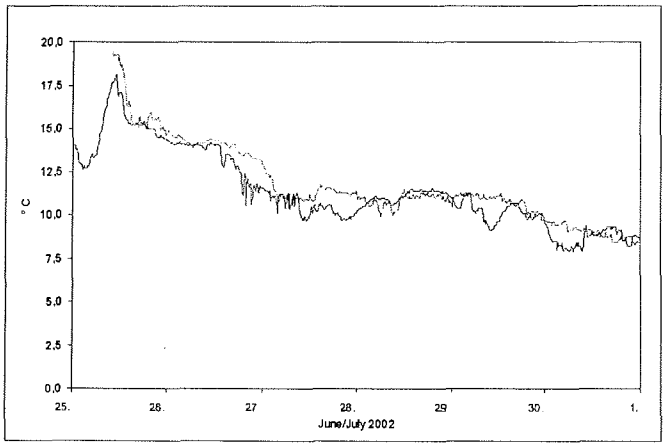

Fig. 1.3: Air temperature (solid) and sea surface temperature (dotted)

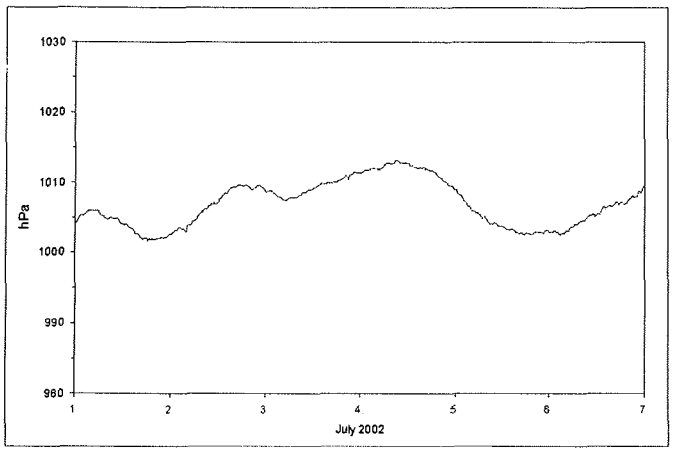

Fig. 1.4: Air pressure

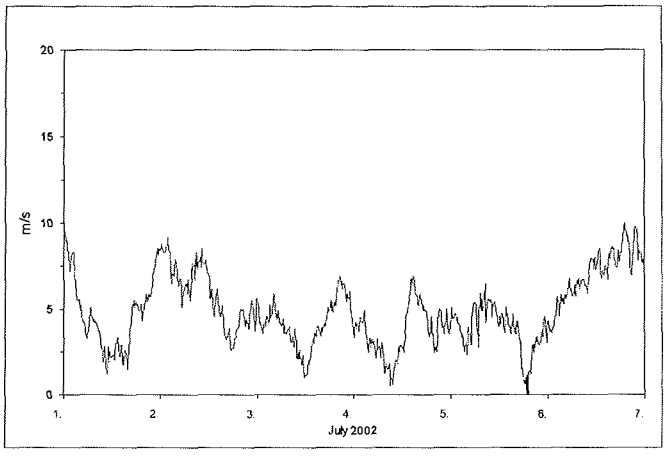

Fig. 1.5: Wind speed

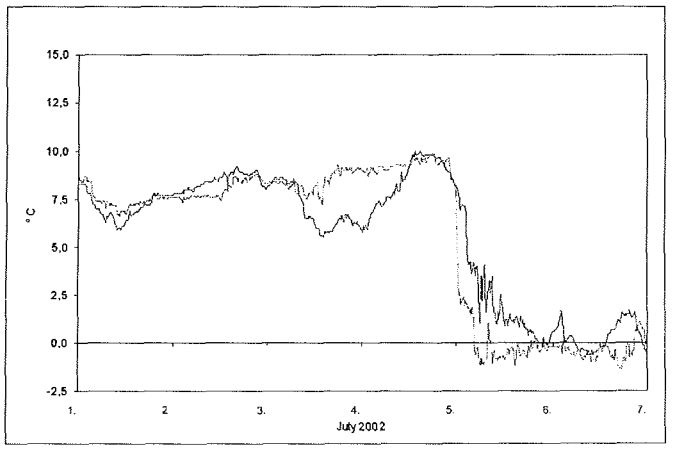

Fig. 1.6: Air temperature (solid) and sea surface temperature (dotted)

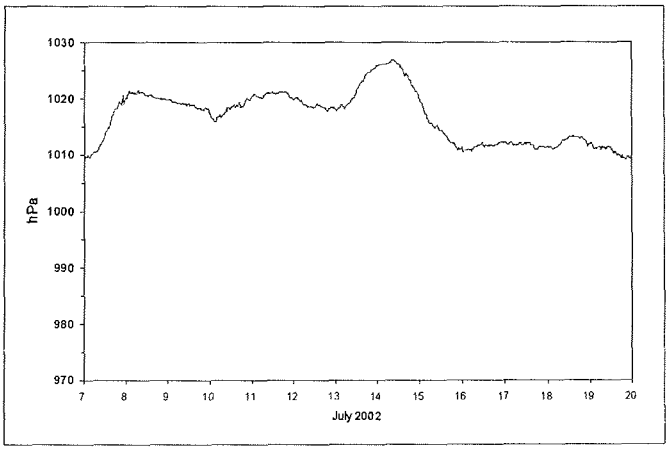

Fig. 1.7: Air pressure

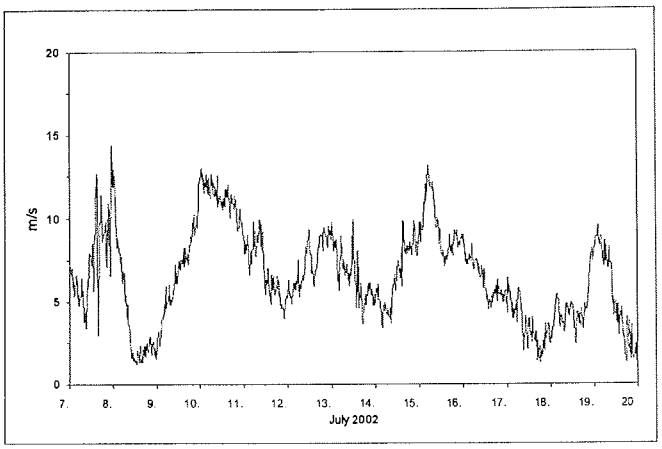

Fig. 1.8: Wind speed

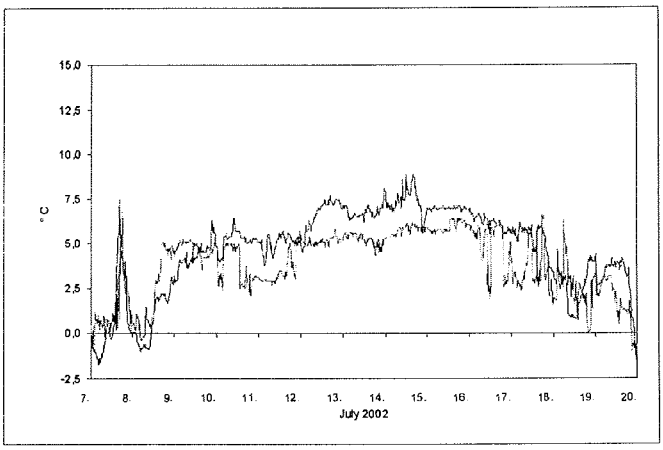

Fig. 1.9: Air temperature (solid) and sea surface temperature (dotted)

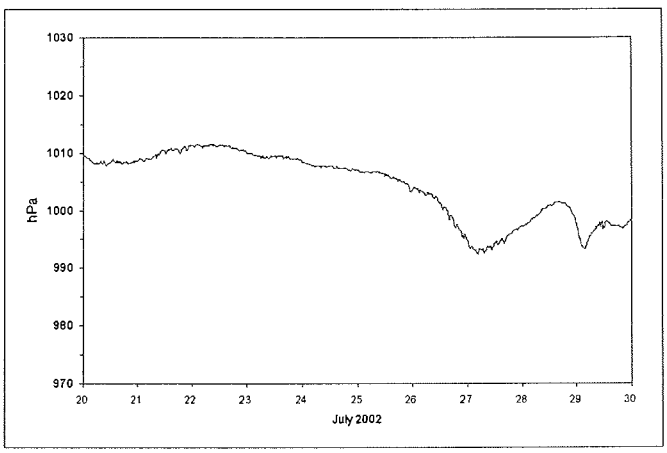

Fig. 1.10: Air pressure

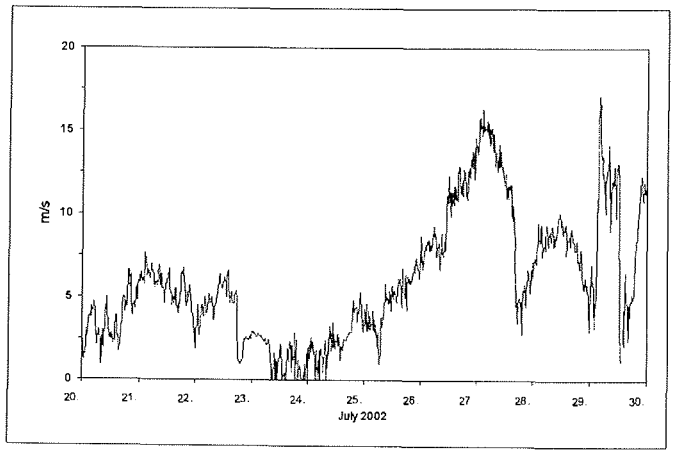

Fig. 1.11: Wind speed

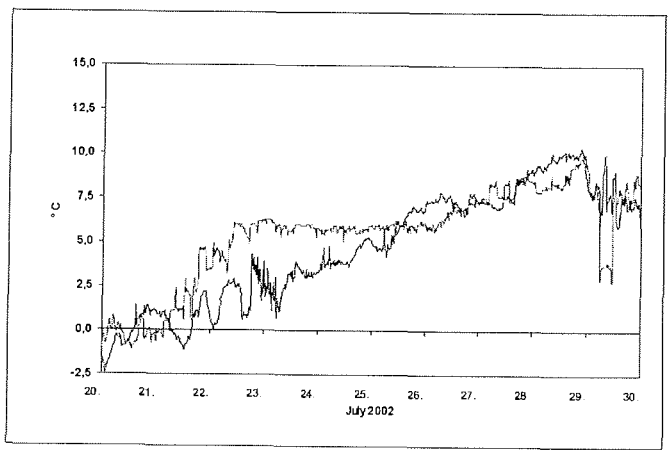

Fig. 1.12: Air temperature (solid) and sea surface temperature (dotted)

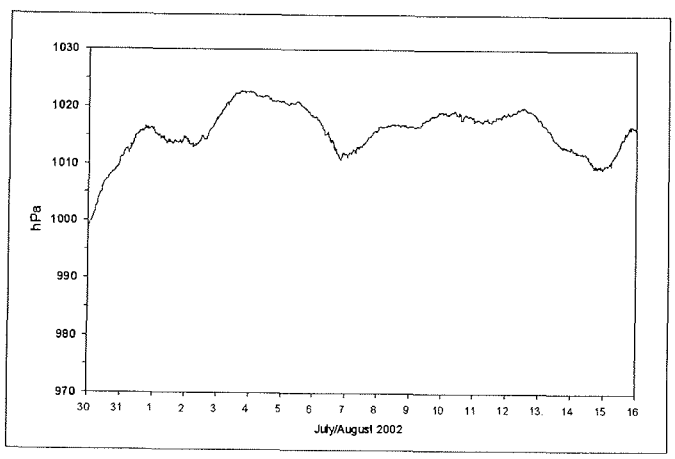

Fig. 1.13: Air pressure

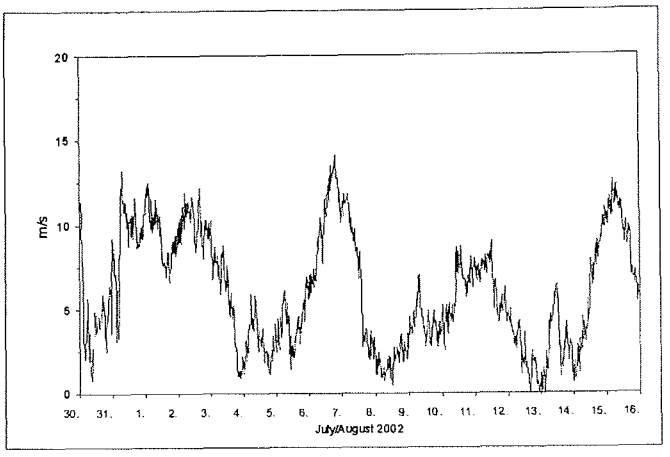

Fig. 1.14: Wind speed

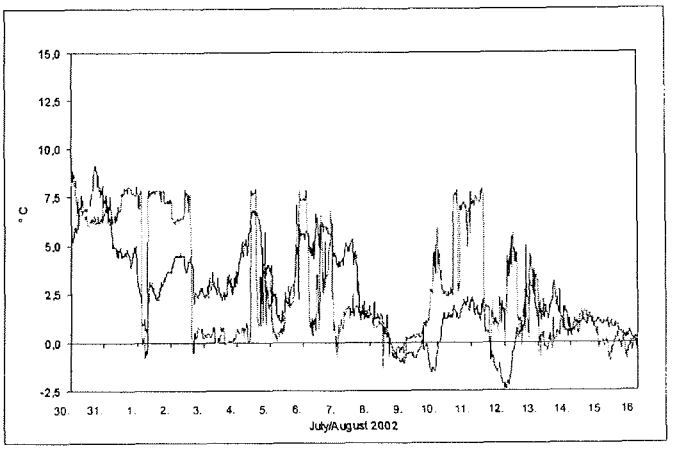

Fig. 1.15: Air temperature (solid) and sea surface temperature (dotted)

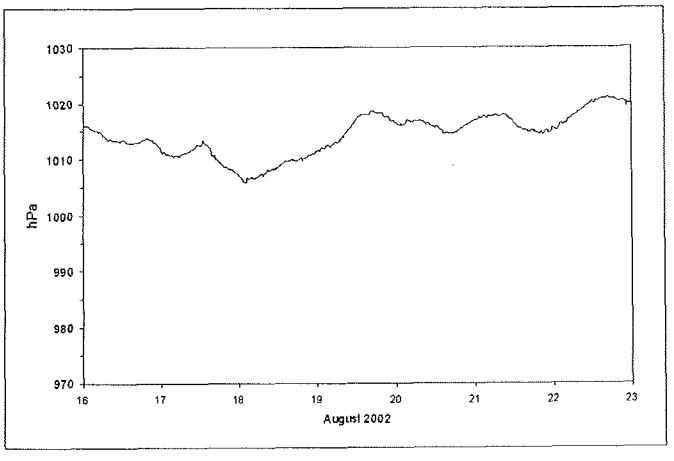

Fig. 1.16: Air pressure

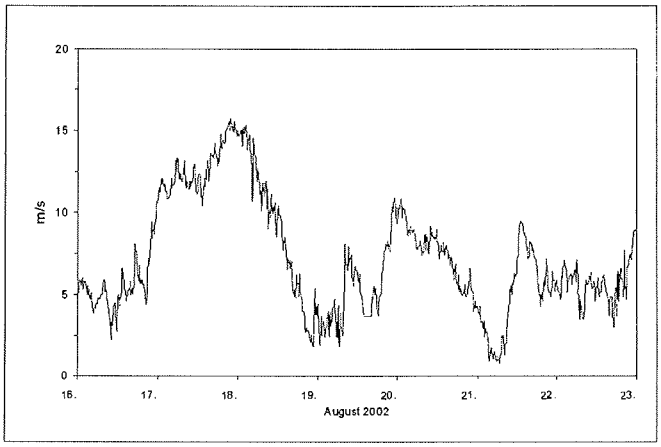

Fig. 1.17: Wind speed

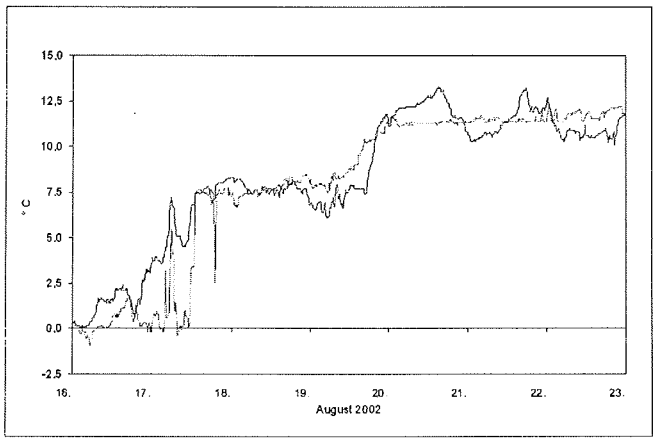

Fig. 1.18: Air temperature (solid) and sea surface temperature (dotted)

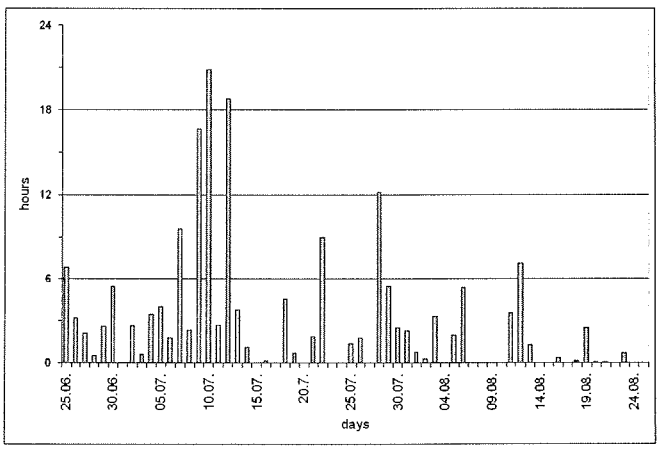

Fig. 1.19: Daily duration of sunshine during ARK XVIII/1

3.2 Determination of the net total radiation and atmospheric turbidity at sea

(Behr)

Information about the spatial and temporal distribution of the net total radiation and its components at the sea surface as well as atmospheric turbidity are one of the most important parameters in resolving numerous meteorological and oceanographic questions. While the role of air-sea transfer in forcing global climate has long been recognised in tropical regions, the importance of Polar Regions has been acknowledged only relatively recently. This has led to increased effort to measure the solar fluxes and derived quantities such as atmospheric turbidity in order to give support to numerous groups building atmospheric or oceanic models.
Therefore, during the cruise, the following radiation components were recorded: global (*G*) [by a ship borne pyranometer] and direct solar radiation (*I*) as well as sunshine duration (*SD*) [by an additional installed sunshine indicator type SONIe-3]. Additional components necessary to close the radiation balance: reflected solar radiation (*R*), long wave thermal radiation of the atmosphere (*A*), and ocean surface radiation (*E*) are computed using numerical models successfully tested on former research cruises in the Atlantic, Behr (1990).

As the input of solar radiation at the sea surface is controlled by the content of absorbing constituents, the knowledge of their concentrations is essential. The following constituents reduce solar radiation penetrating through the atmosphere: (*i*) dust and sand exported from landmasses. This can be seen at sea in the area west of the African coast. (*ii*) sea spray in the lower and water vapour in the upper atmosphere. This can be found especially in the vicinity of the ITCZ. (*iii*) anthropogenic aerosol (e.g. biomass burning and industrial pollution). This can be seen east of Brazil and/or in the middle Northern Hemisphere. The loss of solar radiation by extinction (sum of absorption and scattering) is expressed by the optical depth σ or the turbidity factor T. The turbidity factor T is defined as the ratio of the optical depth $\bar{\delta}$ of the actually loaded atmosphere to the optical depth $\bar{\delta}_R$ of the pure and dry atmosphere (so-called Rayleigh atmosphere). Therefore T states how many Rayleigh atmospheres are equivalent to the actual atmosphere:

$$\bar{\delta} = T \cdot \bar{\delta}_R. \qquad (1)$$

The bar indicates that the optical depth is integrated over the entire solar spectrum. If the wavelength dependence of the optical depth is considered, an index λ is added: δ_λ or $\delta_{R\lambda}$. These parameters were first introduced by Foitzik and Hinzpeter (1958).

As optical depths $\bar{\delta}$ and δ_λ are not accessible to direct measurement, they have to be determined by indirect methods. The most common way is to measure direct solar irradiance I at the sea surface after penetrating the loaded atmosphere and to compare these data with computed solar irradiance I_R penetrating a Rayleigh atmosphere. To evaluate the spectral turbidity factors, the corresponding spectral irradiances were used.

As it is not possible to install a sensitive sun-facing system on a rolling and pitching ship in order to record spectral irradiances continuously, a simple hand-held instrument, the **L**inke-**F**eussner-**A**ctinometer (LFA) equipped with three IGY-filters

was used. The filters RG2 and OG1 are commonly used as standard-filters for measuring different spectral direct solar irradiance.

Atmospheric turbidity is expressed by turbidity factors as follows:

- Total-turbidity factor T_g, identical with the Linke-turbidity-factor T_L, describing all radiative processes in the whole solar spectrum: $0 < \lambda < \infty$. T_L runs between 2 (clear dry air) and roughly 10 (air from an highly industrialized area),
- short-turbidity factor T_s, comprising the solar spectrum between: $0 < \lambda < 0.62$ µm. It is essentially determined by aerosol extinction within the atmosphere. T_s runs between 1 (aerosol-free air) and 5 (air originating from sand outbreaks e.g. from the Sahara).
- red-turbidity factor T_r, comprising the solar spectrum between: 0.62 µm $< \lambda <$ 2.8 µm. This factor is essentially influenced by water-vapour absorption. The filter RG2 is designed to span the significant absorption bands of water vapour (720 - 740 nm, 810 - 840 nm, 890 - 940 - 990 nm, and 1070 - 1110 - 1200 nm). T_r runs between 4 (dry air originating from polar regions with absolute humidity about 4 kg/m^2) and 50 (humid air originating from the tropics with absolute humidity about 60 kg/m^2),

The factors $T_x \equiv \{T_L, T_s, \text{and } T_r\}$ can be computed by:

$$I_x = I_{0x} \exp(-T_x \cdot m \cdot \delta) \quad (2)$$

with:

- I_x: direct solar radiation received from a surface normal to the beam of the sun, e. g. measured with a Linke-Feussner-Actinometer during the cruise.
- I_{0x}: extraterrestrial solar radiation received from a surface at the top of the atmosphere normal to the beam of the sun. Its quantity depends on the distance sun - earth only. The quantities I_{0g} [total-solar constant], I_{0r} [red-solar constant] and I_{0s} [short-solar constant] are calculated from the data of the extraterrestrial spectrum. Dehne and Kasten (1983) published the corresponding data. The spectral integration of the data according to the characteristics of the filters used results in:

  $I_{0g} =$ 1367.13 W/m^2 $\quad I_{0r} =$ 818.52 W/m^2 $\quad I_{0s} =$ 516.60 W/m^2 (3)

- m: optical path length, dependent on the solar elevation angle.
- δ: optical thickness of the atmosphere.

  $m \cdot \delta$ are expressed:

  $$- m \cdot \delta_{R\lambda} \cong - [\delta_R(\lambda) \cdot m_R(\gamma) + \delta_Z(\lambda) \cdot m_Z(\gamma)] \quad (4)$$

  with $\delta_R(\lambda)$ and $\delta_Z(\lambda)$ spectral vertical optical depths of the atmosphere related to:
  R: Rayleigh scattering by air molecules,
  Z: ozone absorption,
  $m_R(\gamma)$ and $m_Z(\gamma)$ are the corresponding relative optical air mass and ozone mass, respectively, at solar elevation angle γ.

  The spectral optical depth $\delta_R(\lambda)$ due to Rayleigh scattering was calculated with help of an equation given by Iqbal (1983):

  $$\delta_R(\lambda) = 0.008735 (\lambda / 1000 \text{ nm})^{-4.08} \quad (5)$$

The spectral optical depth $\delta_Z(\lambda)$ was calculated using a formula from Kasten (1996). He considered ozone absorption and additional absorptions by totally mixed gases (carbon dioxide and oxygen in particular). This absorption has to be considered because it shows considerable values in the UV up to 360 nm and in the Chappius-band between 410 nm and 850 nm.

Exact formulae to compute the air mass m passed by the radiation were published by Kasten and Young (1989). As these formulae would overtax the accuracy of the LFA, a simpler formula is used which is valid for LFA-readings at solar elevation angles $\lambda>10°$. In this case we have:

$$m(\gamma) \cong m_R(\gamma) = m_Z(\gamma) = 1/\sin\gamma. \quad (6)$$

The hand-held LFA was focussed on the sun only at times when clouds or any obstacles of the ship did not obscure the sun for at least 10 min. A sunshine-indicator measuring sunshine-duration and direct solar radiation continuously was installed on the highest point on the ship, but there was still some shading by the nearby masts. The readings of this instrument spanning over a period with 100 % sunshine-duration for at least 10 min were extracted from the data set to compute T_L additionally. These continuous records were used to close the gaps between the hand-held LFA-measurements.

As the sky was obscured for most of the cruise (see weather-log) it is difficult to present catchy results from the Arctic region. Data from two days taken from the scarce data set may illustrate the different characteristics of air masses reaching R/V Polarstern. The time used in the figures is **t**rue **s**olar **t**ime (TST); 12 TST is defined as the noon position of the sun bisecting the day in two equal parts. Atmospheric turbidity factors calculated from the LFA-measurements are given in both figures as: T_L (•), T_s (Δ), and T_r (+). As T_L comprises the contributions of all extinging substances in the air, it is necessary to examine the results of T_s and T_r additionally.

10. 07. 2002 (Figs. 1.20-1.22)

Cold and dry air masses reached our working position (74.3° N/8.2° W) originating in all levels from the north. Their flux is illustrated in Fig. 1.20 comprising 108-hours-backward trajectories in the levels: surface, 950, 850, and 700 hPa. A circle marks our working position. Due to this clear air mass, the readings of global solar radiation (G, pink line) and direct solar radiation (I, green line) follow the ascent of the sun very directly in the morning (Fig. 1.21). At 2 TST and 6 TST there was some shading of the instruments by the masts. After 16 TST growing clouds reduce G and I remarkably. In contrast to these continuous readings (Fig. 1.21) the hand-held LFA was applied only during time-intervals with a cloud-free sun (Fig. 1.22). Due to the quality of the air, T_L did not change significantly throughout the day. The data of T_L are around 2.5, representative of clear, unloaded air. T_r is up to 12 with a tiny decrease to 10 at the end of the recording period expressing a water-vapour content of about 11 kg/m^2 computed from the data of the radiosonde ascent on this day. In the tropical Atlantic we obtained values for T_r of 30 to 60, cf. Figs. 4 and 5 in Behr (2001). This stands for a water vapour content of 40 to 60 kg/m^2, cf. Fig. 6 in Behr (2001). The data for T_s are about 1.2 due to clean maritime aerosol.

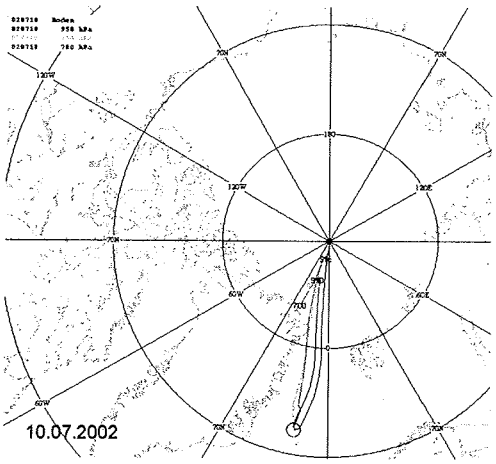

Fig. 1.20: Backward trajectories in different levels started 108 hours ago reaching the position of R/V Polarstern on 10. July 2002, 00 UTC. The pressure levels used are: surface, 950 hPa, 850 hPa, and 700 hPa.

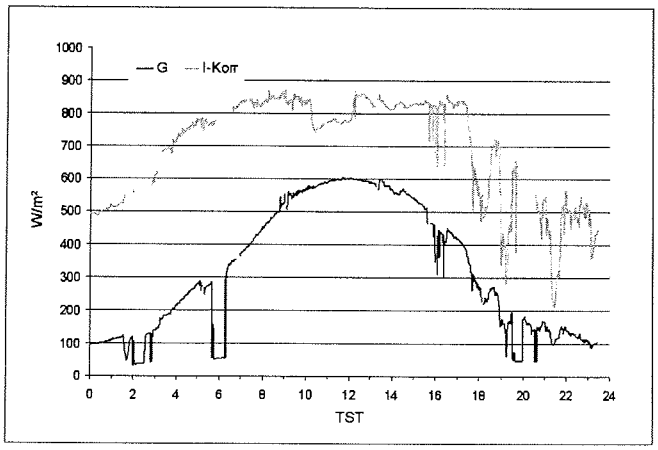

Fig. 1.21: Daily cycles of solar global radiation and direct solar radiation on 10. July 2002. Time used is true solar time

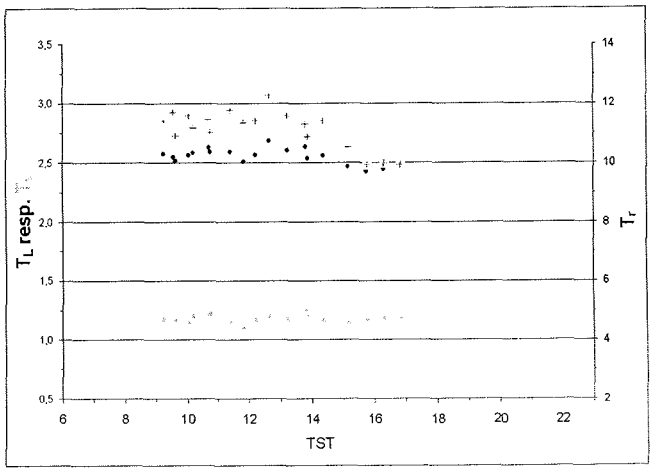

Fig. 1.22: Daily cycles of the turbidity factors T_L (•), T_s (Δ), and T_r (+) on 10. July 2002, time used is true solar time.

12. 07. 2002 (Figs. 1.23 - 1.25)

The synoptic situation had changed two days later: two types of air masses reached our working position at 74.9° N/3.9° W: on the one hand they originate from the polar region (surface up to 950 hPa) transporting clear air, and on the other from the mid-Atlantic (850 hPa and higher) transporting humid air towards R/V Polarstern, cf. Fig 1.23. Our working position (marked by a circle) was in the vicinity of an anticyclone combined with sinking air masses diminishing clouds in the afternoon. Therefore LFA-measurements could be performed until the sun-elevation angle was lower than 5° over the horizon (21 TST). Due to this air mass *G* and *I* show a variable course before noon and a very stable course in the afternoon. (Fig. 1.24). The masts were shading both instruments around 6 TST and from 06:30 TST to 10:00 TST the SONIe-3 only. The LFA-readings (Fig. 1.25) reveal: there is a reduction of T_L from 2.5 to 2.0 during the day caused by a drying of the atmosphere. This is characterized by a reduction of T_r from 11 to 6. The daily variation of T_s around 1.2 is not worth mention. This quantity was similar to that two days ago.

Further examination of the solar radiation data are planned in order to fit the turbidity data originating from the Arctic Region into those obtained on further cruises of R/V Polarstern (Behr, 1990, 1992) and R/V Meteor (Behr, 2001).

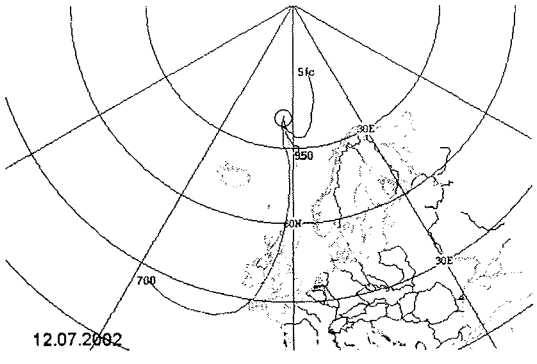

Fig. 1.23: Same as Fig. 1.20 but for 12 July 2002, 00 UTC

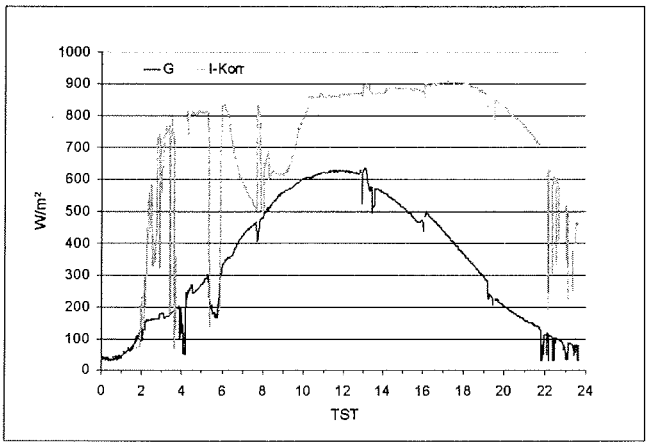

Fig. 1.24: Same as Fig. 1.21 but for 12 July 2002, 00 UTC

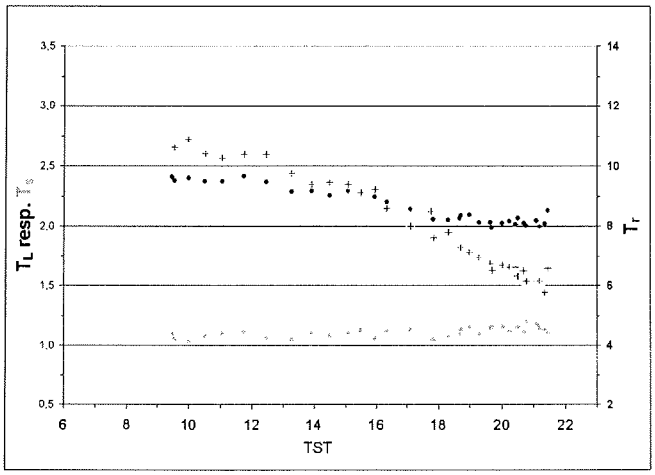

Fig. 1.25: Same as Fig. 1.22 but for 12 July 2002, 00 UTC

References

Behr, H. D., 1990: Radiation Balance at the Sea Surface in the Atlantic Ocean Region between 40° S and 40° N, Journal of Geophysical Research, D95, 20633-20640.

Behr, H. D., 1992: Net total and UV-B Radiation at the Sea Surface, Journal of Atmospheric Chemistry, 15, 299-314.

Behr, H. D., 2001: Atmospheric Turbidity West of the Westafrican Coast in January and July - a Comparison. Meteorol. Z., 10, 373-385.

Behr, H. D., 2001: Atmospheric turbidity at sea (prelim. results from ARK XVI/2), Ber. z. Polarforsch., **389**, 88-91.

Dehne, K.; F. Kasten, 1983: The spectra of extraterrestrial solar radiation and global radiation in the UV range as basis for defining "reference sunny days", Licht-Forschung, **5**, 85-87.
Foitzik, L., H. Hinzpeter, 1958: Sonnenstrahlung und Lufttrübung, Leipzig, 309 pp.

Iqbal, M., 1983: An Introduction to Solar Radiation, Academic Press Toronto, New York, London, 390 pp.
Kasten, F., 1996: The Linke Turbidity Factor Based on Improved Values of the Integral Rayleigh-optical Thickness, Solar Energy, **56**, 239-244.
Kasten, F., A. T. Young, 1989: Revised Optical Air Mass Tables and Approximation Formula, Applied Optics, 28, 4735-4738.

4. CORING A SEDIMENT RECORD OF VARIATIONS IN THE DENMARK STRAIT OVERFLOW

(Sarnthein, Weinelt, Larsen, Bartoli, Blümel, Budeus, Dunhill, Gai, Kierdorf, Kißling, Kösters, Lorenz, Matthiessen, Millo, Mühr)

4.1. OBJECTIVES

The cold Denmark Strait Overflow presents a giant near-bottom outflow from the Greenland Sea to the south across a sill of 400-600 m depth and forms a cataract of 3 Sverdrups (Sv; million m^3 water per second) down to the abyss of the northwestern North Atlantic. Here this water is a major source of the global thermohaline-circulation (THC) system. The Overflow and the overlying East Greenland Current (EGC; also 3 Sv) to a large part compensate for the advection of warm North Atlantic water from the subtropics into the Nordic Seas. Thus the Overflow intensity contributes significantly to the control of climate quality in northwest Europe.

In particular, this cruise served to test some major factors that may have controlled past reductions in Overflow intensity. (1) Ice breakouts from eastern Greenland may have induced changes in the salinity of the EGC and subsequent variations in deep-water convection in the Greenland Sea and in Overflow intensity in the context of the millennial-scale Dansgaard-Oeschger (DO) climate cycles (van Kreveld et al., 2000). (2) The coeval advance of shelf ice sheets from both sides, eustatically and isostatically controlled changes in the vertical cross section, and "iceberg traffic congestions" in the Denmark Strait may jointly have short-term constricted its diameter and throughflow (Sarnthein et al., 2001). (3) Finally, the cruise helped to trace the exchange and depth zonation of planktic and benthic foraminifera species, which have strongly differed to the north and south of the Denmark Strait during glacial stages and possibly may be also depicted in a differential molecular genetic code of some benthic species.

Hemipelagic sediment piles from the lower Greenland continental margin to the southwest and north of the Denmark Strait promise to contain a highly sensitive record of past changes in the Overflow on subcentennial to millennial time scales back to several hundred thousand years B.P. and thus have formed an attractive target for coring on this cruise. To decipher the history of Overflow changes, planktic and benthic foraminifera tests in the sediment cores will be analyzed for establishing

ventilation, paleosalinity, and paleodensity records through analyzing stable-isotope and temperature signals. Furthermore, differential paleo-^{14}C ages of coeval benthic and planktic foraminfera species will help to distinguish different paleowater masses in comparison to the modern distribution of ^{14}C radioactivity measured in water samples retrieved on this cruise. Biomarker analyses may help tracing paleowater masses and their nutrient content. In addition, grain size studies may provide new insights into past variations of current speeds in the bottom water. Finally, extended shallow-seismic (4 kHz; Parasound) records will provide the necessary insights into the spatial extension of paleoceanographic signals deduced at only few core sites and transects. Studies of benthic-foraminifera ecology and genetic composition may help tracing past changes in the marine environments to the south and north of the Denmark Strait and in defining the mobility of these species.

4.2. METHODS AND SAMPLING GEAR

4.2.1 Reading Parasound Echosound Records

On board of PFS Polarstern high-resolution acustostratigraphy is based on the Parasound echosounder system which provides a strongly focussed (4°) reflection signal that results from the frequency difference of two narrowly bundled seismic signals at approximately 18 and 22 kHz (described in detail by Rostek et al.; Spieß, 1992) and penetrates the sea floor as deep as conventional 3.5 kHz echosounders, but is focussed more closely.

On this cruise Parasound records mainly served for identifying proper sites to core undisturbed, largely continuous hemipelagic sediment sections needed to establish paleoceanographic records (see Appendix figures for each core site). On the basis of long-term ship-board experience (e.g. Sarnthein et al., 1994), hemipelagic sediments were identified from coarsely-to-finely laminated sediment reflectors which drape the underground and frequently form (standing or migrating) "sediment waves".

Numerous precise informations on the prevailing regime of sediment deposition or erosion on the deep-sea floor were deduced from micromorphological features in the Parasound record that actually reflect erosion. They included (1) angular micro-channels cut into the layered or non-layered hard sediment sections below, and (2) minihyperbolae which led to a "coarse", that is crimped reflector which in fact represents a crinkled, rough sediment surface. The crinkling was either produced by sand transport (e.g., fine-sand ripples), current winnowing (lag sediments consisting of washed out pebbles and stones lying on top of a hardground), or by (3) minor and major angular fine-sediment boulders contained in sediment slides and slumps. In addition, the slides are clearly marked as thick, pancake- or worm-shaped sediment bodies with an acoustically transparent center, only extending over short distances of a few hundred meters or less. Sediment slumps usually showed a slide scar at their upper and a bulge at their lower end. (4) Turbidite layers were easily distinguished from the hemipelagic drape by means of coarse, crimped reflectors and abundant minor to major unconformities and minichannels in a non-draping, but flat, board-shaped sequence of generally coarse sediment beds.

4.2.2 CTD and Rosette Water Samples (for $d^{13}C$ and ^{14}C analyses)

The water column was sampled down to the sea floor at 3 stations (Table 4.1, Figure 4.1) to measure the distribution of $d^{13}C$ and ^{14}C in modern intermediate and deep-water masses.

A Rosette sampler with 21 bottles of 12 l each served to sample the intermediate and deep water masses with high vertical resolution according to the CTD profile.

In addition, the uppermost water column was sampled to extend a data base of C and O stable isotope signatures of the surface water in northern high latitudes, a data base assembled at the Leibniz Laboratory of the University of Kiel since 1989. Further surface-water samples were collected with a simple bucket at each station.

The water samples were filled into 100 ml bottles and poisoned with HgCl to stop bacterial growth and further respiration of CO_2. The bottles were cramped and stored at 4°C. $d^{13}C$, $d^{18}O$, and ^{14}C data will be measured at the Leibniz Laboratory of Kiel University.

Table 4.1. Sediment and water sampling

Cruise No.	Event No.	Date	Latitude	Longitude	Water depth	Gear	Parasound time
PS 62/002	1	01.07.2002	61°47,668	39°22,433	1887	MUC	
	2	01.07.2002	61°47,744	39°22,351	1888	KOL, TWC	09:22
	3	01.07.2002	61°47,685	39°22,423	1891	GKG	
PS 62/003	1	01.07.2002	61°42,010	39°04,028	2158	GKG	
	2	01.07.2002	61°42,003	39°04,041	2159	KOL, TWC	08:10
	3	02.07.2002	61°42,062	39°04,065	2157	GKG	
PS 62/004	1	02.07.2002	61°31,896	38°07,924	2557	CTD, ROS, ADCP	
	2	02.07.2002	61°31,544	38°07,391	2564	MUC	
	3	02.07.2002	61°31,559	38°07,387	2565	KOL, TWC	04:55
PS 62/006	1	02.07.2002	62°15,053	37°18,403	2436	KOL, TWC	15:14
	2	02.07.2002	62°15,078	37°18,341	2436	MUC	
PS 62/007	1	03.07.2002	62°42,913	37°40,288	2133	GKG	
	2	03.07.2002	62°42,827	37°40,307	2131	KOL	23:02
PS 62/010	1	03.07.2002	64°59,766	32°54,535	1698	GKG	
	2	03.07.2002	64°59,666	32°54,367	1702	GKG	
PS 62/012	1	04.07.2002	64°37,449	31°41,805	2399	CTD, ROS, ADCP	
	2	04.07.2002	64°37,459	31°41,593	2404	GKG	
	3	04.07.2002	64°37,449	31°41,679	2404	KOL	04:56
	4	04.07.2002	64°37,900	31°44,210	2426	CTD, ROS, ADCP	
PS 62/015	1	05.07.2002	67°55,896	25°25,414	987.9	GKG	
	2	05.07.2002	67°55,899	25°25,480	986	GKG	
	3	06.07.2002	67°55,855	25°25,590	980.2	KOL, TWC	21:02
	4	06.07.2002	67°55,841	25°25,748	980.2	GKG	
PS 62/017	1	06.07.2002	67°51,058	24°34,917	1458	GKG	
	2	06.07.2002	67°51,045	24°34,714	1452	KOL	
	3	06.07.2002	67°51,307	24°35,003	1454	CTD, ROS	
	4	06.07.2002	67°51,014	24°35,116	1458	KOL, TWC	05:22
PS 62/020	1	08.07.2002	70°59,935	18°54,903	1322	MUC	
PS 62/021	1	08.07.2002	71°30,150	16°50,230	1704	MUC	

MUC= Multicorer, GKG=box corer, ROS=Rosette, ADCP=current profiler, KOL=Piston corer, TWC= trigger weight corer

4.2.3 Sediment Coring

For deep-sea sediment sampling we deployed a piston corer ('Kolbenlot', KOL) with split piston. The weight stand ('bomb') had a weight of 1.5 t to drive 10 m and 15 m long pipes, respectively, into the sea floor. The inner diameter of the liners was 122 mm. A pilot corer (46 mm inner liner diameter) was used to trigger the free fall of the piston corer over 5 m depth above the sea floor and for sampling the actual sediment surface down to 150 cm depth. Weather conditions were favorable and allowed fast retrieving times (speed of slacking: 0.8 m/s down to 150 m above the sea floor and 0.5 m/s until the TWC arrived at the sea floor; heaving speed: 1.2 m /s). Each deployment of this gear, but one was successful.

The multicorer (MUC) is designed to penetrate the top-sediment layer with 8 pipes, 61 cm long and with an outer diameter of 10 cm. This gear was unsuccessful in hard and/or coarse-grained surface sediments and thus not deployed at most sites. Accordingly, most surface sediment were sampled with a spade box corer ('Großkastengreifer', GKG; 50x50x60 cm), a generally reliable gear with a slacking speed of 0.8 m down to 150 m above sea floor and of 0.5 m down to the sediment surface. Where the closing mechanism failed, the GKG was deployed for a second or third time.

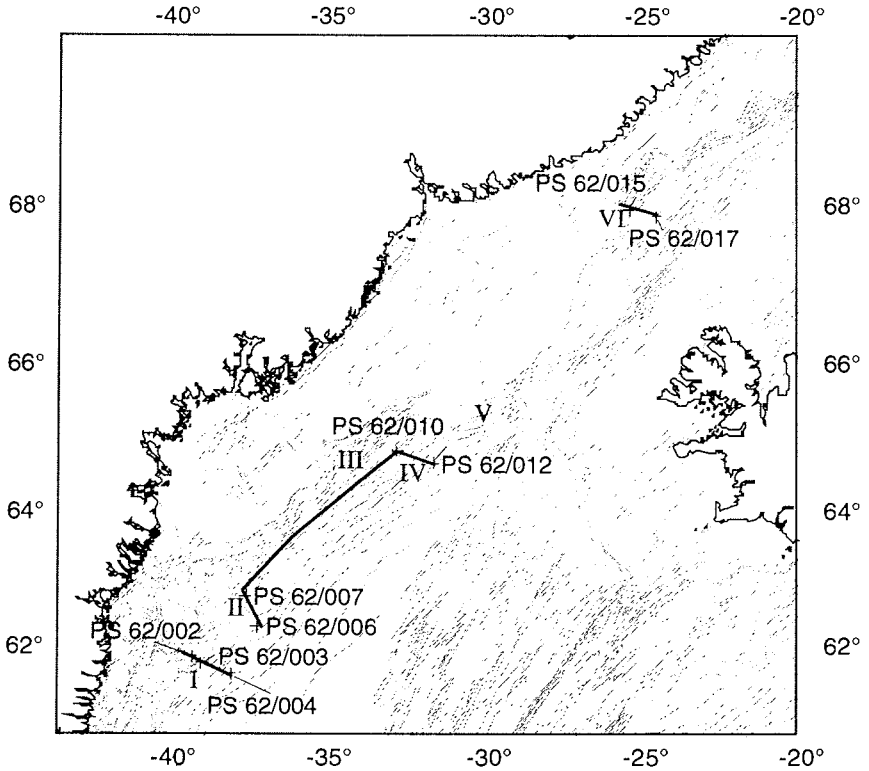

Figure 4.1. Position of cored sites and Parasound profiles I – V

4.2.4 Core Logging (Magnetic susceptibility, P-wave velocity, Color Reflectance, etc.)

Before sediment cores were cut non-destructive logging methods were applied to measure color reflectance and physical properties. The spectrophotometer "Minolta CM-2002" was used to measure color reflectance on the archive half of sediment cores at 1 cm intervals. The "Multi Sensor Core Logger" (MSCL, Geotek, UK) was used to determine P-wave velocity, bulk density and magnetic susceptibility of whole-core sections. The methods are described in detail by Niessen (1995) and Kuhn (2002).

4.2.5 Sampling Schemes of MUC and GKG

The use of the multicorer (MUC) was limited, because fine and coarse sandy sediments blocked the core closing mechanism at most stations. Here the box corer (GKG) was deployed instead.

MUC (providing 8 cores at each station):
To measure stable isotopes and trace metals in foraminifera and to study the faunal composition of planktonic / benthic foraminifera 1 core was entirely cut into 1-cm slices.
To analyse the molecular genetics of benthic foraminifera 3 cores were sampled with cm-thick slices at 0-1 cm and 1-5 cm, respectively.
To study living benthic foraminifera, 3 parallel sediment samples were obtained from 3 cores each. Two of them were sampled with 1-cm thick slices from 1-5 cm bsf, and 7, 10, and 15 cm bsf (below sea floor).
To analyse the biomarkers 1 core was cut into 1-cm slices.

GKG sampling:
After visual description and photography of the sediment surface, the macrofauna was collected, in particular porifera (F. Hoffmann). Metal frames of known spatial extent (10 x 10 cm; 15 x 27 cm) were used to demark the sediment surface and to sample the top-1 cm of sediment with a so called ´Lutze Spoon´ according to the following scheme:
– 50 cc were obtained for measuring stable isotopes and the composition of planktonic and benthic foraminifera faunas (Weinelt, IfG Kiel);
– 405 cc were obtained for molecular genetic analyses of living benthic foraminifera (Blümel, IfM Kiel);
– 200 cc served for life observations on benthic foraminifera (Lorenz, IPÖ Kiel);
– Undefined volumes served for biomarker analyses (Kierdorf, AWI Bremerhaven).

An archive core with a diameter of 12.2 cm was taken for core logging, and for 1-cm wise sediment sampling of the core top sequence (on shore).

4.2.6 Methods of Foraminifera Preservation

A) Sample preservation for genetic analyses
Immediately after a MUC or GKG sample had arrived on board, 405 cc were sampled for molecular genetics and an untreated subsample (4.5 ml in a Cryo tube) was taken for measuring the total DNA content of the sediment. This Cryo tube was shock-frozen in liquid nitrogen and stored at –25°C. The remaining portion of the sample was sieved with cold saltwater and split into 6 grain size fractions (> 2 mm, > 500 µm, > 200 µm, > 112 µm, > 63 µm, > 32 µm). Minor parts of these fractions were shock-frozen in liquid nitrogen and maintained at –25°C in a 2 ml Cryo tube. Another portion of the samples was preserved in Ethanol in a 1.5 ml Eppendorf tube.

The major part of the samples was preserved at 4°C for the analysis of morphological communities of benthic foraminifera under the binocular. The communities will be documented by a Nikon Coolpix 995 digital camera attached to the binocular. Individual foraminifera cells will be sorted out and determined morphologically and subsequently prepared for DNA extraction. Membranous allogromiid individual cells will be put into 50 µl Guanidin solution. Agglutinated, rotaliid, and miliolid foraminifera were preserved on micropaleontological slides for DOC extraction in the shore-based laboratory.

B) Ecology and taxonomy
Sediment samples out of each GKG or MUC core were fixed in ethanol mixed with Rose Bengal. In the shore-based laboratory living (stained) and dead foraminifera will be counted separately to determine the following faunal parameters: Number of individuals, number of species, abundance, diversity, evenness, and average living depth. To investigate the microhabitat requirements of benthic foraminifera a second subcore of the GKG or MUC, respectively, is used to measure biotic and abiotic parameters, in particular, temperature, salinity, water depth, oxygen content, pH-value, chlorophyll and phaeopigments, sediment grain size, pore water content, POC, DNA content, carbonate, silicic acid, and carbon-nitrogen-ratio. Sediment samples from a third subcore down to 5 cm bsf were used for observations at living organisms.

4.2.7 Sampling Scheme of KOL cores

One-meter long sections of piston cores PS 62/002, -003, -004, -006, -007, -010, -12, -015 were split into two halves ("A" = Archive half and "W" = Working half) on board of PRV Polarstern. "A"-halves were visually described and documented by photographs. Color variability was measured cm-wise with a Minolta-color scanner. "A"-halves are stored at the core depository at AWI, Bremerhaven. "W"-halves of cores PS 62/002, -004, -006, -007, -010, -12, -015 were cut into 1-cm slices for stable-isotope, ^{14}C, Mg/Ca, and faunal analyses. 1-cm slices of Core PS 62/003 were subsampled for biomarker analyses (1/3 of the slice). Biomarker samples were freeze-dried on board.

4.3. FIRST RESULTS

4.3.1 Introduction: Summary of core and water sample recovery

To trace the variability of the Denmark Strait Overflow, nine sediment sites were cored (Figure 4.1) and three water profiles were sampled on four different transects (#1, 2, 4, 5) across the lower continental margin of Greenland. These transects each run across the eastern margin of the near-bottom Overflow, three transects to the south and one transect to the north of the Denmark Strait. Generally, the core transects extend just as far west / uphill as hemipelagic sedimentation prevails sediment winnowing. Only Site PS62/010 sampled a coarse lag sediment from the strongly current-washed erosional sediment surface right below the center of the Overflow.

Moreover, Parasound echosound profiles were recorded from five transects and various connection routes in between (Figure 4.1). Of particular interest is profile III which followed in its northern part the old airgun line 79-16 of GEUS, Copenhagen, running along the northern slope of the Irminger basin at approximately 1600-1400 m water depth, moreover, profile V which crossed the former IMAGES Site MD99-2260 in the center of the southern entrance to the Denmark Strait (Labeyrie et al., 2002). In total, the echosounder tracks sum up to 1300 nm of echosound profiles.

The vertical composition of the water column down to the sea floor and its variation downstream the EGC and the Overflow was sampled at one station immediately to the north (67°51'N, 24°24' W) and at two stations to the south of the Denmark Strait, one lying far southwest at 61°32'N, 38°8'W, one more proximal to the strait at 64°38°N, 31°42'W. CTD profiles revealed the upper level of the dense Overflow water by a sharp temperature decrease at 2200 m and 2300 m, respectively, reaching down to >2500 m depth at the two stations to the south of the Denmark Strait (PS 62/004 and PS 62/012). The upper level of the Labrador Intermediate Water was marked by a temperature maximum of 3.65°C near 1300 m. To the north of Denmark Strait station PS 62/017 reached a water depth of 1500 m and shows a distinct temperature maximum of 1.7°C, marking the Atlantic Central Water near 720 m.

4.3.2 Parasound echocharacter reflecting the deepwater regime

The Denmark Strait Overflow exerts a dominant control on sedimentation and sea floor morphology at the East Greenland continental rise and lower slope. Echo signals related to this current activity were observed on the slope below approximately 500 m to the north of the Strait and below 1000 m and down to 2300 m to its south, in regions that were not disturbed by iceberg ploughmarks, sediment slides, and/or turbidites.

To the north of the Denmark Strait a pair of crimped surface reflectors on Profile VI reach from <700 m down to approximately 1300 m, indicating a current-winnowed sediment surface. Widespread sediment slides destroyed any evidence of bottom current activity from 1300-1470 m depth. Further below, deep (>50 m) acoustic penetration and fine seismic laminations characterized large portions of the almost

flat deep sea floor at 1500 m and were revealed as clay-rich sediments in the cores of Site PS62/017. We assume that the Overflow may have led to quasi-stagnation near the floor of this semi-enclosed basin close to the northern luv side of the Greenland-Iceland Ridge. This barrier has entailed an extensive deposition of suspended fines in a basin acting similar to a sand box upstream of a hydroelectric power station.

On the Ridge itself ice scourings are pervasive in the Parasound record at water depths less than 450 m and no direct evidence of current erosion was found. However, erosional features were obvious further south, especially at the northern end of Parasound Profile III, and on Profiles IV. This erosion cut deep 'windows' into the underlying sediment units, for example, it led to a partial destruction of (subfossil) sediment slides at the upper slope near the southern entrance of the Denmark Strait (e.g., on Profile IV and V). We identified three categories of (decreasing) erosion intensity.

1) Near to the northern end of Profile III and at the upper part of Profile IV (down to 2200 m) maximum erosion intensity led to a great number of (dendritic) narrow downslope channels, steeply incised down to more than 25 m depth into older sediment deposits (Figure 4.2). On the long-slope, S.S.W.-N.N.E. running airgun profile 79-16 of GEUS, Copenhagen, the channels produced a series of huge, but spurious megaripple-style structures near 1500 m water depth. The channels clearly mark the center of giant cataract activity expected at the northernmost margin of the Irminger basin to the W.S.W. of the Denmark Strait, where the Overflow penetrates down to the abyss of the northwest Atlantic. Similar broad, but long-slope horizontal channel erosion can be traced near 1400-1500 m water depth far to the southwest along the uppermost Greenland continental rise, up to the southern tip of Greenland.
2) A washed sea floor is characteristic of vast regions above 800 m depth within and immediately to the north and south of the Denmark Strait, where the Overflow current perhaps is less erosive because of a wide current profile.
3) Fine-sand deposits mark the proximal periphery of the Overflow erosion (e.g., at station PS062/002). The sand ripples produce small-scale microhyperbolae in the Parasound records, reflected as highly characteristic thick, crimped reflectors.

On Parasound Profiles I and II (Figure 4.1) hemipelagic clays and oozes only start to fully replace the sand and silt enriched sediments at water depths greater than 2150 m, where they drape the sea floor and finally form standing sediment waves at water depths greater than 2350 m. Several crimped subbottom reflectors possibly reflect sand layers and a former extension of intensive current action farther downslope during certain past climate stages, probably during warm extremes (Sarnthein et al., 2001).

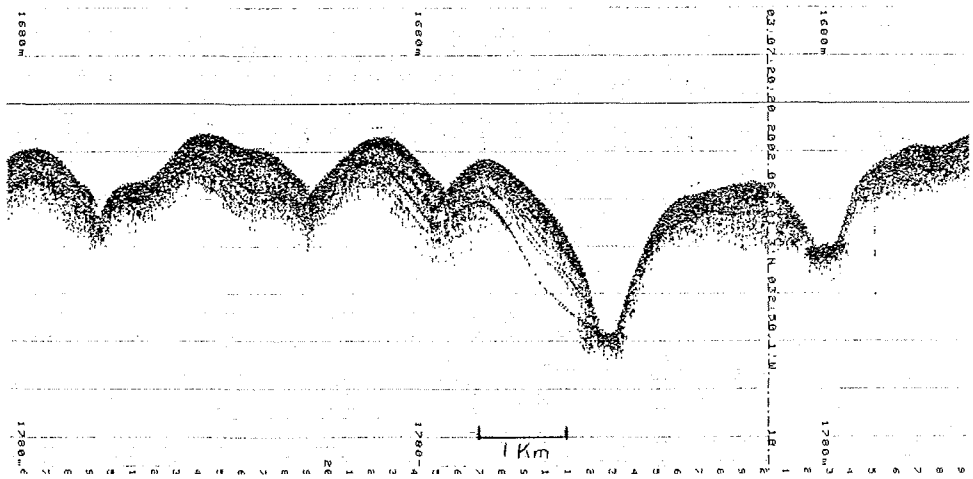

Figure 4.2. Parasound record of "Channel Land"

4.3.3 Description of Box Core and Multicorer Sediments and Fauna

We recovered 7 box cores from the study area to observe possible effects of Denmark Strait Overflow Water on the sea floor surface. Box cores collected south of Denmark Strait from the Irminger Basin show strikingly similar lithologies. The samples (PS62/002-3, PS62/003-3, PS62/007-1, PS62/010-2 and PS62/012-2) were obtained from the slope in water depths ranging from 1698 to 2157 m. All core-top sediments contained abundant planktonic foraminifera tests.

Two of these cores (PS62/010-1 and -2) were obtained from areas with sediment ridges with up to 25 m relief, where the seismic reflectors were crimped and narrow, angular incisions suggest strong channel erosion. The sea floor surfaces produced high-amplitude reflectors suggesting a hardground surface. Accordingly, we found coarse lag sediments and a macrofauna characteristic for hard substrates including porifera, anthozoans, and bryozoans, moreover sessile foraminifera attached to large dropstones (reaching 8 cm in diameter). Below the lag sediment, clay rich ooze contained a rich planktic foraminifera fauna with significant minor portions of *Neogloboquadrina pachyderma* (dextral), *Turborotalita quinqueloba*, and *Globogerinita glutinata*, but dominated by *N. pachyderma* (sinistral). Rich sediment portions of pteropods indicate minimum carbonate dissolution at this site.

Box core PS62/002-3, also retrieved from an area with a crimped, coarse bottom reflector, showed a thick sand layer at the surface. The remaining box and multicores from the region to the south of the Denmark Strait were collected from sites the seismic reflectors of which show parallel, laminated, draped sediments. These five cores PS62/ 003-3, 004-2, 006-2, and 007-1, which recovered up to 32 cm of sediment, reveal a sea floor composed of yellowish brown, well sorted, foram-rich sands which are 3-7 cm thick. This uppermost unit has either an abrupt or erosional basal contact. The surface sediments contained mm- to cm-scale black rocks, possibly basaltic dropstones, with abundant porifera, ophiuroids, and polychaets, moreover, gastropods and bivalves. However, living benthic foraminifera were only rare in the fine sands. Below this top layer the sediments become finer and darker.

The lower units are sandy-to-silty muds. The most notable characteristic about these cores is the well sorted sandy nature of the sediments suggesting ongoing current winnowing by the Denmark Strait Overflow.

The 2 box cores (PS62/017-7 and PS62/015-4) collected along a transect immediately north of Denmark Strait reveal a different type of sea floor sediment. Parasound data at Site PS62/015-4 show two parallel crimped reflectors such as south of the Denmark Strait. However, the echosound record at Site PS62/017/1 has a surface reflector, which is not crimped and does not have a particularly high amplitude, indicating well laminated, soft sediments. These two cores, which were obtained from water depths of 980 and 2402 m respectively, penetrated deeper, recovering 48 and 50 cm thick sections. The top 6-7 cm layer consisted of dark yellowish brown clay to silty clay with some coarse sand sized black lithic fragments, possibly basalt. The lower interval was a homogeneous dark gray clay. In the section from the shallower site along the transect (PS62/015-4) two large, dark, fine grained rocks were found with a maximum diameter of 10 and 20 cm.

2 MUCs (PS62/020 and PS62/021) were collected along a transect at the northern entrance to the Denmark Strait at approx 71^0N. Both of them were obtained from well stratified sequences without a strong bottom reflector indicating normal deposition 0f clay rich sediments at 1322 m and 1704 m depth, respectively. The MUCs penetrated to ca 35 cm bsf. The topmost 1 cm were almost fluid, moderately yellowish brown, silty mud with few sand grains and dropstones. The layer below was a rather soft, homogenous looking silty clay with open worm? holes extending both into horizontal and vertical directions.

The most important difference between the box cores collected to the south and north of Denmark Strait is the nature of the sea floor surface sediment. In the sediments south of the Strait silty or coarse sands are frequent, some of which appear to be lag deposits, while the sediments to north of the strait primarily contain clayey sediments.

4.3.4 Core logging results (magsus, color reflectivity, etc.) and first tentative core correlations

On the basis of magnetic susceptibility records we tentatively correlated the stratigraphy in five cores obtained from Profile I and Profile II (Figure 4.3). Most important result of this preliminary reconstruction are:
In general fairly constant sedimentation rates found over the entire region;
A differential preservation of the sediment surface. The top-sediment records in cores PS 62/003 and 004 may be best preserved. Both sites are most distal to current action of the Overflow.
The record at the shallow site PS62/002 (near to 1900 m depth) may be incomplete because of current-induced stratigraphic gaps.

Since no age-stratigraphic marker has been found yet, moreover, since these magnetic susceptibility records cannot be tied yet to a dated core (GIK 23519; C. Millo, in prep.) obtained nearby, to the southeast of the Denmark Strait (Pflaumann et al., 1996), there was no way to establish on board any rough age control and to estimate proper sedimentation rates in these sediments below the East Greenland Current, in the proximity of the Overflow.

Figure 4.3. Core transects I, II: preliminary correlation via magnetic susceptibility

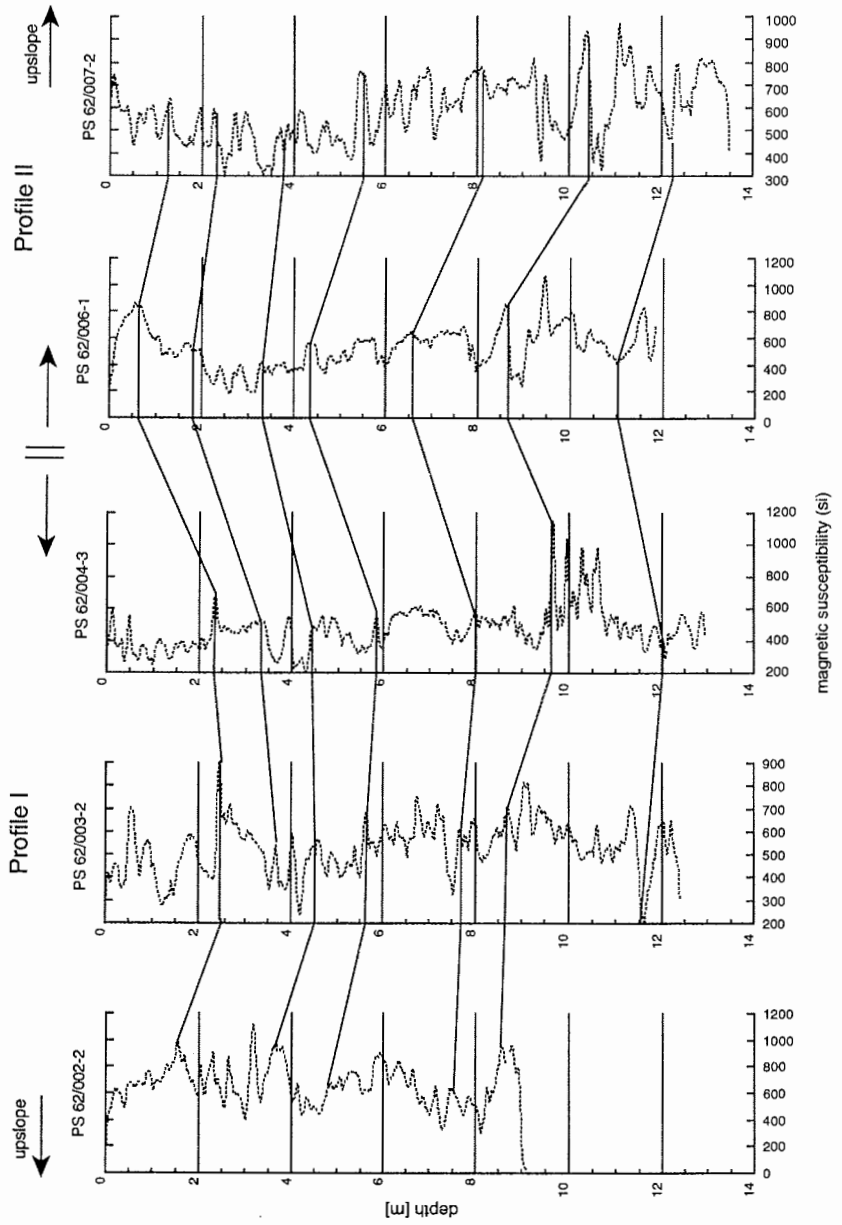

4.3.5 Observations of benthic foraminifera

For future genetic analyses living benthic foraminifera in the grain size fractions >500µm and >200µm from each station were picked out for species determination under the binocular microscope (Figure 4.4, Picture 1). Table 4.2 provides an overview of the species found at each station.

Table 4.2. Benthic foraminifera assemblages in (MUC and GKG) core-top samples south and north of DK Strait.

Station No.	Sediment type	Genera identified
PS62/ 002-1	Silty clay	Adercotryma, Cassidulina, Pelosina, Allogromiid sp., Hyperammina, Ammolagena, Rupertina, Bathysiphon, Saccammina, Psammosphaera, Reophax, Proteonina, Haplophragmium
PS62/003-3	Sandy surface layer	Saccammina, Psammosohaera, Rhabdammina, Ammolagena, Crithionina, Reophax, Rhizammina
PS62/004-2	Fine silt	Rhabdammina, Bathysiphon, Crithionina, Allogromiid sp., Textularia, Reophax, Ammobaculites, Haplophragmium
PS62/007-1	Sand	Ammonia, Epistominella, Psammosphaera, Textularia, Saccammina, Allogromiid sp., Haplophragmium
PS62/010-2	Coarse Sand	Rupertina, Psammosphaera, Crithionina, Cassidulina, Cibicidoides, Textularia, saccammina, Hyperammina
PS62/012-2	Sand	Ammolagena, Psammophaga, Reophax, Rupertina, Textularia, Cibicidoides, Haplophragmium
PS62/015-4	Silt	Bathysiphon, Crithionina, Haplophragmium, Cibicidoides, Psammosphaera, Hyperammina, Reophax, Proteonina,
PS62/017-1	Clay	
PS62/020-1	Silty Clay	
PS62/021-1	Silty Clay	

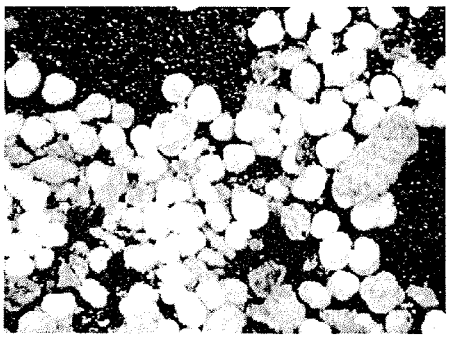

Picture 1:
Sieved, but unsorted foraminifera species with a sample (>500µ) under the binocular microscope

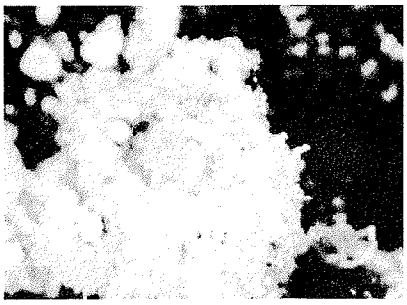

Picture 2:
Allogromiid species with a membranous test

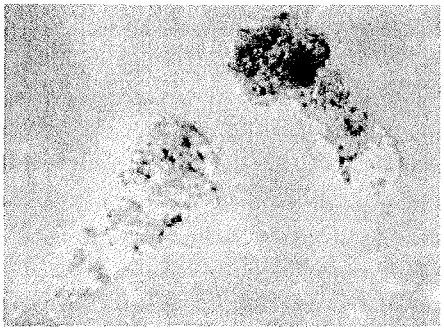

Picture 3:
Allogromiid species with a membraneous wall

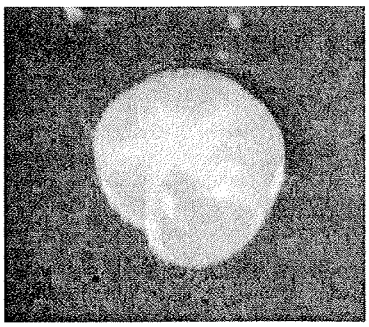

Picture 4:
Epistominella, species which produces a calcareous test

Figure 4.4. Four pictures of foraminifera

All species were documented by a digital camera (Figure 4.4). Rotaliid and agglutinated species were preserved on micropaleontological slides, whereas allogromiid species were put in 50 µl Guanidin solution. In the shore-based laboratory DNAs will be extracted, followed by PCR amplification of the 18S rDNA, subsequent cloning experiments, and sequencing. The phylogenetic analyses based on sequenced DNA fragments will serve for a better understanding of the molecular genetic relationshipsbetween the different foraminiferal species, hitherto only defined on a morphometric
basis.

For future ecological studies cultivated benthic foraminifera will be monitored in special, 1-cm wide aquaria to study the preferred habitat depth and possible migration behaviour of different foraminiferal species. These observations will be supplemented by experiments on petri dishes to investigate the movements and ingestion of foraminifera specimens.

ACKNOWLEDGEMENTS

We thank the Alfred Wegener Institute für Polarforschung for generously providing us with shiptime, moreover, Master Jürgen Keil and his crew for their most efficient support on board of this cruise. The chief scientist, Professor Peter Lemke, warmly supported us with ongoing advise and patience. We acknowledge with thanks the German Bundesanstalt für Geologie und Rohstoffe (BGR) in Hannover for sending their core technician, Mr. Peter Mühr, to this cruise for getting acquainted with the multicorer system. His skill and great and never ending efforts helped us to successfully retrieve good piston cores. Dr. Birger Larsen and Dr. Antoon Kuypers from the Geological Survey of Denmark and Greenland (GEUS) in Copenhagen, strongly contributed to the success of this cruise by providing us with published and unpublished seismic lines and sedimentary records from the Greenland continental margin. Our project "Impact of Gateways on Ocean Circulation, Climate, and Evolution" was generously funded by the Deutsche Forschungsgemeinschaft (DFG), Bonn (FOR 451-1).

REFERENCES

Kuhn G., Hass C., Censarek, B., Rudolph, M., Forwick, M., Quirós-Alpera, S., 2002: Meeresgeologie. In Thiede, J., Oerter, H.; Die Expedition ANTARKTIS XVV/2 des Forschungsschiffes POLARSTERN 2000. Ber.Polarforsch. Meeresforsch., 404, 136-157.

Labeyrie, L. et al., 2002: Report of IMAGES Cruise V, 1999 to the western equatorial and northern North Atlantic. Institut Francaise pour la Recherche et la Technologie Polaires, Brest.

Niessen, F., Henschel, H., 1994: Physical properties in marine sediments. In. Hubberten, H.-W. (ed.), The Expedition ARKTIS-X/2 of RV "Polarstern" 1994. Ber. Polarforsch. Meeresforsch., 174, 75-82.

Pflaumann, U., D. Adelung, T. Anders, et al., 1996: Bericht über die „POSEIDON"-Reise 210/2 Reykjavik – Reykjavik, 13.08. bis 29.08.1995. – Bericht Sonderforschungsbereich 313, Univ. Kiel, Nr. 62, 1-62.

Rostek, F., V. Spieß, & U. Bleil, 1991: PARASOUND Echosounding: Comparison of analogue and digital echosonder records and physical properties of sediments from the equatorial South Atlantic. – Mar. Geol. 99:1-18.

Sarnthein, M., Pflaumann,U., Wang, P.X., and H.K. Wong, 1994: Preliminary report on SONNE.95 cruise „Monitor Monsoon" to the South China Sea.– Berichte-–Reports, Geol.-Paläont. Inst. Univ. Kiel, Nr. 68, 1-225.

Sarnthein, M., K. Stattegger, D. Dreger, H. Erlenkeuser, P. Grootes, B. Haupt, S. Jung, T. Kiefer, W. Kuhnt, U. Pflaumann, C. Schäfer -Neth, H. Schulz, M. Schulz, D. Seidov, J. Simstich, S. van Kreveld-Alfane, E. Vogelsang, A. Völker, M. Weinelt, 2001: Fundamental modes and abrupt changes in North

Atlantic circulation and climate over the last 60 ky - Concepts, reconstruction, and numerical modelling. - In: P. Schäfer et al. (eds): The northern North Atlantic: A changing environment (Springer Verl.) 365-410.

Spieß, V., 1992: Digitale Sedimentechographie – Neue Wege zu einer hochauflösenden Akustostratigraphie. -Unveröff. Habil.-schr., Univ. Bremen, 199 pp.

Van Kreveld, S., M. Sarnthein, H. Erlenkeuser, P. Grootes, S. Jung, M.J. Nadeau, U. Pflaumann, and A. Voelker, 2000: Potential links between surging ice sheets, circulation changes, and the Dansgaard-Oeschger cycles in the Irminger Sea. - Paleoceanography 15: 425-442.

5. GEOLOGY AND BIOLOGY OF A DEEP-SEA CHANNEL SYSTEM IN THE GREENLAND SEA

5.1 Introduction

During the expeditions ARK XVI/1 and ARK XVII/1 in 2000 and 2001 a deep-sea channel system was studied in the western Greenland Basin in the frame of the multi-disciplinary research programme "ARKTIEF" (Krause & Schauer, 2001; Fahrbach, in press). Work concentrated on the continental margin in water depths of ca. 1500 to 3500 m where more than 200 km of the channel system was mapped by the HYDROSWEEP and PARASOUND systems and oceanographical, biological and geological sampling was conducted at selected sites. The principal goal of ARK XVIII/1a was to extend the studies into the deep central Greenland Basin to study the depositional regions in the distal part of the channel system which were first mapped by a GLORIA long-range side-scan sonar survey (Mienert et al. 1993; Hollender, 1996).

The geological programme aimed at (1) characterizing the large-scale subsurface structure of the channel and the adjacent areas, (2) mapping the various sedimentary facies, and (3) sampling surface and near surface sediments for a detailed study of sedimentological, organic geochemical and micropaleontological tracers which may reflect the various sedimentation processes, in particular gravitative mass transports, on geological time-scales (± 1000-2000 years). Additionally, the history of sediment transport in the channel will be elucidated by analysing sediment cores.

During the previous expeditions, biological studies focussed on distribution patterns of benthic organisms and sediment turnover processes in and around the western part of the channel system. Based on activity and biomass data it might be possible to estimate the frequency and intensity of particle-loaded near-bottom currents within the channel. So far, the deep-sea megafauna in the vicinity of the channel seemed to be dominated by echinoderms and small-growing sponges. Results from optical surveys of the larger epibenthic fauna and small-scale topography are combined with activity and biomass data for small sediment-inhabiting organisms to determine the habitat heterogenity, distribution patterns, as well as biomass and activity patterns of benthos communities in the vicinity of the channel system. The biological programme includes seafloor imaging, sampling of mega-/epibenthos, as well as sediment sampling for biochemical analysis and the assessment of small benthic organisms.

The biological and geological studies will be used to evaluate the significance of the channel system as modern tranport pathway for sediments and nutrients that may establish specific ecological conditions for deep-sea benthos in the channel compared to the adjacent deep sea.

5.2 Bathymetrical survey

(Frahm, Hohmann, Matthiessen)

The swath sounding system HYDROSWEEP was used during expedition ARK XVIII/1a for a bathymetric survey in the study area of „ARKTIEF" at the East Greenland continental margin. Based on the results of the survey during expeditions ARK XVI/1 and XVII/1 in 2000 (Krause and Schauer, 2001; Fahrbach, in press), the adjacent deep-sea area was visited to continue the detailed mapping of the course of the channel and to study the transition from the channel to the deep-sea sedimentation area. Furthermore, selected transects were conducted in the central portion of the system that was studied last year to fill gaps in the bathymetric chart of this area (Fig. 5.1).

The large-scale mapping with the GLORIA long-range side-scan sonar revealed the general pattern of a system with three major channel systems in the western Greenland Basin (Mienert et al., 1993; Hollender 1996) but only single separate segments of the channel system that was selected for a detailed study in the project „ARKTIEF" could be mapped. The bathymetric surveys revealed that a single channel meanders from the lower continental slope to the abyssal plain over a distance of about 200 km (Fig. 5.2). The channel was tracked back from the Greenland Basin in ca. 3500 m water depth at ca. 74°45´N and 6°30´W to the continental rise at ca. 74°N and 13°15´W in about 2600 m water depth. The preliminary evaluation of the HYDROSWEEP data of ARK XVIII/1a suggests that the channel divides in the distal part east of 5° 30´W into several distributary channels. These channels are difficult to track because of their shallow depth (< 10m). In the depositional area, the southern major channel system of the Greenland Basin joins the ARKTIEF channel and the distributary channels cannot clearly be attributed to one of these channels. The evaluation of the complete dat set and the construction of a new bathymetric map of the area is in progress (Hohmann; Frahm (master thesis).

Fig. 5.1. Preliminary digital terrain model of the channel system based on the surveys from 2000 to 2002. Note that this model is based on the initial shipboard processing of the raw data

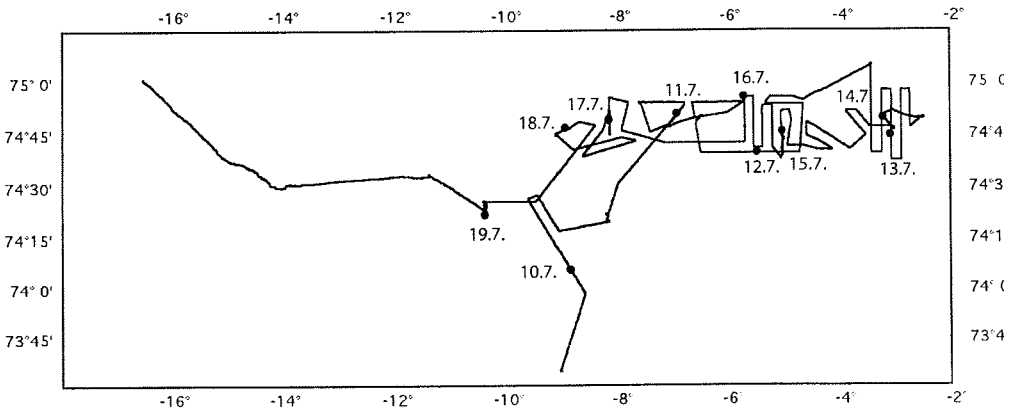

Fig. 5.2. Cruise track of the HYDROSWEEP and PARASOUND surveys during expedition ARK XVIII/1a.

5.3 Sediment echosouding

(Matthiessen, Rogenhagen, Usbeck, Clausing, Hoffmann, Kierdorf, v. Seggern)

The ship-mounted PARASOUND echosounding system of RV "Polarstern" was in operation during the work in the Greenland Sea in order to characterize the acoustic behaviour of the uppermost sediment layers. The PARASOUND transects were conducted partly perpendicular to the axis of the channel in order to identify lateral variability of sedimentary facies. Furthermore, PARASOUND profiling was used to select coring locations and transects for the OFOS surveys. The data were digitized by two different systems: 1) the PARASOUND system for simultaneous printing on a chart recorder (Atlas Deso 25), and 2) the PARADIGM system (Spiess 1992). For details of the method and standard settings used during the expedition see e.g. Niessen & Whittington (1995).

The acoustic penetration was on the average down to a sediment depth of 25 to 40 m, except in the channel bottom and in the abyssal plaine where penetration was usually less than 5 to 10 m. The channel system can be tentatively divided into 4 segments based on morphological and acoustic characteristics (see Fahrbach, in press). In the Greenland Basin east of ca. 6°35'W PARASOUND profiles show a notable change of cross sections. The channel is much shallower and wider than further to the west (compare Figs. 5.3 and 5.4.), possibly terminating in larger depositional lobes. Several shallow distributary channels (< 1000 m width, < 10 m deep) are incised into the sea floor between 74° 40'N, 5° 30'W and 74°50'N, 4°30'W (Fig. 5.4). Acoustic penetration is 5 to 10 m into the channel floors showing several subparallel reflectors. However, it is not clear whether these small channel segments are connected to the main channels. A few distinct onlap structures adjacent to these channels indicate basin infill. Furthermore, paleochannels are filled in with younger sediments that flatten the subbottom topographies.

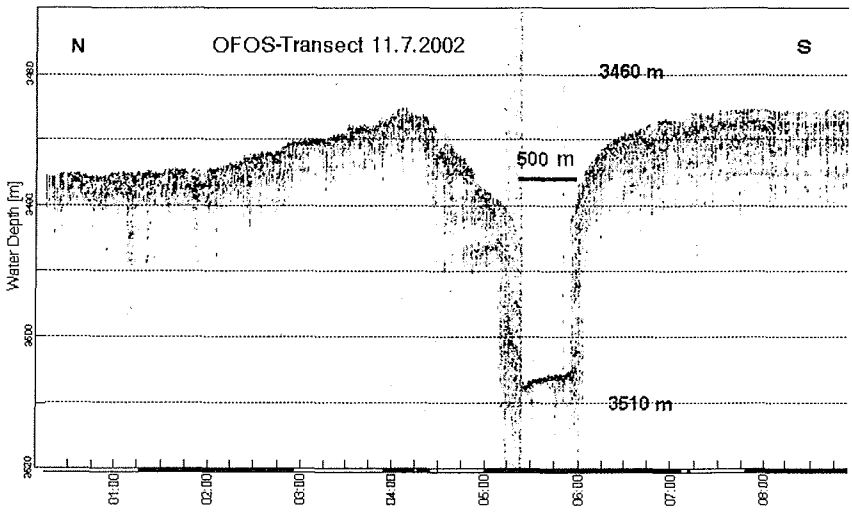

Fig. 5.3. Parasound profile along OFOS transect at Station PS62/029. The channel is located at 74° 49,3´N, 007° 00,6´W.

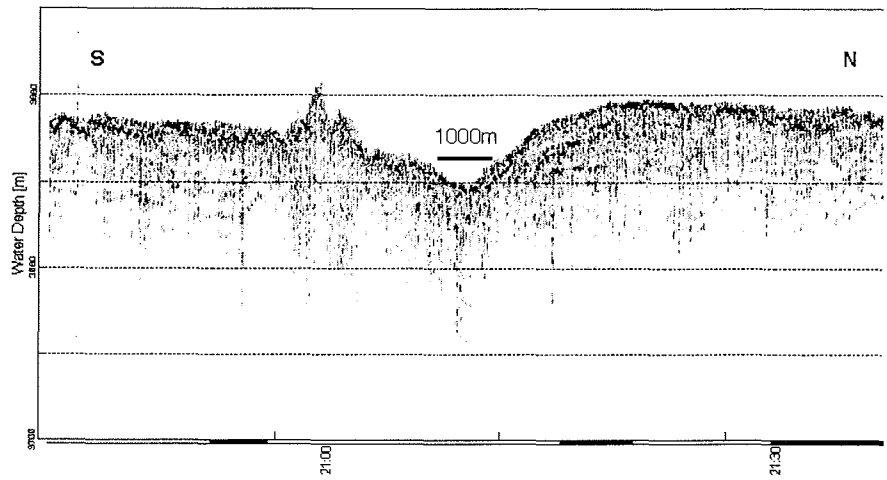

Fig. 5.4. Parasound profile in the abyssal Greenland Basin across channel segment at 74° 50,6´N 3° 16,0´W.

5.4 Bottom sediment sampling

(Matthiessen, Clausing, Hoffmann, Kierdorf, v. Seggern)

Surface and near-surface sediments were collected in the study area on transects across the channel and the depositional lobes to sample the various sedimentary environments. A more detailed sampling was done along the OFOS seafloor imaging transects in collaboration with the biology group. In order to get undisturbed surface and near-surface sediments, the giant box corer (GKG) with a size of 50x50x60 cm and the multi corer (MUC) with a tube diameter of 10 cm were used. The sampling was routinely done by MUC because of the better recovery of sediment surfaces. Gravity corers (SL) were used to obtain long sediment cores from the channel, the adjacent levees and the deep sea. Before sediment cores were cut non destructive logging methods were applied to measure colour reflectance and physical properties. The spectrophotometer "Minolta CM-2002" was used to measure colour reflectance on the archive half of sediment cores at 1 cm intervals. The "Multi Sensor Core Logger" (MSCL, Geotek, UK) was used to determine P-wave velocity, bulk density and magnetic susceptibility of whole-core sections. The methods are described in detail by Niessen and Henschel (1995) and Kuhn (2002).

Bottom sediment sampling was conducted along the whole channel system (Fig. 5.5).The initial macroscopic analysis of the surface sediments suggests that the composition of sediments in the channel, the adjacent levees and the deep-sea areas is similar. The lack of erosional surfaces and the comparable sediment composition along the course of the channel suggest continuous recent and sub-recent deposition. Only short sediment cores were recovered from the depositional areas. They show bioturbated sandy to silty clays at the surface underlain by laminated silts and clays which may indicate that the channels are in an inactive phase today. Gravity cores did not penetrate into the sediments from the depositional lobes. Longer sediment cores were only retrieved from levees showing distinct changes from laminated to crossbedded units consisting of clays to silts and bioturbated silty clays. This reflects episodic deposition of distal turbidites or bottom current activity.

Further detailed land-based sedimentological (graunlometry, mineralogy), geochemical and micropaleontological studies as well as analysis of the HYDROSWEEP and PARASOUND records are required to evaluate the variability of sediments in the study area with respect to sedimentation and transport processes.

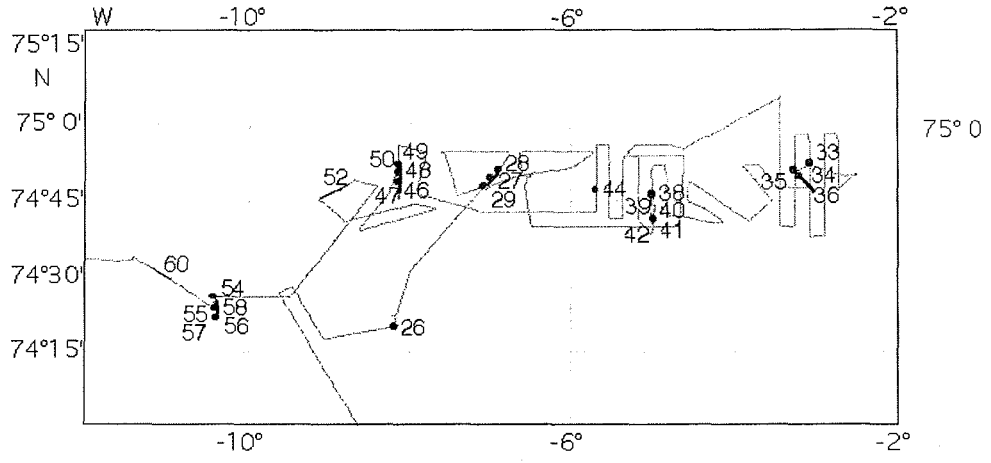

Fig. 5.5. Bottom sediment sampling stations during expeditions ARK ARKXVIII/1a.

5.5 Sources of organic matter in sediments

(C. Kierdorf)

During expedition ARK XVIII/1a and b surface sediment samples were collected to study the composition of the organic matter in the Greenland Sea and Fram Strait. Organic-geochemical bulk parameters (TOC and carbonate contents, C/N-ratios, HI/OI-ratios) and different biomarkers (*n*-alkanes, sterols, alkenones, fatty acids) will be measured to evaluate the importance of terrestrial and aquatic organic matter in sediments. Important sources for organic matter in surface sediments of the Greenland Sea and Fram Strait are (1) planktic and benthic organisms, (2) organisms living in sea-ice and meltwater ponds on sea ice, and (3) terrestrial sediments transported from coastal areas to the deep-sea by sea-ice. To determine the specific biomarker signature of the different sources, ice floes and the water column were systematically sampled. Altogether 14 stations on ice floes were conducted, and sediment samples and samples from sea-ice and meltwater ponds were taken (Table 5.1). Furthermore, 20l of water from 3 different water depths were taken on 16 CTD-stations in the Greenland Sea and Fram Strait All water and ice samples were filtered through GF/C Whatman filters. Sediment samples and filters were stored deep-frozen in amber glass bottles.

Station	Latitude	Longitude	Date	Samples
1-1	75°07.37'N	16°31.69'W	20.07.02	Sediment, Sea Ice, Meltpond
2-1	75°00.53'N	13°38.45'W	20.07.02	Sediment
2-2	75°01.04'N	13°34.31'W	20.07.02	Sea Ice, Meltpond
3-1	79°11.97'N	02°40.34'E	08.08.02	Sediment, Sea Ice, Meltpond
4-1	79°09.01'N	03°01.60'E	09.08.02	Sediment, Sea Ice, Meltpond
5-1	78°59.41'N	00°00.21'W	12.08.02	Sediment, Sea Ice, Meltpond
5-2	78°57.99'N	00°39.28'E	12.08.02	Sediment
6-1	79°02.06'N	02°02.31'W	13.08.02	Sediment, Sea Ice, Meltpond
6-2	78°46.93'N	02°00.10'W	13.08.02	Sediment, Sea Ice, Meltpond
7-1	78°56.58'N	04°35.98'W	14.08.02	Sediment, Sea Ice, Meltpond
7-2	78°55.39'N	04°55.77'W	14.08.02	Sediment
8-1	78°45.37'N	07°06.75'W	14.08.02	Sediment, Meltpond
9-1	78°54.55'N	14°38.90'W	15.08.02	Sediment, Sea Ice, Meltpond
10-1	78°50.64'N	17°39.42'W	15.08.02	Sediment, Sea Ice, Meltpond

Table 5.1: List of sea-ice stations during the expedition ARK XVIII-1a/b

5.6 Benthic distribution patterns and turnover processes

(v. Juterzenka, Kolar, Krusche)

5. 6.1 Megafauna/Epifauna and habitat characteristics

Seafloor imaging

The investigations on mega-/epifauna in the vicinity of the channel system had been continued by means of the towed deep-sea camera system OFOS (Ocean Floor Observation System), which had been also used in 2000 and 2001 (for technical details see Krause & Schauer 2001, Fahrbach in press). The whole system was towed across the seafloor in a distance of approx. 1.50 m with a drift velocity of approx. 0.5 knots. Kodak Ectachrome 100 ASA film provides up to 800 shots per track. During the cruise, 6 OFOS tracks had been performed in the central to eastern part of the channel and the area of the suspected depositional lobe. Where the channel profile has a distinct shape, tracks had been layed across the channel axis (Fig. 5.5: Sts. 29, 49, 57). They cover a distance of 2-4 nm. In the area of the depositional lobe, two short tracks were performed (Fig. 5.5: St. 39, St. 40). The easternmost transect at St. 36 started in the center of a deep-sea plain between small seamounts and ended up in the central depression of one of the prolonged seamounts.

A first impression of the benthos fauna in the vicinity of the eastern channel system is given by b/w video information and short pieces of slide film, which were developed on board for quality control reasons. They reveal elpidiid holothurians (*Elpidia glacialis*), actinaria, gastropods, small pantopods and sponges, fish and some octopus specimens (probably *Cirroteuthis muelleri*) (Fig. 5.6) as well as a variety of traces, tracks and mounds. Furthermore, the eastern part of the study area is

characterized by the presence of large-growing stalked hexactinellid sponges (*Caulophacus sp.)*. The southern slope of the central channel area is colonized by large-growing anthozoans, a finding that corroborates the results of ARK XVI/1. A typical example of a seafloor view in the channel area is given in Fig. 5.7.

Fig. 5.6. Seafloor image of the eastern part of the ARKTIEF study area (PS62/49): hexactinellid sponge Caulophacus sp. (identification by F. Hoffmann/C. Kamcke).

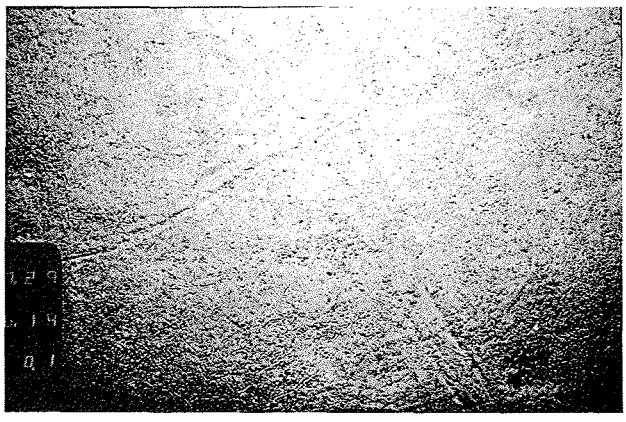

Fig. 5.7. Seafloor image of the central part of the ARKTIEF study area (see Fig. 5.5).

Megafauna sampling
A small Aggassiz-Trawl (1m in width) was used at three sites (Sts. 42, 52, 60) to sample reference material for species identification as well as for the evaluation of population parameters of dominant species. On the eastermost location („deep-sea depositional plain"), the sampled fauna was dominated by sponges and their remains (mainly *Caulophacus* sp., *Thenea* cf *abyssorum*). Furthermore, the catch contained *Elpidia glacialis*, Gastropoda, Bivalvia, several species of Amphipoda and Decapoda, and few Pantopoda.

At St. 52, the trawl was towed along the channel floor and contained *Elpidia glacialis*, *Thenea* cf *abyssorum* and some crustaceans, pantopods and gastropods.

The third trawl station (St. 60) covered the continental slope foot at 3000 m water depth. Here, the echinoderms and sponges dominated in the catch as well. Additional elements in this region were the irregular deep-sea echinoid *Pourtalesia jeffreysii*, which is already known from seafloor imaging at the channels „funnel" area at the slope foot (ARK XVI/1), a second holothuroid species as well as asteroids. In addition to reference samples, sponges were taken by F. Hoffmann/I. Kaesler/C. Kamcke for further taxonomic, microbiological and biochemical analysis (see Chapter 7.)

5.6.2 Sediment biochemistry and small organisms

Along all OFOS imaging transects, sediment samples from the multi corer were taken at overall 13 stations. Were OFOS transects lay across the channel profile, sampling stations have been choosen within and outside the channel on the levees (5.4; see also Krause & Schauer 2001, Fahrbach in press).
Cores are subsampled in 1 cm horizontal sections down to a sediment depth of 5 cm to identify gradients within the sediment column. Samples are fixed with formalin and/or were deep-frozen. They will be analyzed in the home lab for meiofauna and small organisms, phospholipids, protein content. Chloroplastic pigment equivalents (CPE) will be determined to quantify organic matter input from primary production. Microbial exoenzymatic activity (fluorescein-di-acetate (FDA) hydrolysis) was measured directly on board.

References:

Hollender, F.-J. (1996): Untersuchungen des ostgrönländischen Kontinentalrandes mit dem Weitwinkel-Seiten-Sonar GLORIA. Ber. SFB 313, 67, 124p.

Krause, G. & Schauer, U. (2001 eds): The expeditions ARK XVI/1 and XVI/2 of the Research Vessel „Polarstern" in 2000. - Ber. Polarforsch. Meeresforsch. 389, 108pp.

Mienert, J., Kenyon, N.H., Thiede, J., Hollender, F.-J. (1993): Polar continental margins: Studies of East Greenland, EOS, Trans. Amer. Geophys. Union 74(20), 225-236.

Fahrbach, E. (ed.), The expedition ARK XVII/1 of the Research Vessel „Polarstern" in 2001. - Ber. Polarforsch. Meeresforsch.

Kuhn G., Hass C., Censarek, B., Rudolph, M., Forwick, M., Quirós-Alpera, S. (2002): Meeresgeologie. In Thiede, J., Oerter, H.(eds.). Die Expedition ANTARKTIS XVV/2 des Forschungsschiffes POLARSTERN 2000. Ber. Polarforsch. Meeresforsch., 404, 136-157.

Niessen, F., Henschel, H. (1995): Physical properties in marine sediments. In. Hubberten, H.-W. (ed.), The Expedition ARKTIS-X/2 of RV "Polarstern" 1994. Ber. Polarforsch., 174, 75-82.

Niessen, F., Whittington, R. (1995): Marine sediment echosounding using Parasound. In. Hubberten, H.-W. (ed.), The Expedition ARKTIS-X/2 of RV "Polarstern" 1994. Ber. Polarforsch., 174, 62-68.

Spiess, V. (1992): Digitale Sedimentechographie - Neue Wege zu einer hochauflösenden Akustostratigraphie. - Ber. Fachber. Geowiss. Univ. Bremen, 35, 199pp.

6. PHYSICAL OCEANOGRAPHY

6.1 Hydrographic conditions and deep ventilation in the Greenland Sea

(Budéus, Engeler, Kleppek, Marx, Plugge, Schinkel, Walter, Wilkens (AWI, Bremerhaven and IUP, Uni Bremen))

Bottom water renewal in the Greenland Sea by deep convection in interplay with ice coverage and atmospheric forcing is a major element of the water mass modification in the Arctic Mediterranean. Effects influence both the central Arctic ocean and the overflow waters into the Atlantic. Since the hydrographic observations became more frequent in the late 1980s, no bottom water renewal by winter convection took place, however. Under these conditions, the deep water properties change towards higher temperatures and salinities. Furthermore, the doming structure in the Greenland Gyre, as it was observed in the mid-80s, was superseeded by an essentially 2-layered water mass arrangement with a marked density step which is located presently at about 1800 m.

The project is incorporated in the EU funded 'CONVECTION' and the DFG-project 'Ventilation of the deep Greenland Sea'. Specific objectives are to investigate the relative importance of atmospheric forcing parameters for winter convection, to clarify whether ice coverage inhibits or facilitates deep convection, to build a long term observational basis about deep water changes in the Greenland Gyre, and to contribute to the decision which deep water exchange mechanisms are at work under the absence of deep winter convection. A special focus is put on the persistent small scale eddies (diameter of order 10 km) which allow convection to considerably greater depth (about 2500 m) than is generally observed within the gyre. The DFG-project concentrates on the monitoring of changes in deep water ventilation by

continuing the existing time series of CFC measurements, the estimation of diapycnal diffusivities from the vertical shear spectra of the Lowered Acoustic Doppler Current Profiler (LADCP) measurements, the quantification of the deep water renewal due to vertical mixing, and the comparison of LADCP spectra with higher resolution Expendable Current Profilers (XCP) which reveal a spectral correction for short wavelengths.

Work at sea

After a number of profiles performed at geological stations, work at sea is comprised of two main parts: Jojo-CTDs in the ARKTIEF region and the long term east-west transect across the Greenland Gyre. The latter included an extended investigation of a small scale eddy. The two Jojo-CTD stations in the ARKTIEF area were taken at 0.5 kn speed and covered transects from the southern to the northern Levee of the investigated trench.

In the central Greenland Sea, the long term zonal CTD transect at 75°N has been performed with a regular station spacing of 10 nautical miles. CTD and water sampler (SBE 911+, Carousell 24 bottle sampler with 12 L Niskin bottles) worked faultlessly . A few hints may suffice to give an idea about the general procedure of in situ calibration and data processing. We use the same sensors already for a number of years and checked for their performance with respect to unwanted cross dependencies. According to this, one of the temperature sensors shows a pressure sensitivity of roughly 1.5 mK/4000 dbar while no pressure or temperature dependance of the conductivity sensors could be found.

The locations of in-situ comparisons have been chosen carefully by checking for each data point whether a comparison is allowed or inhibited. For drift control, duplicate sensors have been utilized throughout. Time alignment has been optimised for each flow path separately. The data will be corrected by a final post cruise calibration. The difference between pre-cruise and post-cruise calibration is normally in the range of a few mK and a few 1/1000 in salinity. Bottle sample salinities of quadruple samples are determined in the lab on land and by Ocean Scientific. In addition to the standard parameters, transmission has been measured (Seatech, 25 cm).

The ADCP measurements were taken with two RDI Workhorse ADCPs attached to the water sampler. This set-up should allow for a good altogether range (145m for each instrument, 290m altogether) as well as a reasonable vertical resolution of 10m and good data near the bottom. Unfortunately, on of the new instruments failed during the first deep water cast. The problem could not be resolved on board, so the measurements were continued with only one instrument. This resulted in bad data quality below 2500m due to seriously diminished range because of scarcity of scatterers in the bottom waters. Altogether, 75 profiles were taken, 68 of those on or near the 75N section. This repeats the parts of a dataset from 1998 (ARKXIV/2), where high diffusivities were found in the central Greenland Sea.

On 5 occasions, additional high resolution current profiles were recorded by simultaneously launching XCPs while the ship was on station and a LADCP profile was taken. The XCPs were launched from helicopter in a safe distance to the ship,

so that the ships magnetic field could not interfere with the inductive measurement. The data from the XCP were recorded on audio tape and will be analysed later at home.

On a total of 7 stations, 142 CFC samples were taken. It was a so-called "offline" sampling, where the samples are collected in specially designed glass ampoules, which are subsequently sealed by melting. This is done so that no gas exchange can take place, and allows for extended periods of keeping the samples. The samples will be stored at 4 degree C and analysed in lab by gas chromatography. The CFC components of inerest are CFC-11, CFC-12 and CCl4. The 7 stations were spaced along 75N, with stations on the Greenland shelf break, in the central Greenland Sea and near Mohn's Ridge, to give a good horizontal coverage. The vertical resolution was aimed to be between 100 and 200m, with special focus on the deep water.
One station was taken in a small scale eddy filled with exceptionally homogenous cold water.

The three in house developed EP/CC (externally powered/compressibility compensated) Jojo-moorings have been exchanged during splendid weather conditions. Deployments and recoveries revealed no problems. Performance was a mixed success. Two moorings stopped to profile prematurely (after a quarter and half a year), the third measured the entire year with a two day interval and thus provides an unprecedented time series.

Three 4H Jena Drifters have been launched to mark the center of the small scale eddy and are planned to drift in 600 m depth and to surface every 10 days to submit their data and position by satellite. A fourth drifter could not be properly started.

First results

Owing to extremely low ice concentrations the transect could begin unusually close to the East Greenland coast, thus covering the area occupied by fresh Polar Surface Waters almost completely. This will lead to a precise estimate of the actual fresh water transport of the East Greenland Current.

The most outstanding single feature of the survey in the Greenland Sea was certainly the small scale eddy. Similar features represent the deepest convection level observed in recent years. The center of the investigated eddy was found close to the Greenwich meridian (0° 47'W) and slightly north of 75° N. The almost homogeneous water column showed temperatures below -1.000 deg C, lower salinities than the surrounding, and extended to a maximum of 2500 dbar. The ubiquitous temperature maximum (found usually at medium depth levels of some 1700 to 1800 m) was displaced downwards to 2800 m. The feature has been covered with 21 stations. The eddy has a diameter of roughly 20 km and contains water which is denser than the surrounding at low pressure levels (about 600 m), but considerably less dense at higher pressures (Fig. 6.1). This indicates that the water within the eddy is not a good candidate for bottom water replacement. There are indications that the eddy may not have been established during the last winter but may have existed before. This would mean that its lifetime exceeds one year.

The eddy represents an exception from the state of the surrounding waters. In the background, winter convection did not penetrate through the temperature maximum (which is combined with a pycnocline) and is confined mostly to about 1500 m. The Jojo-moorings show in detail that the deepening of the ventilated layer resulted in higher temperatures and higher salinities. This result is not typical for winter convection concepts and can occur in the Greenland Sea because of the subsurface inflow of high saline and warm Atlantic Waters from the gyre's rim. The temperature and salinity increase in the ventilated area is also apparent in the data of the 75° N transect. Although it is somewhat difficult to estimate the general depth level of the temperature maximum because of the eddy induced distortions of the temperature field, from 2001 to 2002 a general increase in its depth level of about 100 m is apparent. It is also unambiguous that the warming of the bottom waters, as observed during the last years, continued with a rate of more than 10 mK/year. The lowest temperatures in the bottom waters increased from -1.145 deg C (potential temperature) in 2000 to -1.131 deg C in 2001 and -1.112 in 2002 at 1° W (Fig. 6.2).

The nature of the CFC and XCP measurements (analysis at home) do not allow for a discussion of first results. The LADCP measurements, however, show an almost barotropic flow on the slope off Greenland; the East Greenland current flows south with velocities up to 40 cm/s at the surface. In the Greenland Sea gyre, the direction and magnitude of the currents is less determined; interpretation of the data is difficult at this stage, because the bad data quality in the lower part of the profiles tend to shift the barotropic component of the flow. It will be attempted to correct for that effect by matching the LADCP profiles with the data from the Vessel Mounted ADCP (VMADCP). In the eastern part part of the basin, the West Spitsbergen current is clearly visible in the data, flowing north in some sort of banded structure, with speeds around 30 cm/s, and a tendency to produce eddies. The overall data quality for the single ADCP is good, except for the problems due to few scatterers at great depth mentioned earlier.

For the last couple of stations, the ship experienced a rough sea state with a lot of swell, which caused the water sampler to tilt quite a bit, and may degrade data quality. However, on first inspection, the data seemed fine.

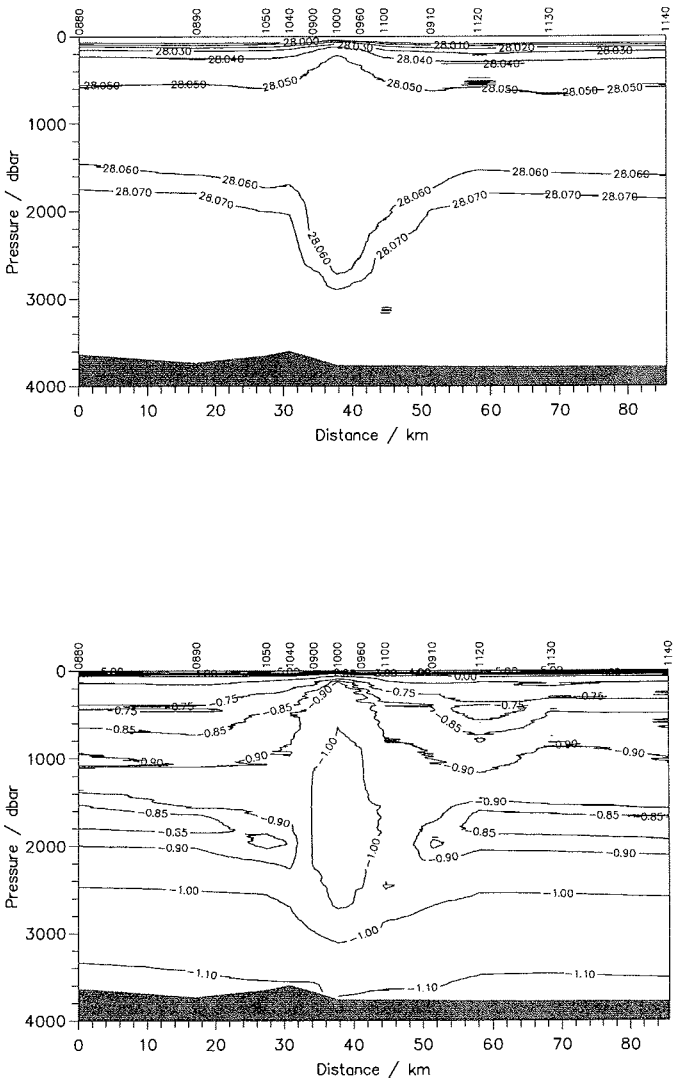

Fig 6.1: Distribution of a) density and b) pot. temperature on a east-west transect across the eddy.

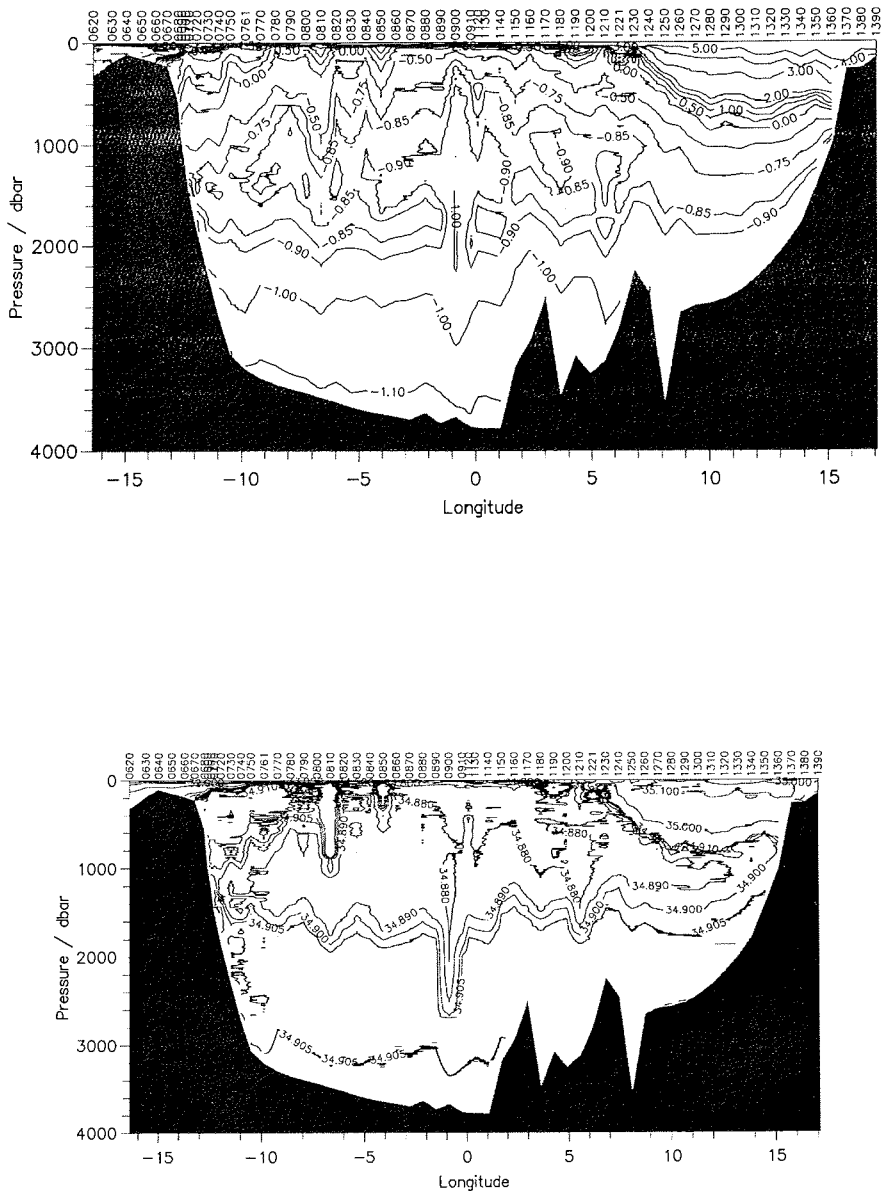

Fig 6.2: Distribution of a) pot. Temperature and b) salinity on the zonal transect along 75 deg N.

6.2 Physical oceanography in Fram Strait

(Schauer, Schütt, Wisotzki, Monsees, Schinkel,
Kleppek, Winkler, Schwarz, Marx, Engeler)

Background

Exchange between the North Atlantic and the Arctic Ocean result in the most dramatic water mass conversion in the world ocean: warm and saline Atlantic water, flowing through the Nordic Seas into the Arctic Ocean, is modified by cooling, freezing and melting to become shallow fresh water, ice and saline deep water. The outflow from the Nordic Seas to the south provides the initial driving of the global thermohaline circulation cell. Knowledge of these fluxes and understanding of the modification processes is a major prerequisite for the quantification of the rate of overturning within the large circulation cells of the Arctic and Atlantic Oceans, and is also a basic requirement for understanding the role of these ocean areas in climate variability on interannual and decadal scales.

The Fram Strait is the only deep connection between the Arctic Ocean and the Nordic Seas. Just as the fresh-water transport from the Arctic Ocean is thought to be of major influence on convection in the Nordic Seas and further south, the transport of warm and saline Atlantic water significantly affects the water mass characteristics in the Arctic Ocean and therefore possibly influences also ice and atmosphere. Since 1997, velocity and hydrography measurements are carried out in Fram Strait with the aim to estimate mass, heat and salt fluxes through the strait as well as fluxes of dissolved substances. This work is done jointly with the Norwegian Polar Institute and until July 2000 was part of the European Union project VEINS (Variability of Exchanges in the Northern Seas). In combination with regional models, the results will be used to investigate the nature and origin of the transport fluctuations on seasonal to decadal time scales.

The complicated topographic structure of Fram Strait leads to a splitting of the West Spitsbergen Current carrying Atlantic Water northward into at least three parts. One follows the shelf edge and enters the Arctic Ocean north of Svalbard. This part has to cross the Yermak Plateau which poses a sill for the flow with a depth of approximately 700 m. A second branch flows northward along the north-western slope of the Yermak Plateau and the third part recirculates immediately in Fram Strait at about 79°N. Evidently, the size and strength of the different branches largely determine the input of oceanic heat to the inner Arctic Ocean. The East Greenland Current, carrying water from the Arctic Ocean southwards has a concentrated core above the continental slope. Therefore, our mooring array is designed to cover the deep part of Fram Strait from the eastern to the western shelf edge. The related hydrographic section is usually extended onto the Greenland shelf as far as the ice allows which meant in this year up to the Greenland coast.

Work at Sea

To continue time series of the current, temperature and salinity fields between Greenland and Spitsbergen, 10 out of 14 moorings which were deployed in summer 2000 (some in summer 2001) along 78° 50'N were planned to be recovered and

replaced by 12 new moorings (Fig. 6.3, Appendix 3). Two moorings could not be recovered: F2 was lost during recovery and F3 probably due to commercial fishery activities (its top buoy with Argos transmitter popped up in March 2002 and was recovered by FS Lance). All other moorings were recovered successfully. The records provide the 5th set of year-long time series since 1997. Evaluation of the data from the previous years have proved the necessity of higher horizontal coverage in the central Fram Strait to capture the western boundary of the West Spitsbergen Current which is variable in its position and to cover the return flow. Therefore moorings were deployed for another year at 12 instead of only 10 positions. The four Norwegian moorings in the west will be exchanged in September 2002.

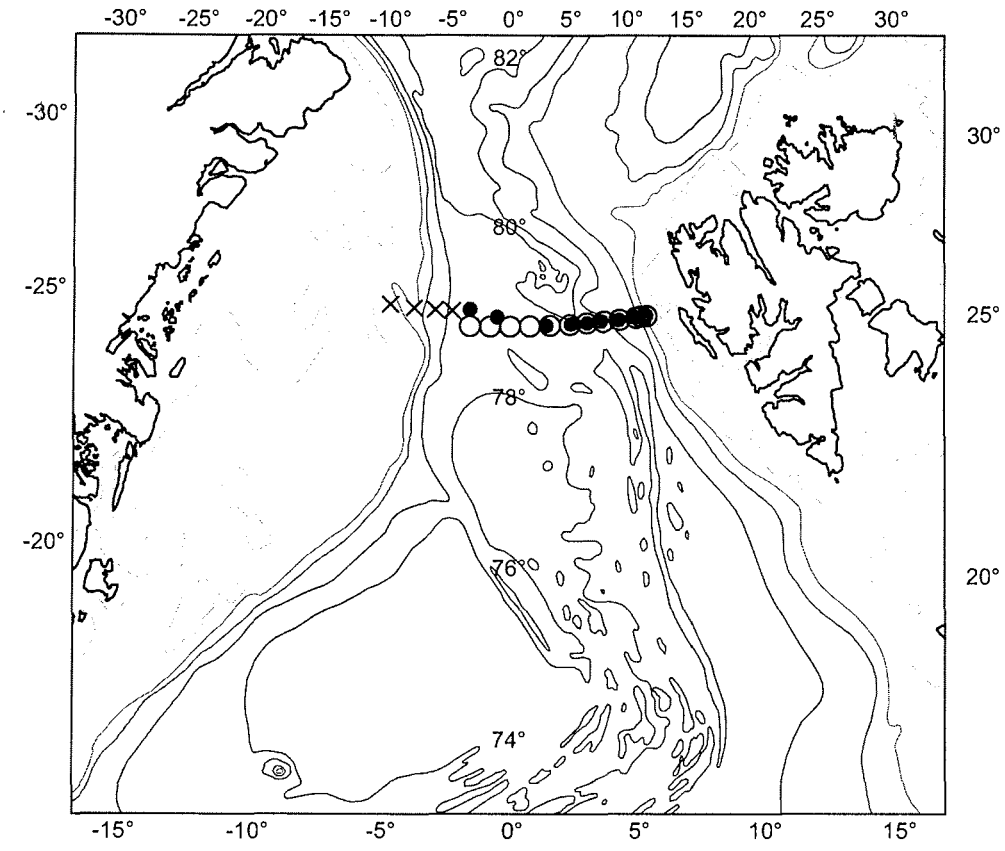

Figure 6.3: Position of recovered moorings (grey filled circles) and deployed moorings (open circles). Crosses mark the positions of Norwegian moorings

The instrumentation of the moorings remained similar as in the last years except that instruments have been induced also at the 700 m level which is about the lower boundary of the warm layer of Atlantic Water is now instrumented. For a sufficient vertical resolution, each mooring carried 3 to 8 instruments like current meters from Aanderaa and FSI, acoustic current profilers (RDI), temperature and salinity probes (Seabird), and Upward looking Sonars for ice thickness measurements (APL). Three moorings carry deep-sea pressure gauges (Seabird) to obtain changes of the sea level slope indicative of barotropic velocity changes.

Hydrographic stations were conducted along the mooring line to supply temperature and salinity at a much higher spatial resolution than given through the moorings (Fig. 6.4). The section was continued westward beyond the shelf edge and, because of favourable ice conditions, could be extended up to the Greenland coast. Two further sections were carried out at the Spitsbergen continental slope at 77°N and 78°N after a plume of dense saline bottom water was discovered between 1100 and 1900 m at 79°N. 9 CTD stations were taken at the Hakon Mosby Mud Volcano (area IV in Fig. 6.4).

For the hydrographic measurements we used the CTD system Seabird Electronics SBE9plus SN 09P21218-0561 with a twin set of standard temperature and conductivity sensors (SBE-3plus SNs 4127 and 2678, and SBE-4 SNs 2325 and 2618), and a digital reversing thermometer SBE 35 RT (SN 27) for in-situ calibration. Pressure was measured by Digiquartz 410K-105 SN 75659. Other sensors were Light transmission - C-Star Wetlabs transmissiometer, SN CTS-403DR, Bottom distance – Benthos Altimeters 2110-2 SNs 189 and 208, Datasonics Altimeter PSA-900 SN 733.

The CTD was used in combination with a SBE32 Carousel Water Sampler SBE32, SN 3221218-0273 which operated 24 12-liter Ocean-Test-Equipment bottles. Samples were taken by the plankton, the microbiology and the geochemistry groups for phytoplankton, methane and oxygen analysis. A total number of 101 samples was taken in low salinity gradient parts of the water column for in-situ salinity calibration of the CTD-sensors; part of the samples were analysed onboard with a Guildline Autosal 8400A salinometer and IAPSO standard sea water Batch #P140. All sensors showed a good performance throughout the cruise – the maximum temperature and salinity deviation between the standard sensors pairs was $2*10^{-3}$ K and $2*10^{-3}$ PSU respectively. Temperature and salinity sensors were calibrated by the manufacturer before and after the cruise.

First results

With the section between Svalbard and Greenland along 78° 50'N the sixth high-resolution survey in an annual sequence was performed (Fig.6.5). In the West Spitsbergen Current the temperature and salinity of the Atlantic Water showed similar high values during the last three years as compared to the beginning of this time series in 1997, but the southward flowing water of the East Greenland Current was considerably colder than in the years before. If this is true for more than a snapshot of one survey (as will be revealed by the data from the moored instruments) it would indicate a change in the circulation pattern of the Arctic Ocean.

At the continental slope west of Spitsbergen at 79°N, a layer of saline warm bottom water was found between 1100 and 1900 m water depth (Fig. 6.6). The plume was also marked by enhanced turbidity. This water is most likely shelf water formed in winter in the Storfjord polynja. Dense water is formed through brine released during freezing and accumulates in appropriate shelf regions. It spreads in plumes along the bottom to the shelf edge and sinks to deeper layers in the basins thereby entraining less saline warm ambient water. Shelf/slope convection is the Arctic Ocean contribution to the thermohaline overturning and the Storfjord polynja is known as one of the major production sites. Throughout the 1990s, brine enriched shelf water in the Storfjord was of too low salinity to ventilate the deep ocean. For the first time since the 1980's, in winter 2002 high salinity water was observed in the Storfjord during a cruise of the Swedish ice breaker Oden. The outflowing water has obviously spread meanwhile northward to about 79°N. Two sections along 78°N and 77°N (II and III in Fig. 6.3) showed also remnants of the plume although the signal was only small.

CTD-stations taken at the Hakon Mosby Mud Volcano showed no temperature/salinity structure indicative of an influence of the volcano. Moreover, optical measurements with the light transmissometer did not reflect the acoustic anomalies detected with the 38 KH echo sounder (see Sauter) in 300 m bottom distance – be these induced by gas bubbles or sound reflecting particles (Fig. 6.7).

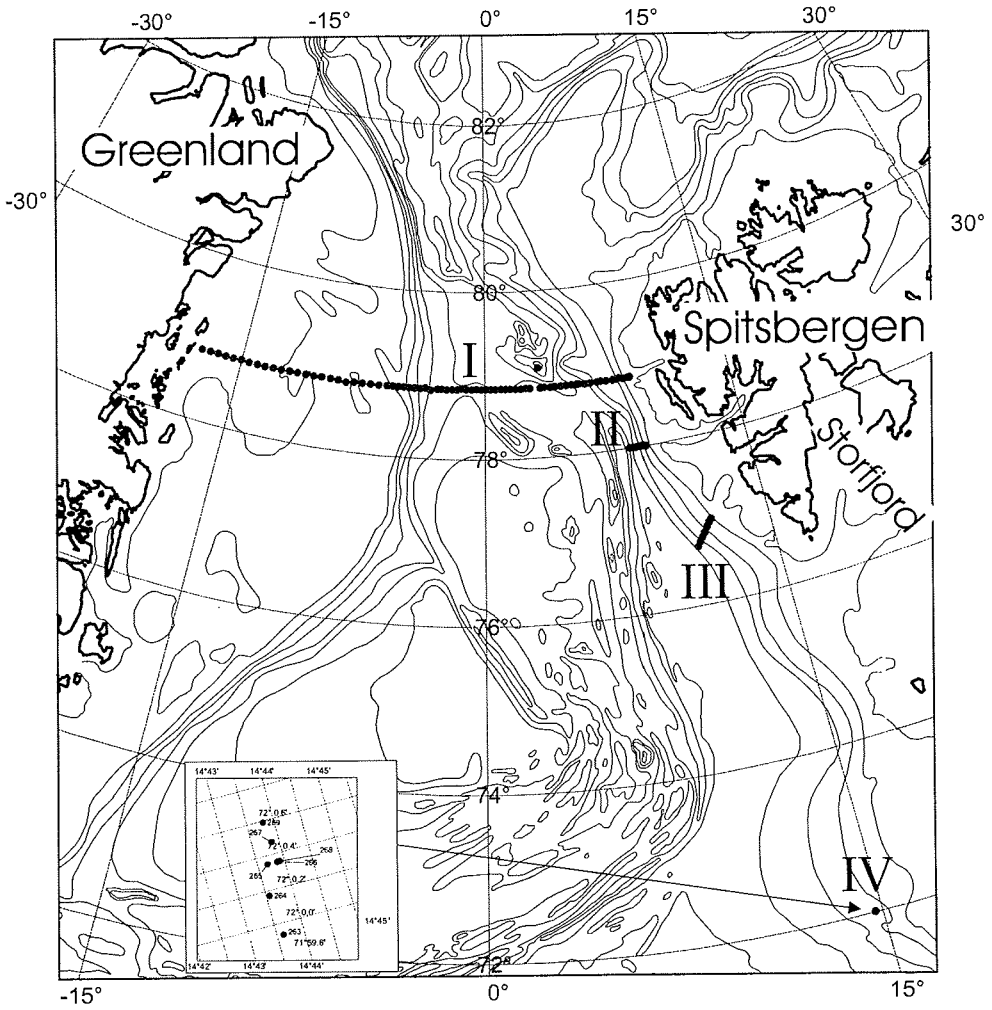

Figure 6.4: Locations of CTD-measurements.

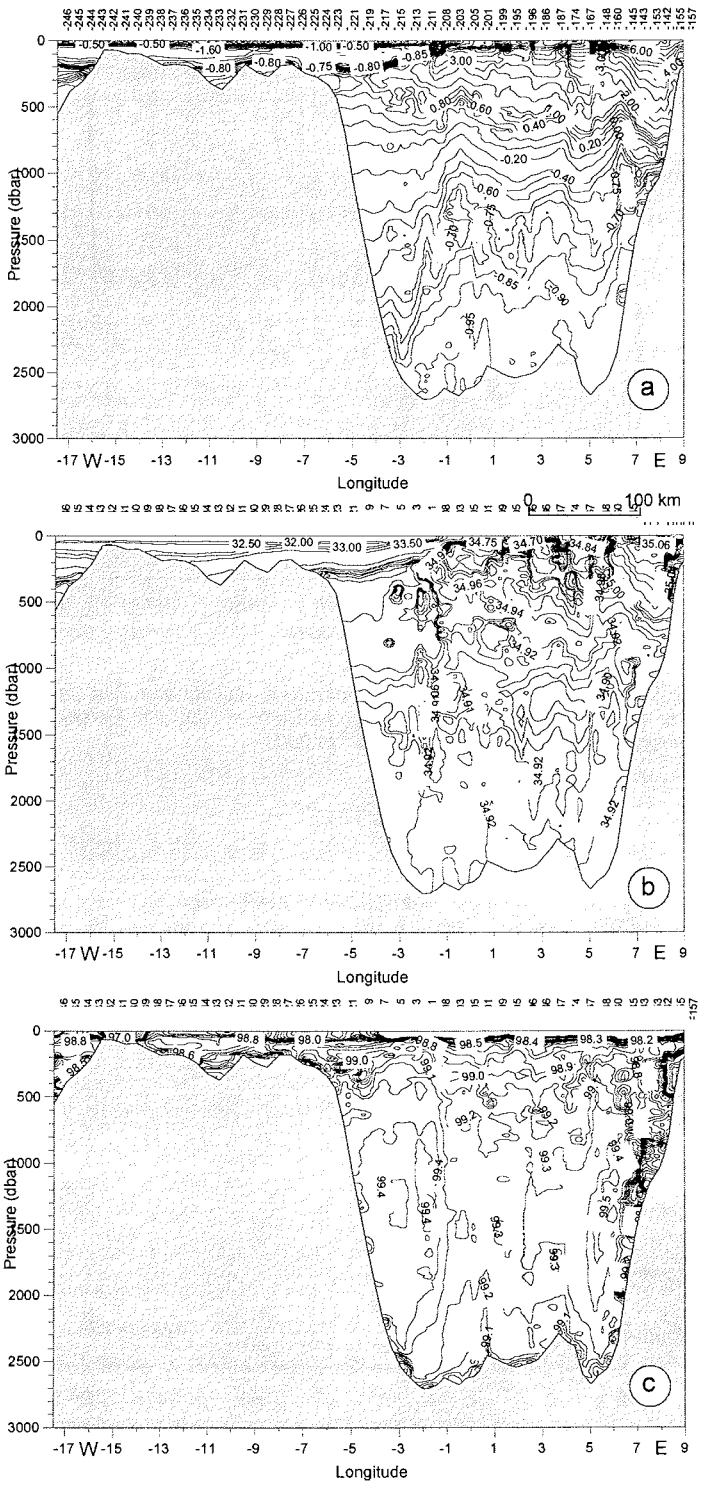

Figure 6.5: Temperature (a), salinity and density distribution along section I (see Fig. 6.3).

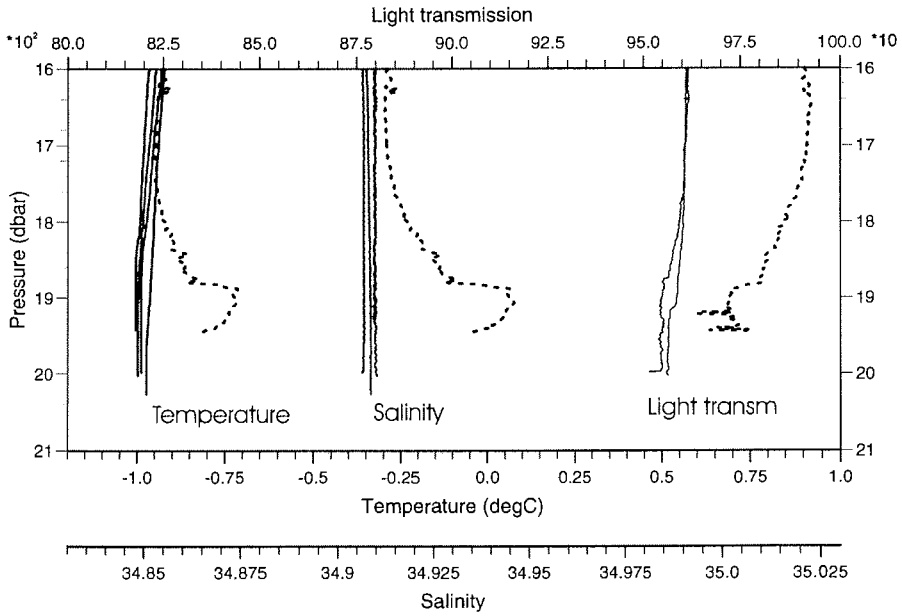

Figure 6.6: Near bottom profiles of temperature, salinity and light transmission at about 78° 50'N, 6° 45'E. The stippled line shows the profile from 2002 with the shelf water plume. The other curves are from the years 1997 to 2001.

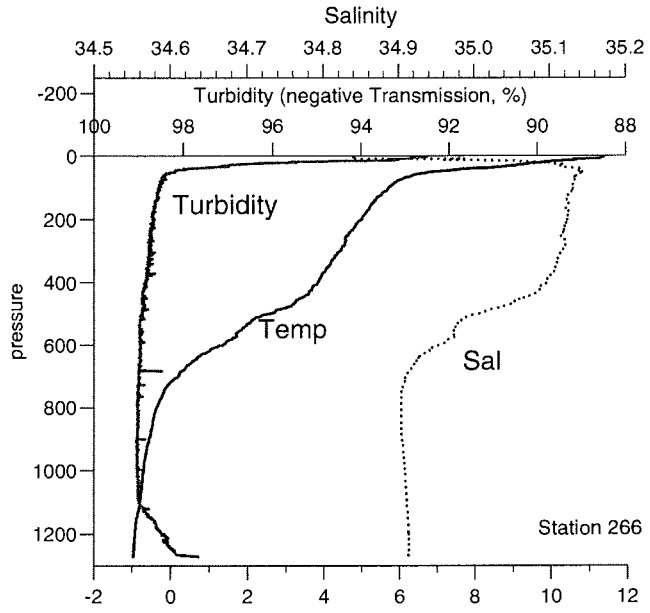

Figure. 6.7: Profiles of temperature, salinity and light transmission at the Hakon Mosby Mud Volcano.

7. GEOBIOLOGY AND BIODIVERSITY OF PORIFERA FROM ARCTIC AUTOCHTHONOUS SPICULITE MATS AND ABYSSAL SOFT BOTTOM SEDIMENTS

(Hoffmann, Kamcke, Friedt, Kaesler)

Sponges belong to the most ancient phyla of the animals, representing the onset of Metozoa evolution. As sessil dwellers of the sea bottom, most sponges produce a braod range of secondary metabolites for defence against predation. During the past few years scientific interest in sponges has increased due to the increasing interest in these metabolites for application in the pharmaceutical and cosmetical industry. Sponge associated bacteria, which can account for a major part of the sponge tissue, are suspected to contribute to the production of the secondary metabolites.
Scientists and students from the Universities of Göttingen and Berlin participated on cruise ARK XVIII 1 a and b to collect arctic sponges from different habitats.
Sponge communities on arctic spiculite mats of Vesterisbanken and Jan Mayen Sporn (PS 62/022-025) were sampled with a giant box corer. In co-operation with the Deep Sea Group from AWI, Bremerhaven (K.v. Juterzenka, T. Soltwedel), soft bottom species were sampled with an Agassiz Trawl in the area of the ARKTIEF project (central Greenland Sea – PS 62/042-1, 052-1, 060-1), as well as in the "AWI-Hausgarten" northwest of Spitsbergen (PS 62/180-1,182-1, 191-2). Aerobic and anaerobic sponge associated bacteria were cultivated from 4 sponge species. Subsamples of all collected sponges were fixed in formaline for determination and further histological investigation. Remaining samples were frozen for chemical investigation by BOSMAN-project partners in Hamburg and Berlin (see below). Spicule preparations and sponge sections were made in the laboratories on board, and sponge species were determined by microscopical examination of the spicules. Microscopical pictures were taken with a digital camera. At least 26 species from 16 families could be determined until the end of the cruise (see table 7.1). The samples cover a broad range of sponge taxonomy: Both Hexactinellida, Calcarea and Demosponges are represented. The majority of the sponge samples, both in respect to the number of species and individuals, belong to the tetracinellid sponges from the order Astrophorida.

Part of this project is connected to the BOSMAN project (Boreal sponges as a source of marine natural products – BMBF No. 03F0256A-D). Frozen sponge samples are passed to the project coordination at Hamburg University (Prof. Michaelis, Institute of Biogeochemistry and Marine Chemistry, Dep. of Geosciences) for chemical investigation and for distribution to other project partners.

Probennahme

ARK XVIII 1a (insgesamt 22 GKGs)

Anzahl, Aktion	Stationsnummer	Stationsbeschreibung
4 GKG	PS 62/022-1 bis 4	Jan Mayen Sporn
4 GKG	PS 62/023-1 bis 4	Vesterisbanken mittel
9 GKG	PS 62/024-1 bis 9	Vesterisbanken flach
5 GKG	PS 62/025-1 bis 5	Vesterisbanken tief

ARK XVIII 1b (insgesamt 3 AGTs)

Anzahl, Aktion	Stationsnummer	Stationsbeschreibung
1 AGT	PS 62/180-1	Hausgarten
1 AGT	PS 62/182-1	Hausgarten
1 AGT	PS 62/191-2	Hausgarten

Table 7.1: Taxonomy of sponges from ARK XVIII 1 a + b

Calcalrea
- *div. sp. indet*

Hexactinellida
- Hexasterophora
  - **Lyssacinosida**
    - Rossellidae
      - Rossellinae
        - *Schaudinnia artica*
        - *Scyphidium sp.*
        - *Asconema sp.*
      - Caulophacidae
        - *Caulophacus arcticus*
      - Acanthascinae
        - *Rhabdocalyptus sp.*

Demospongiae
- Tetractinomorpha
  - **Spirophorida**
    - Tetillidae
      - *Tetilla sp.*
  - **Astrophorida**
    - indet
    - Ancorinidae
      - *Dragmastra normanni*
      - *Stelletta lactea*
    - Geodiidae
      - indet
      - *Geodia sp.*
      - *Geodia mesotriaena*
    - Pachastrellidae
      - *Stryphnus ponderosus*
    - Theneidae
      - *Thenea cf. abyssorum*
  - **Hadromerida**
    - Polymastiidae
      - *Polymastia sol*
      - *Weberella bursa*
    - Suberitidae
      - *Tentorium semisuberites*
      - *Pseudosuberites hyalinus*
- Ceractinomorpha
  - **Poecilosclerida**
    - indet
    - Microcionidae
      - *Clathria barleei*
    - Raspailidae
      - *Eurypon sp????*
    - Coelosphaeridae
      - *Lissodendoryx sp.*
    - Cladorhizidae
      - *Cladorhiza gelida ?* (Lundbeck 1905)
  - **Halichondrida**
    - Axinellidae
      - *Phakellia ventilabrum*
  - **Haplosclerida**
    - Chalinidae
      - *Haliclona sp.*
      - *Haliclona sp.*
      - *"Gellius porosus"* Fristedt 1887
      - *Haliclona urceolus*
  - **Verongida**
    - Aplysinsidae
      - *Aplysilla sulphurea*

8. DEEP SEA RESEARCH IN FRAM STRAIT (AWI-HAUSGARTEN)

8.1 Interdisciplinary research at a deep-sea long-term station
(Soltwedel, Quéric, Sauter, Schewe)

Due to its enormous dimensions and inaccessibility, the deep-sea realm remains the world's least known habitat. Till today, numerous deep ocean processes and their relevance to global climate and ecosystem issues are still not sufficiently understood. Single sampling campaigns or measurements only generate snap shots, not allowing extrapolation on temporal variability. Long-term investigations at selected sites will provide the information necessary to describe natural variations and changes due to anthropogenic impacts. The opportunity to measure processes on sufficiently long time scales will finally help to differentiate spatial and temporal variability from long-term trends.

AWI's long-term station "Hausgarten" in the eastern Fram Strait off Spitsbergen (Fig. 8.1) represents the first long-term station in polar deep-sea regions. It was established during Polarstern expedition ARK XV/1 in summer 1999. Beside a central experimental area of 3 x 3 km^2 at about 2500 m water depth, we defined 9 sampling sites along a depth transect between 1000-5500 m, which will be revisited yearly to analyse seasonal and interannual variations in various biological, geochemical and sedimentological parameters.

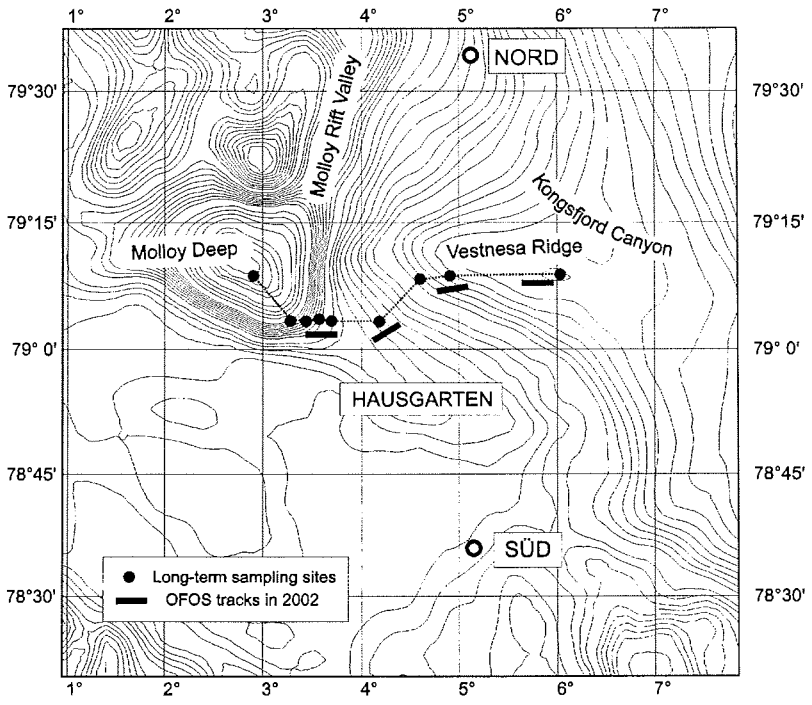

Fig. 8.1: Deep-sea long-term station AWI-"Hausgarten" in eastern Fram Strait.

Fluxes of particulate organic matter to the seafloor were characterised and quantified using moorings carrying sediment traps. The exchange of solutes between the sediments and the overlaying waters as well as the bottom currents were studied with various instruments (profiling units, incubation chambers, water sampler) to investigate major processes at the sediment-water-interface. Sediment samples were analysed for various biogenic compounds to estimate the flux of organic matter to the seafloor (pigment concentrations as an indicator for the input of phytodetritus), benthic activities (e.g. bacterial exo-enzymatic activity) and the total biomass of the smallest sediment-inhabiting organisms, to describe the eco-status of the benthic system. The quantification of benthic organisms from bacteria to megafauna is a major goal in the biological investigations.

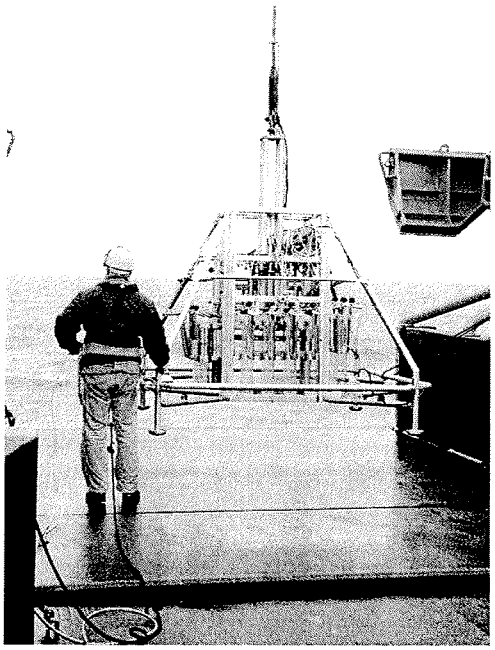

Fig. 8.2: New-designed multiple corer for 4x4 sediment cores.

This year's sampling and observation programme at AWI-"Hausgarten" was a big success. A new designed, video-controlled multiple corer (Sequential Multiple Corer, S-MUC; Fig. 8.2) was used to obtain virtually undisturbed sediments from all sampling sites along the "Hausgarten" transect to study depth-related gradients in benthic activity and biomass, thereby extending a time series which was started in summer 1999. Two additional sites ("Hausgarten"-Nord, "Hausgarten"-Süd; Fig. 8.1) were sampled to analyse latitudinal gradients in the area of investigations. The zone of investigations was extended from the sediment-water interface by the near-bottom water column (approx. 2 meters above ground). For this purpose a newly developed multi-horizon bottom water sampler (Fig. 8.3) was deployed at most stations of the "Hausgarten" transect in order to get more information about interfacial fluxes and the geochemical millieu within the bottom water.

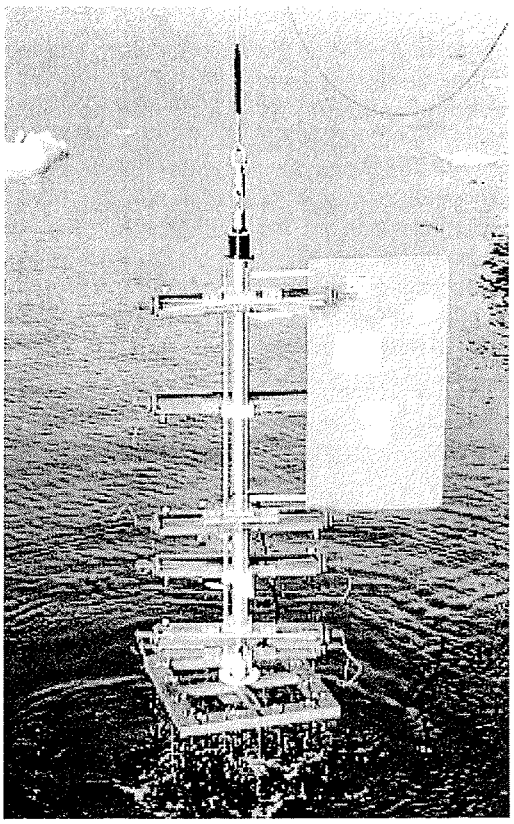

Fig. 8.3: Bottom water sampler able to sample 6 layers within the lowermost 2 m of the water column

A mooring with sediment traps and current meters at different depths above ground was successfully replaced. Two free-falling devices ("bottom-lander") carrying a micro-profiling unit and respiration chambers, respectively, were repeatedly deployed for *in situ* measurements of oxygen concentrations at the sediment-water interface (see below). One bottom-lander, equipped with a time-lapse still camera (12 h time interval) and a current-meter, was finally anchored at the central "Hausgarten" site at about 2500 m water depth. The lander will be recovered during the Polarstern expedition in summer 2003. Large-scale distribution patterns of epifauna organisms were assessed using imaging techniques: the so-called "OFOS" (Ocean Floor Observation System, Fig. 8.4) carrying a video and a still camera was towed at 1.5 m above ground at different depth intervals (1200-1300 m, 1400-1700 m, 2400-2600 m, 3000-4000 m) along the "Hausgarten" transect (Fig. 8.1), producing about 18 hours of video recordings and approx. 3200 colour slides. High-resolution Hydrosweep and Parasound recordings along the transect completed this year's work at AWI-"Hausgarten".

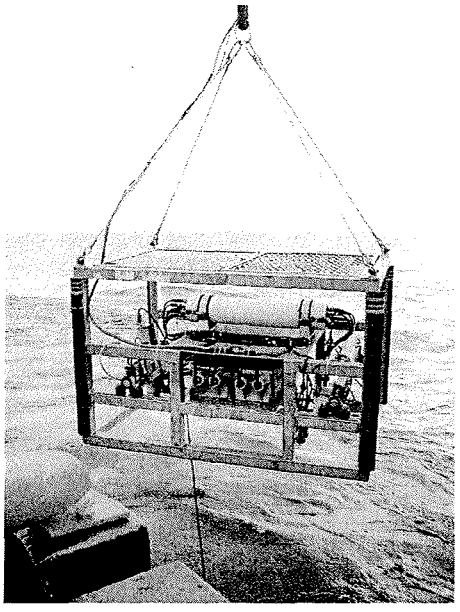

Fig. 8.4: Ocean Floor Observation System, OFOS

8.2 Carbon remineralisation by the benthic community

(Soltwedel, Sauter, Sablotny, Wegner)

The seafloor plays an important role in the regulation of the chemical composition of water masses in the oceans. The conventional approach to study geochemical and biological processes at the seafloor is to collect a sediment sample from the seabed, bring it up to the surface and there make observations and carry out experiments on it either on-board ship or in the laboratory. It is difficult, if not impossible, to obtain accurate data from the deep-sea, because artefacts are induced when the samples are subjected to large changes in hydrostatic pressure and temperature as they are brought up to the surface. Therefore, it's preferable to carry out experiments and measurements with the use of bottom landers directly at the sea floor (*in situ*).

To assess and quantify the role of the benthos in the recycling of carbon and to calculate the fluxes of solutes across the sediment water interface, we performed measurements of *in situ* oxygen consumption at the seabed. Sediment community oxygen consumption was measured using a free-falling grab respirometer. The lander consists of a flotation tripod and four integrated incubation chambers (Fig. 8.5). Each chamber encloses approx. 6000 cm^3 of sediment and about 6 l of water. A new-designed subsystem of the respirometer draws off (and stores) 8-times 60 ml of the overlying water for ship-board Winkler titrations, to measure the decrease of dissolved oxygen due to the respiration of sediment-inhabiting organisms within the chambers. The free-falling grab respirometer was deployed twice at the central "Hausgarten" station at approx. 2500 m water depth. Incubation times were 16 and 24 hours, respectively.

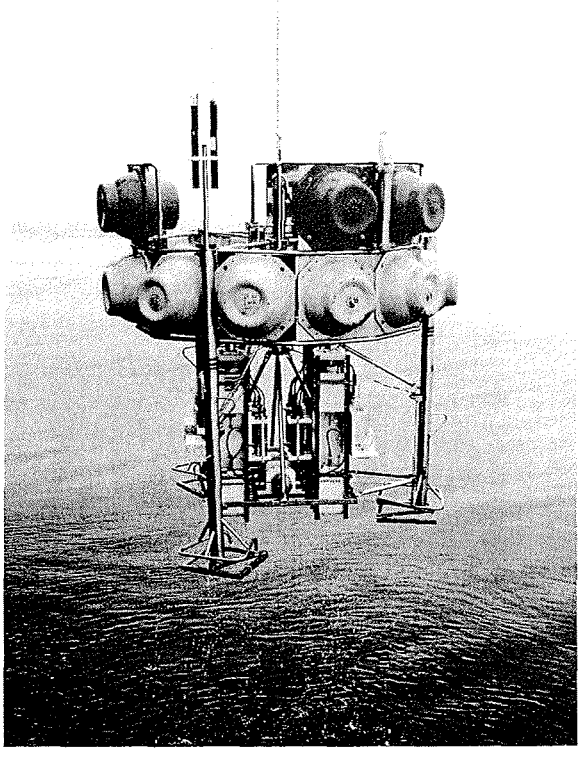

Fig. 8.5: Recovery of the free-falling grab respirometer

In order to obtain information about the sedimentary depth distribution of O_2-consumption rates, a second free-falling device was equipped with an *in situ* micro-profiler. Such device allows to measure pore water oxygen concentrations in very high vertical resolution (e.g. in steps of 0.1 mm). These high resolution profiles will be used for exact calculation of diffusive oxygen fluxes through the water-sediment interface, from which organic carbon fluxes to the seafloor can be derived. Since macro- and epifauna activity in general does not affect the shape of O_2-microprofiles but is included in respiration measurements, the specific respiration rates of these organisms can be quantified by comparing both method's results obtained at the same location. Fluxes quantified by microprofiles can be considered to be the basic O_2 turnover within an oxic sediment, mainly caused by microfauna. Besides oxgen microsensors the profiler was equiped with a special probe to to measure the electrical resistivity of sediment and bottom water. From this parameter the sediment porosity can be derived in high vertical resolution.

At water depths of 1500, 2500, and 3500 m the micro-profiler was carried down to the seafloor by the freefalling lander which was additionally equiped with a sequential deep-sea video camera and an acoustic doppler current-meter.
Due to a severe ice coverage at the Molloy Deep station (5500 m) the micro-profiler was mounted into a steel frame and lowered to the seafloor on the wire (Fig. 8.6).

During the two hours of micro-measurements the bridge officer managed to keep exact position, so that undisturbed measurements could be performed. The relatively small oxygen penetration depth revealed by the microprofiles obtained at this location, and, thus the high rates of oxic remineralisation confirm other sedimentary findings that the Molloy Deep functions as a huge sediment trap rather than a deep-sea dessert.

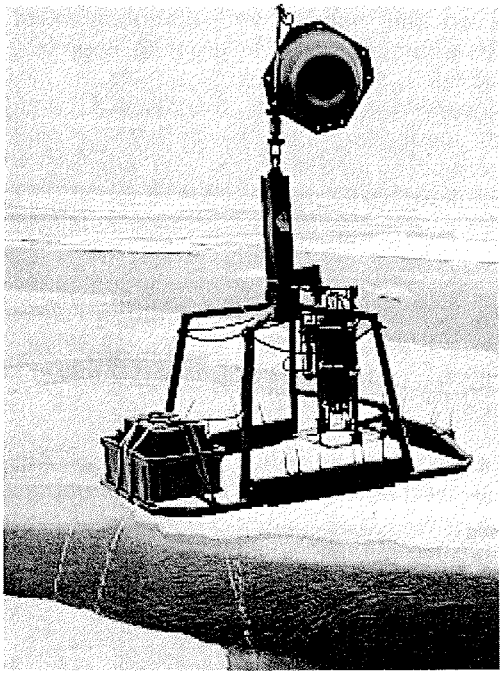

Fig. 8.6: Since the sea-ice cover prohibited the deployment of the freefalling landers in the Molloy Deep, the micro-profiler was deployed in a special wire-driven frame.

8.3 Investigations on the impact of alternating hydrostatic pressure on the dynamics of benthic bacterial communities in Arctic deep-sea sediments

(Quéric, Sablotny)

The importance and extent of the microbial influence on biogeochemical parameters at the sediment-water interface remains object of several investigations on the complexity of sedimentary habitats in the deep sea. With no pressure-constant sediment sampling system, samples are exposed to large changes in temperature and hydrostatic pressure according to depth during heaving to the surface. Incubation experiments of decompressed samples for bacterial activity estimations have to be conducted directly on board, at least in compliance with *in situ* temperature. There is still a lack in information about possible effects of variations in hydrostatic pressure on the status of deep-sea microbial communities from different depths. Thus comparative recompression experiments were carried out in newly

developed incubation chambers (Fig. 8.7), reflecting the possibility for a gradually building up and reducing of pressure according to *in situ* conditions of the sampling site. Sediment samples were taken by means of a new-designed, video-controlled multiple corer sampling system (Fig. 8.2). Regarding known small-scale bacterial population differences, the uppermost and the 5 centimetre of sediment core subsamples were prepared for incubation series evaluating decompression effects.

Aim of the study was to estimate a long-term, time-depending impact of alternating hydrostatic pressure on the activity and composition of complex bacterial communities from deep-sea sediments. In order to keep any specific adaptation properties on the same level, sediment samples from the AWI's long-term station "Hausgarten" (Fig. 8.1) were taken for the time-series (48 h and 72 h, 1 and 2 weeks, 2 and 4 months). After incubation, samples were partly conserved on –80°C for further molecular fingerprinting revealing re- and decompression effects on the population-specific activities, partly preconditioned for FISH analysis for following potential time-dependent community shifts on the level of individual cell counts.

Short-time incubation experiments (18 h) were conducted with sediment samples from different depths (2500 m, 3500 m, 5000 m) revealing any re- and decompression effects on the bacterial activity by measuring specific incorporation rates. Samples were rinsed and conserved on –24°C for further processing at the institute's laboratory.

These test series are expected to contribute to the rating of previous investigations on the activity of deep-sea bacteria being conducted under unadjusted pressure conditions and to represent a clue for the planning of long-term experiments on interspecific interactions among benthic deep-sea organisms.

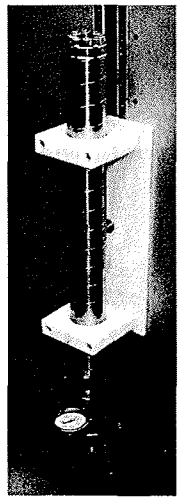

Fig. 8.7: Pressure incubation chamber for gradual pressure adjustment according to in situ conditions (max. 1000 bar).

9. MARINE MICROBIOLOGY

9.1 The role of protists in the food web of the Arctic Ocean. Investigations of the microbial communities of the water column and sea ice.

Dietrich (FU Berlin), Moorthi (AWI), Weitere (AWI)

During the expedition a broad study on the ecology of arctic protists was conducted. The special role of mixotrophic protists (unicellular eukaryotes with photoautotrophic and heterotrophic nutrition modes) and the complex trophic interactions within the microbial food web (bacteria, algae, flagellates and ciliates) were studied experimentally in the water column and sea ice. For an insight into the trophic interactions between the microbial food web and the metazooplankton (e.g. copepods) further experiments were undertaken. In addition the abundances of picoplankton (bacteria, up to 2µm) and nanoplankton (up to 20µm) were followed along depth gradients. All studies were based on the privotal ecological role of free-living protists in the aquatic carbon cycle. The studies are embedded in work previously undertaken in the same geographical regions (ARK XVII) or related work on mixotrophy and its control mechanisms in different habitats. The deep sea gradients are related in part to insights from the oceanographers on this expedition.

9.1.1 Deep sea gradients

The distribution of organisms in the water column is dependent on physical water properties (e.g. pressure, temperature, salinity, light),on the availability of resources (i.e. organic and inorganic nutrients) and on other biotic interactions (e.g. competition, predation). The history and origin of a water mass plays an important role hereby. In the first 200m of the clear, nutrient poor polar seas light and nutrients are availably for part of the year and form the basis for the abundances of planktonic organisms (algae, bacteria, flagellates, ciliates, copepods). The lightless deeper realms of the ocean are generally habitated with much fewer organisms because the microbial communities are dependent to a great extent on the primary production, biomass and exsudation of organic carbon by phytoplankton. Therefore abundances of bacteria and heterotrophic flagellates are much higher in the surface waters.
In the course of the expedition we crossed the path of a so called deep sea eddy, which forms a small (10km in diameter) discrete water body (see contribution by Gereon Budéus). In contrast to the normal deep sea salinity, temperature and density gradients monitored in the Greenland Sea, the deep sea eddy was characterized by having a much deeper homogeneous layer and a very deep temperature maximum at approximately 3000m. Sampling of the water column in the eddy as well as outside enabled us to analyse whether the physical properties of the eddy are mirrored in higher abundances of pico- and nanoplankton to a greater depth.
The bacterial abundance in surface water was generally in the order of 10^6 ml^{-1}. Within the layer of high density of the first 200m the abundances decreased to approximately $0.5*10^5$ ml^{-1}. Bacterial abundances also decreased in the first 200m of the eddy, but not to such an extent. Abundances in the homogeneous layer from 500-2500m remained approximately two-fold higher. At the temperature maximum, numbers were comparable to those found at that depth outside the deep sea eddy.

9.1.2 Trophic Interactions

For the study of trophic interactions within the food web the dilution technique (Landry and Hasset) and the size-fractionation technique (Landry) were employed.
In all experiments samples were taken to determine abundance and biomass of bacteria, heterotrophic and photoautotrophic protists and, in the case of the size-fractionation experiments, zooplankton. All samples were fixed with the appropriate fixatives. Water samples were also filtered through glasfiber filters (GF/F) for a latter chlorophyll a and phaeophytin determination.

Dilution experiments
Under the assumptions that the growth rate of a prey is not density dependent and that the probability with which a prey organism is ingested by a predator is a direct function of predator meeting prey, a step wise reduction in the grazing pressure can be made with the help of dilution. For this <0,2µm filtered biotope water is added in different portions to a sample of whole water. To exclude larger metazooplankton which might be negatively influenced due to the small size of the respective incubation bottles, the whole water was pre-filtered through a 100µm mesh. This procedure was applied in all dilution experiments.
The experiments will yield data on abundances of bacteria, photoautotrophic and heterotrophic protists, community net and gross growth rates, community grazing rates, biomass estimates and secondary production. Some species-specific growth and grazing rates should be also be ascertainable in successful experiments.

Plankton
Five dilution experiments with five set-ups each were conducted. The portion of undiluted water was 1, 0.9, 0.7, 0.45 and 0.25, with 1 being the "whole water" treatment. The experiments were carried out with water from a depth of 10m in 2.24 l polycarbonate bottles incubated for 48 hours in large flow through deck-incubators with *in situ* water-temperature and light regime. To two bottles of each set-up inorganic nutrients and vitamins were added while two others were left untreated to determine possible effects due to resource limitation in the untreated bottles.
Preliminary data on bacterial growth rates showed no such nutrient effect in three experiments. The maximum assumable bacterial community doubling times seem lie in the order of a few days. Although the data needs further analysis, the results point toward a utilisation of all the bacterial production by higher trophic levels.

Sea Ice
Studies on the brine channel community have focussed especially on the taxonomy and the origin of the organisms found. All components of the microbial food web are abundant in this habitat, with numbers often exceeding those in the plankton. Results from the conducted experiments should help answer questions on the production of functional and taxonomic groups as well as on potential trophic interactions within the brine channel food web.
Three experiments were conducted, two in combination with the tracer experiments on mixotrophy and the direct quantification of bacterivory (see below). This combination should enable a very broad view on the possible trophic interactions in brine channels.
Due to the experience obtained in the first tracer experiment with sea ice, a method to washing-out the bacteria and protists with <0.2µm filtered sea water was employed

(see below). Pre-filtration, portions of unfiltered sea ice extract, incubation time and temperature were as described for the plankton.
Our preliminary results of the first two ice dilution experiments demonstrate no resource limitation for the heterotrophic bacteria. Doubling times of the sea ice bacterial community seem to lie in the order of a few days. As described for the plankton dilution experiments, all of the bacterial secondary production seems to be utilised by higher trophic levels.

a) Size-fractionation experiments Plankton
In size fractionation experiments, predator and prey are separated by means of a gauze with a defined mesh size under the assumption that the predator is larger than the prey. We employed this method to study the trophic interaction between the microbial community and the larger zooplankton organisms. Untreated water (normal metazooplankton abundance), water without large metazooplankton (<100µm) and water with threefold metazooplankton abundance was incubated in 25,25 l polycarbonate bottles in flow-through deck incubators under quasi *in situ* temperature and light regime. Three parallels per treatment were incubated for 48 hours parallel to the dilution experiments. The successful experiments should give information on possible direct and indirect top-down control of components of the microbial food web by metazooplankton.
In the first size-fractionation experiment the sampled water body contained numerous large colonies of the haptophyte *Phaeocystis* spp., which in its unicellular form belongs to the nanoplankton First results also showed that zooplankton abundances were low and the trophic interactions seem to have been limited to within microbial food web processes.
The bacterial growth rates showed no significant differences in the three set-ups in the first experiment. Bacteria seemed unaffected by the presence or absence of metazooplankton. Mean growth rates corresponded to the bacterial net growth rate obtained in the dilution experiments for the <100µm "whole water" set-up.

b) Mixotrophy
Another part of our study focussed on the role of mixotrophic flagellates in the water column, in sea ice and in meltwater ponds on sea floes. So called "tracer experiments" were conducted, where food tracers (fluorescently labelled bacteria, FLB) are added to the system to quantify their ingestion by predators. Bacterivory can be quantified and mixotrophs can be identified with an epifluorescence microscope by the simultaneous fluorescence of ingested food tracers and chlorophyll a autofluorescence.
The following experiments were performed during the first part of the cruise:

Date	**Ecological System**	**Station / Coordinates**
4.07.02	Plankton	PS 62/012 64°37,42'N, 31°41,67'W
6.07.02	Sea Ice	PS 62/018-2 67°57,75'N, 24°13,75'W
13.07.02	Plankton	PS 62/032-3 74°49,91'N, 2°27,22'W

19.07.02	Sea Ice	PS 62/061 – 1 74°33,92'N, 11°24,04'W
20.07.02	Meltwater Pond	Without station number 75°07,37'N, 16°31,69'W
21.07.02	Sea Ice	PS 63/075 – 2 75°0,79'N, 10°16,00'W

All experiments were conducted in 2,7 l-bottles, which were incubated after FLB addition on deck for approximately 20 hours in a seawater flow system to assure natural light and temperature conditions. Before FLB addition and after incubation subsamples were taken and fixed with Glutardialdehyde, which were then filtered on a polycarbonate membrane to count the organisms on the filters. Furthermore subsamples were taken for phytoplankton, ciliates, zooplankton, chlorophyll a and nutrients to characterize the community in general.
Apart from assessing general patterns within the different microbial food webs like species composition, grazing pressure etc., we wanted to investigate the quantitative and qualitative role of mixotrophs and their ability to switch between photosynthesis and phagotrophy depending on environmental conditions such as light. Hence, all experiments were conducted with light and dark incubations, each treatment replicated four times.
In plankton experiments microbial communities out of 10m depth and out of 200m depth were compared. It was assumed that communities in 10m depth are adapted to good light conditions in contrast to communities in 200m, where light could be a limiting factor for photosynthesis. We wanted to investigate which trophic mode mixotrophs use in each environment and possible switches between phagotrophy and photosynthesis in light and dark incubations.

Sea ice is a very heterogeneous environment with many gradients within the brine channels of an icefloe. Mixotrophic nutrition could be an important feature for many species to survive there. In the three sea ice experiments we crushed a big ice floe (10-30m width) and caught freshly broken pieces of this ice floe where organisms were not washed out yet. To assure an even distribution of added FLB, a liquid phase was necessary for the experiments. Due to higher salinities within the brine channels it was not possible to just thaw the ice because of a possible osmotic shock of many species caused by decreasing salinity. In the first ice experiment two different methods were used and compared to get a liquid phase out of the ice without damaging the organisms. In both cases the ice was crushed to small pieces. On the one hand the organisms were "washed" out of the ice crush with sterile filtered seawater; on the other hand the ice crush was put into dialyzing tubes and melted in a seawater flow system to attain a salinity adaptation. Since the washing method was very efficient (85% of the bacteria could be washed out) and the dialyzing method very time consuming, especially with regard to community changes within the 18 hours the ice needed to thaw, the washing method was used in following two experiments. FLB were added to the liquid phase followed by on-deck incubation for 20 hours.
One tracer experiment was conducted with water out of a meltwater pond on a seafloe. Meltwater holes within the ponds, where sediments and organisms

accumulate, were pumped out. This water was pooled with plankton out of the pond and again incubated with FLB for 20 hours.
Since it was not possible to count the flagellates on the filters during the cruise, no results can be presented at this point yet. But test filters indicated that the expeirments worked and that a broad microbial community was present in all systems as an adequate basis for our investigations.

9.2 Structure and abundance of oligotrophic bacteria

(Tan, Spahic)

Structure and abundance of oligotrophic bacteria were studied by using seawater samples, taken with a CTD-Rosette from 25, 100, 200, and 400 m depths. Eight stations along 74°-75°N, five stations along 78°-79°N, and two other stations at 72°N (HMMV) were visited (see Table 9.1).

Table 9.1: Microbiological stations

Station No.	Date	Latitude	Longitude	Amounts of seawater (filtered with tangential flow)	from depth
PS62-025-1	09.07.2002	73°35.59`N	9°2.01`W	100 litre	25m
PS62-032-3	13.07.2002	74°49.92`N	2°37.26`W	100 litre	25m
PS62-042-2	15.07.2002	74°38.34`N	5°2.82`W	100 litre	25m
PS62-047-1	17.07.2002	74°49.28`N	8°7.96`W	100 litre	25m
PS62-059-1	19.07.2002	74°23.95`N	10°25.51`W	100 litre	25m
PS62-075-1	21.07.2002	74°59.71`N	10°37.44`W	100 litre	25m
PS62-090	23.07.2002	75°0.526`N	0°56.393`W	100 litre	25m
PS62-107	25.07.2002	75°04.92`N	0°46.96`W	100 litre	25m
PS62-152	01.08.2002	78°50.109`N	7°55.444`E	160 litre	25m
PS62-166	04.08.2002	78°50.10`N	5°2.70`E	160 litre	25m
PS62-174	06.08.2002	78°49.99`N	4°2.76`E	160 litre	25m
PS62-186	09.08.2002	78°50.6`N	2°33.81`E	200 litre	25m
PS62-204	12.08.2002	78°50.034`N	0°6.11`E	200 litre	25m
PS62-263	20.08.2002	71°59.876`N	14°43.632`E	200 litre	1100m
PS62/281-1	22.08.2002	71° 58.47' N	14° 48.91' E	200 litre	25m

After getting the seawater on board, subsamples were taken in glass (500 and 1000 ml) bottles, and immediately processed in a cold laboratory at 10°C. The glass bottles were placed on a cold tray at 2°C. Twelf portions of 50 ml were filtered on nylon (10 µm pore seize) and white polycarbonate (0.2 µm pore size; 25 mm diameter) filters, and the cells treated with 4% paraformaldehyde and saline phosphate buffer. Later on, these filters with the bacteria cells, frozen at -30°C, will be used for quantitative determinations of the phylogenetic compositions of the bacterial community by means of phylogenetic-specific oligonucleotide probes and fluorescence in situ hybridizations.

For acridine orange direct counts, two parallel samples (10 and 20 ml) were filtered on black polycarbonate filters (0.2 µm pore size; 13 mm diameter) and the filters on the slides covered with immersion oil and stored at -30°C. Estimations of bacteria numbers and biomasses will be done in the home laboratory.
For DOC determinations, 50 ml amounts were filtered through 0.45 µm glass fibre filter in a glass ampoule and the ampoule sealed and store at -30°C. DOC concentrations will be analyzed with a TOC-Analyzer for seawater samples.

Seawater bacteria from 25 and 200 m depths (1000 ml) were separated by using nylon (10 µm pore seize) and polycarbonate (0.2 µm pore size; 47 mm diameter) filters, and the cells resuspended in 50 ml of sterile seawater. The cell suspension was sucked in a 50 ml-syringe and injected through the sampling hole into the dialysis chamber. After locking the two sampling holes with screw-on caps, the chamber was subsequently put on a magnetic stirrer holder (9-fold) in a seawater aquarium at 4°C. Further processing of the enrichment cultures (27 chambers) to isolate cold-adapted, oligotrophic bacteria will be done in the home laboratory.

The enrichment cultures in nutrient broths with carbon and nitrogen compounds (N-acetyl-glucoseamine, formamide, methylamine, methanol, dibromomethane) were inoculated each with 3 ml, and peptone-yeast extract-medium with 1 ml of seawater. The Erlenmeyer-flasks were incubated at 4°C, and further isolation procedures will be done later.

The amounts of 100, 160, or 200 litre of seawater were filled in 20 litre polypropylene bottles and stored at 4°C overnight, before further processing have been done on the next day.
The abundance of bacteria in arctic seawater is normally in the of 10^4 to 10^5 cells/ml range. It is necessary to separate and concentrate the bacteria to about 1000-fold to get enough DNA from the bacterial biomass. This can be achieved by applying tangential flow microfiltration (Filter holder Sartocon Slice, Sartorius) of 100 to 200 litre seawater, after separation of the phyto- and zooplankton organisms by pressure filtration, using a 10 µm-nylon prefilter. Three Hydrosart Slice Mini Cassettes, pore size 0.2 µm, each having an effective filtration area of 0.1 m^2, were used by peristaltic pumping the seawater with silicone tubing (inner diameter: 9 mm) at a flow rate of about 254 litre per hour (pressure: 1-2 bar). The 100 to 200 ml of concentrated bacterial cells in polypropylene flasks were kept frozen at - 30°C. DNA extraction, DNA multiplication by PCR, separation of cDNA by gelelectrophoresis, and sequencing of 16S rRNA will be done in the home laboratory.

For determinations of POC/PON concentrations, 3 litres of seawater from each depth were filtered on glass fibre filters (0.45 µm pore size). After filtration, the particulate organic matter were dried at 60°C for 3 d. Later on, the organic carbon and organic nitrogen analyses will be done with an Infrared-C/N-Analyzer.

10. GEOCHEMICAL AND BIOLOGICAL INVESTIGATIONS AT HÅKON MOSBY MUD VOLCANO

(Sauter, Baumann, Harms, Hohmann, Kolar, Quéric, Schewe, Soltwedel, Wegner, Wisotzki)

The fieldwork carried out at Håkon Mosby Mud Volcano (HMMV) during the R/V Polarstern cruise ARK XVIII/1b stands in the context of methane research. Methane acts as a very efficient greenhouse gas in the atmosphere. Thus, it is important to identify the earth's major methane sources and to understand their contribution to the methane cycle. HMMV is of great interest as a spot emitter for methane at the seafloor of the polar ocean. Mud volcanoes can be considered as a surface manifestation of diapirism deeper down in the earth's crust. Density inverted, fluidised sediments are squeezed upwards, often along fault structures, carrying high amounts of mud and gas up to the seafloor (Milkov, 2000). Upward migrating methane is able to form gas hydrates if allowed by temperature and pressure conditions. Those gas hydrates fix large amounts of methane that potentially could be used for future energy supply but also could be released due to hydrate degradation under elevating seawater temperatures. HMMV possibly was formed as a result of a submarine landslide at the Barents Sea slope.

Investigations tie on to the R/V L'Atalante cruise in 2001 (Klages et al., 2002) aiming to assess the amount of methane release from the sediment surface and to follow the fate of methane within the water column. For this purpose the methane inventory of the surface sediment as well as the methane content of the adjacent water column was determined at three key locations of HMMV (Fig. 10.1, see also Sauter et al., 2002a), at reference sites outside the volcano, and along a transect over the volcano, respectively.

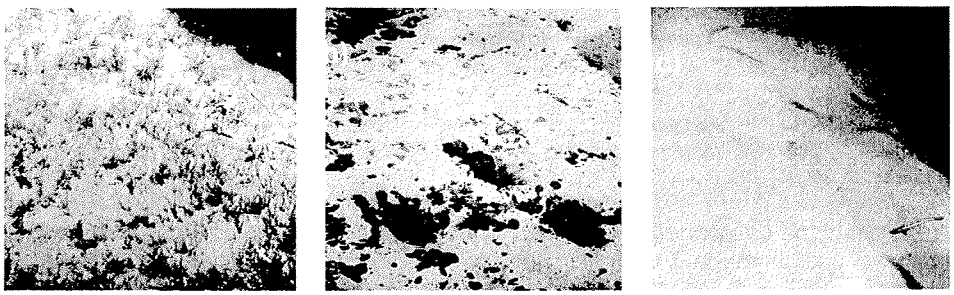

Fig. 10.1: The three key areas to be distinguished at HMMV:
(a) Pogonophora at the outer rim,
(b) bacterial mats,
(c) naked sediment an the mud volcano's center
(Photographs from Victor 6000 operations in 2001).

Before taking water samples along this south-north transect (Fig. 10.2 and Tab. 10.1), we moved the ship in slow speed across HMMV surveying the water column with a 38 kHz fishery echo-sounder. A surprisingly clear acoustic signal above the centre of the volcano indicated the appearance of a large methane plume. Strongest acoustic indication for methane discharge was found at 72° 00.29'N, 14° 43.77'E where the plume extended up to 800 meters above the seafloor. Water samples were taken by CTD throughout the whole water column and, in high resolution by means of a special bottom water sampler (Sauter et al., 2002b) at 6 locations along this transect. Water samples were poisoned for subsequent GC analysis to avoid oxidation of methane within the sample. Whereas CTD data do not show distinct temperature and salinity anomalies within the plume but there was found a distinct drop in the oxygen concentration below 500 m water depth.

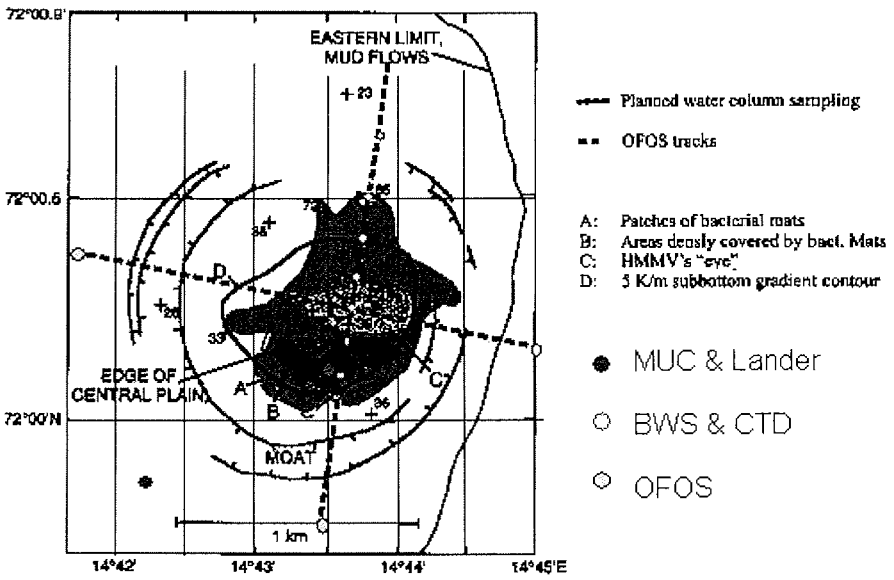

Fig. 10.2: Key locations of HMMV with OFOS and CTD/BWS transects. (Map modified from Pimenov et al., 1999)

Accompanying direct methane investigations, sediments and pore waters where also sampled for subsequent analysis of porosity, nutrients and sulphur-chemistry. This is hoped to provide insights into the geochemical milieu of methanogenesis, sulphate-reduction and other reaction processes dominating those habitats. Sediment sampling at the volcano's centre and within bacterial mat fields turned out to be very difficult due to the high gas content; sediments degassed during recovery of the multicorer thereby disrupting the sediment texture.

To circumvent those difficulties, geochemical profiles were intended to be determined *in situ*, i.e. at the seafloor. For this purpose a microprofiler equipped with microsensors for O_2, H_2S, pH, and electrical resistivity was deployed by means of a freefalling system (bottom-lander) staying about 8 hours on the seafloor performing

autonomous measurements. Three successful bottom-lander deployments could be performed at HMMV (only one was originally scheduled for this location). The obtained microprofiles show that sulphate reducing bacteria release a maximum of H_2S in about 5 cm of sediment depth at the bacterial mats field. Oxygen is already consumed below a few millimetres underneath the sediment-water interface. Whereas exact fluxes will be derived from the microgradients of the respect solutes, the small oxygen penetration depth indicates already qualitatively that a large oxygen respiration takes place right at the sediment surface.

The pattern is different at sediments populated with pogonophora where almost no H_2S could be detected by the microsensors meaning that the consortia of organisms taking up methane under release of H_2S are not present here. Accordingly, oxygen is able to penetrate the sediment deeper down without being respired close to the sediment surface.

To determine, how HMMV affects benthic life, we carried out an extensive sampling programme with a video-guided multiple corer (MUC) and photo/video observations with the "Ocean Floor Observation System" (OFOS). The MUC was used to sample sediments (and associated benthic organisms) within the key areas of the volcano and also at reference sites to the North-west, to the South-west and to the East of the volcano. This approach will provide informations about the ecological relevance of the mud volcano for its surrounding areas.

The quantitative assessment of sediment-bound bacteria and meiofauna organisms, and the analysis of a series of biogenic sediment compounds indicating the activity and biomass of sediment-inhabiting organisms will allow to obtain substantial information on the ecological status of the benthic system in the different parts of the HMMV region. Sediment-bound chloroplastic pigments equivalents, CPE (i.e. chlorophyll *a* plus degradation products) were determined to quantify (vertical and/or lateral) organic matter input from primary production. Differences in activities and biomass within the sediment samples were assessed by a series of biochemical assays commonly used in ecological investigations of the deep sea (e.g. Soltwedel et al., 2000; Schewe, 2001). To evaluate bacterial exoenzymatic activities, esterase turnover rates were determined with the fluorogenic substrates fluorescein-di-acetate (FDA). Phospholipids were analysed specifically as indicators for 'living biomass', i.e. small sediment-inhabiting organisms; more stable compounds like particulate proteins were determined to estimate the bulk of 'living' plus 'dead biomass', i.e. organisms and the proportion of detrital organic matter in the sediments.

Molecular fingerprinting of the natural bacterial community will be performed with DNA as well as with RNA allowing the assessment of spatial shifts in bacterial populations amended by the according population-specific activity: while DNA-derived PCR-amplified 16S rRNA gene fragments are related to the presence of different bacterial populations, analyses of rRNA-derived PCR products can provide an indication of which bacterial populations contribute to the RNA pool. As the cellular concentration of ribosomal RNA is related to the recent activity of cells, this method may help in surveying changes in the activity of bacterial populations established in relation to the spatial characteristics of the HMMV area.

Photo/video observations were carried out to assess large-scale distribution patterns of geological and biogenic structures as well as bacterial mats and larger epibenthic

organisms in the HMMV area. Three transects crossing the HMMV, two in east-westerly direction and one from the North to the South, revealed a total of approx. 1200 colour slides. In contrast to observations made by the ROV "Victor 6000" in 2001 (Schlüter et al., 2002) and by Russian scientists (e.g. Pimenov et al., 1999), we did not succeed to observe a centre of naked sediment. Similarly, the lander intended to be placed in the centre at its second deployment sat in fact within fields of pogonophora.

Although sedimentary changes at the surface of a mud volcano are assessed to be possible also within short time scales, we hesitate to interpret this lack of visual evidence to be a significant change in surface properties or sedimentary habitats (population of originally uncovered sediments by organisms) at HMMV. Since the centre structure of HMMV extends in the order of a few hundred meters it is more likely that the centre was missed: Towing OFOS with 0.5 kn over ground against a current of about 1 kn and wind of different direction with a 118 m long ship (i.e. the location of the GPS receiver distances considerably from the ship's stern) might have caused that OFOS was towed off target. Anyhow, it can be hoped to clarify this issue during the next Polarstern cruise ARK XIX/3 with "Victor 6000" in 2003.

Fortunately the cruise schedule was not hampered by weather conditions or technical problems. Therefore the originally planned 2 days of at HMMV could be extended by one extra day. Consequently, we extended the target area by a multitude of smaller mud diapirs south of HMMV. Against the background of the methane discharge of HMMV it was planned to investigate whether the satellite diapirs also emit methane. Beside an additional OFOS survey over the southern satellites, the whole area was surveyed for by the Hydrosweep bathymetry system of R/V Polarstern. The preliminary bathymetric map (Fig. 10.3) shows topographically protruding satellite mounds whereas HMMV itself is hardly identifiable by its topography.

The OFOS survey over the satellite mounds revealed that sediments are not covered by bacterial mats nor are populated with pogonophora. Instead, many larger stones, possibly glacial remnants, were observed throughout large parts of the surveyed transect. Although, above some of the mounds plumes patterns were observed acoustically by the 38 kHz fishery echo-sounder running in parallel to the OFOS deployment. To determine whether these patterns are the acoustic manifestation of methane plumes seawater and sediment samples were taken by TV-guided multicorer, bottom water sampler and CTD-rosette at one of these satellite diapirs. Subsequent analysis of methane and other geochemical parameters will be performed back home.

If the southern satellite mounds of HMMV confirm to emit methane as well, the whole area gains more importance in respect to its contribution to the global methane cycle. Further investigations are needed to clarify the extension of methane discharge and to understand possible linkage of HMMV and satellites.

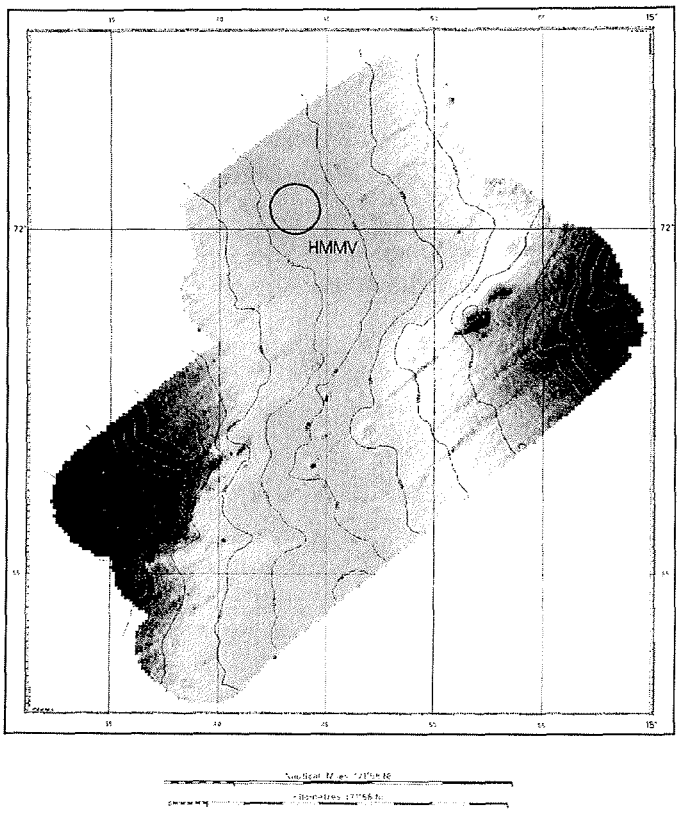

Fig. 10.3: Preliminary bathymetric map of the HMMV and southern satellite diapirs.

References:

Klages, M., Mesnil, B., Soltwedel, T, Christophe, A. (2002) The expedition "AWI" of RV "L'Atalante" in 2001. Reports on Polar and Marine Research. 422, 65 pp.

Milkov, A.V. (2000) Worldwide distribution of submarine mud volcanoes and associated gas hydrates. Marine Geology 167, 29–42.

Pimenov, N., Savvichev, A., Rusanov, I, Lein, A., Egorov, A., Gebruk, A., Moskalev, L., Vogt, P. (1999) Microbial processes of carbon cycle as the base of food chain of Håkon Mosby Mud Volcano benthic community. Geo-Marine Letters 19, 89-96.

Sauter, E., Schlüter, M., Boetius, A., Baumann, L. (2002a) Geochemistry of Håkon Mosby Mud Volcano (HMMV) bottom water and sediments. In: Klages, M. et al. (eds) The expedition "AWI" of RV "L'Atalante" in 2001. Reports on Polar and Marine Research. 422, 47-53.

Sauter, E., Schlüter, M., Baumann, L. (2002b) Geochemistry of deep-sea sediments and the bottom water. In: Klages, M. et al. (eds) The expedition "AWI" of RV "L'Atalante" in 2001. Reports on Polar and Marine Research. 422, 29-34.

Schewe, I. (2001). Small-sized benthic organisms of the Alpha Ridge, central Arctic Ocean. Internat. Rev. Hydrobiol., 8 (3): 315-333.

Soltwedel, T., Mokievsky, V., Schewe, I. (2000). Benthic activity and biomass on the Yermak Plateau and in adjacent deep-sea regions northwest of Svålbard. Deep-Sea Res. I., 47 (9): 1761-1785.

Schlüter, M., Boetius, A., Klages, M., Sauter, E., Soltwedel, T. (2002) Video observation of the Håkon Mosby Mud Volcano terrain. In: Klages, M. et al. (eds) The expedition "AWI" of RV "L'Atalante" in 2001. Reports on Polar and Marine Research. 422, 34-36.

Tab.10.1: Station list HMMV.

Station	Date	Time	Latitude	Longitude	Depth [m]	Gear	Action
PS62/263-1	20.08.02	03:55	72° 00.04' N	14° 43.50' E	1291	S-MUC	on the bottom
PS62/263-2	20.08.02	05:17	71° 59.81' N	14° 43.68' E	1293	CTD/RO	on depth
PS62/263-3	20.08.02	06:57	72° 00.12' N	14° 43.52' E	1291	BL_P	deployment
PS62/263-4	20.08.02	08:05	72° 00.50' N	14° 43.82' E	1273	FLS	start
PS62/263-4	20.08.02	09:28	72° 00.15' N	14° 43.54' E	1271	FLS	end
PS62/264-1	20.08.02	10:12	72° 00.14' N	14° 43.61' E	1289	BWS	on the bottom
PS62/264-2	20.08.02	11:25	72° 00.11' N	14° 43.57' E	1290	CTD/RO	on depth
PS62/265-1	20.08.02	12:31	72° 00.20' N	14° 43.68' E	1290	BWS	on the bottom
PS62/265-2	20.08.02	13:41	72° 00.18' N	14° 43.64' E	1289	CTD/RO	on depth
PS62/266-1	20.08.02	15:00	72° 00.30' N	14° 43.76' E	1288	BWS	on the bottom
PS62/266-2	20.08.02	16:06	72° 00.28' N	14° 43.82' E	1290	CTD/RO	on depth
PS62/267-1	20.08.02	17:27	72° 00.40' N	14° 43.78' E	1287	BWS	on the bottom
PS62/267-2	20.08.02	18:35	72° 00.41' N	14° 43.82' E	1292	CTD/RO	on depth
PS62/263-3	20.08.02	19:25	72° 00.22' N	14° 43.67' E	277	BL_P	recovery
PS62/268-1	20.08.02	20:50	72° 00.37' N	14° 43.84' E	1288	CTD/RO	on depth
PS62/268-2	20.08.02	21:52	72° 00.34' N	14° 43.56' E	1288	BWS	on the bottom
PS62/269-1	20.08.02	23:00	72° 00.47' N	14° 43.86' E	1287	BWS	on the bottom
PS62/269-2	21.08.02	00:02	72° 00.53' N	14° 43.89' E	1294	CTD/RO	on depth
PS62/270-1	21.08.02	01:11	72° 00.26' N	14° 43.85' E	1289	S-MUC	on the bottom
PS62/271-1	21.08.02	04:17	71° 59.85' N	14° 43.56' E	1295	OFOS	start
PS62/271-1	21.08.02	04:49	71° 59.59' N	14° 43.12' E	1302	OFOS	end
PS62/272-1	21.08.02	06:08	72° 00.35' N	14° 43.77' E	1288	BL_P	deployment
PS62/272-2	21.08.02	07:17	72° 00.29' N	14° 43.77' E	1288	S-MUC	on the bottom
PS62/273-1	21.08.02	10:56	72° 00.22' N	14° 45.35' E	1282	OFOS	start
PS62/273-1	21.08.02	11:22	72° 00.44' N	14° 45.80' E	1272	OFOS	end
PS62/274-1	21.08.02	12:10	72° 00.10' N	14° 45.89' E	1278	S-MUC	on the bottom
PS62/275-1	21.08.02	13:54	71° 59.86' N	14° 42.12' E	1306	S-MUC	on the bottom
PS62/275-2	21.08.02	15:19	71° 59.89' N	14° 42.58' E	1305	BWS	on the bottom
PS62/276-1	21.08.02	16:53	72° 00.25' N	14° 43.53' E	1287	BWS	on the bottom
PS62/272-1	21.08.02	17:41	72° 00.44' N	14° 43.67' E	1286	BL_P	recovery
PS62/277-1	21.08.02	18:54	72° 00.01' N	14° 38.90' E	1338	Hydrosweep	start bathymetry
PS62/277-1	22.08.02	02:53	71° 58.42' N	14° 57.23' E	1152	Hydrosweep	end bathymetry
PS62/278-1	22.08.02	03:41	72° 00.21' N	14° 43.64' E	1290	BL_P	deployment
PS62/279-1	22.08.02	04:01	71° 59.85' N	14° 43.62' E	1294	CTD/RO	on depth
PS62/280-1	22.08.02	04:53	72° 00.78' N	14° 42.96' E	1295	S-MUC	on the bottom
PS62/281-1	22.08.02	06:49	71° 58.64' N	14° 48.89' E	1215	CTD/RO	on depth
PS62/281-2	22.08.02	07:54	71° 58.58' N	14° 48.52' E	1214	BWS	on the bottom
PS62/281-3	22.08.02	09:12	71° 58.61' N	14° 48.75' E	1206	S-MUC	on the bottom
PS62/282-1	22.08.02	11:50	71° 55.92' N	14° 39.73' E	1335	OFOS	start
PS62/282-1	22.08.02	12:20	71° 56.39' N	14° 40.37' E	1331	OFOS	end
PS62/282-2	22.08.02	15:40	71° 55.90' N	14° 39.21' E	1342	OFOS	start
PS62/282-2	22.08.02	16:02	71° 55.98' N	14° 38.64' E	1350	OFOS	end
PS62/278-1	22.08.02	16:43	72° 00.28' N	14° 43.93' E	1288	BL_P	recovery
PS62/283-1	22.08.02	17:55	72° 00.19' N	14° 43.17' E	1288	CTD/RO	on the bottom
PS62/283-2	22.08.02	19:09	72° 00.10' N	14° 43.12' E	1289	BWS	failure
PS62/283-3	22.08.02	20:22	72° 00.09' N	14° 43.02' E	1291	BWS	repetition
PS62/283-4	22.08.02	21:30	72° 00.03' N	14° 43.20' E	1290	S-MUC	on the bottom
PS62/284-1	23.08.02	01:17	71° 59.83' N	14° 45.91' E	1283	OFOS	start
PS62/284-1	23.08.02	01:53	71° 60.00' N	14° 44.86' E	1289	OFOS	end

APPENDIX

Stationsliste ARK 18 1-a/b

Station	Date	Time	PositionLat	PositionLon	Depth [m]	Windstrength [m/s]	Course [°]	Speed [kn]	Gear	Gear Abbreviation	Action	Comment
PS62/001-1	01.07.02	05:43	61° 30.06' N	38° 30.07' W	2503.0	N 4	288.7	8.1	HydroSweep/ParaSound profile	HS_PS	start track	Parasoundprofil, HS und DWS laufen mit
PS62/001-1	01.07.02	11:21	61° 57.75' N	39° 51.12' W	1348.0	ENE 2	308.0	8.3	HydroSweep/ParaSound profile	HS_PS	profile end	
PS62/002-1	01.07.02	13:46	61° 47.66' N	39° 22.43' W	1929.0	NE 3	208.2	0.5	MultiCorer	MUC	at sea bottom	1926 m ausgesteckt
PS62/002-2	01.07.02	15:44	61° 47.74' N	39° 22.35' W	1929.0	ENE 2	346.8	0.4	Piston corer	PC	at sea bottom	1929 m ausgesteckt
PS62/002-3	01.07.02	17:41	61° 47.68' N	39° 22.43' W	1928.0	NNE 6	227.7	0.3	Large Box Corer	GKG	at sea bottom	GE 52.2 1913 m Draht
PS62/003-1	01.07.02	20:24	61° 42.01' N	39° 4.03' W	2194.0	NNE 6	87.3	0.5	Large Box Corer	GKG	at sea bottom	
PS62/003-2	01.07.02	22:36	61° 42.00' N	39° 4.05' W	2192.0	NNE 7	44.3	0.3	Piston corer	PC	at sea bottom	
PS62/003-3	02.07.02	00:58	61° 42.06' N	39° 4.06' W	2192.0	NNE 8	144.2	0.1	Large Box Corer	GKG	at sea bottom	2173 m ausgesteckt
PS62/004-1	02.07.02	05:43	61° 31.77' N	38° 7.85' W	2560.6	NE 5	9.4	0.1	CTD/rosette water sampler	CTD/RO	at depth	EL 31 Draht 2537m
PS62/004-2	02.07.02	07:42	61° 31.55' N	38° 7.39' W	2563.9	NNE 6	350.5	0.2	MultiCorer	MUC	at sea bottom	GE 52. 2 Draht 2541m
PS62/004-3	02.07.02	10:03	61° 31.56' N	38° 7.38' W	2567.0	NE 8	54.6	0.0	Piston corer	PC	at sea bottom	winde52.2 2522m ausgesteckt
PS62/005-1	02.07.02	15:05	62° 13.42' N	37° 17.35' W	2487.0	ENE 5	340.3	12.3	HydroSweep/ParaSound profile	HS_PS	start track	
PS62/006-1	02.07.02	16:52	62° 15.05' N	37° 18.41' W	2469.0	E 3	53.2	0.3	Piston corer	PC	at sea bottom	GE 52.2 2423 m Draht
PS62/006-2	02.07.02	18:42	62° 15.08' N	37° 18.34' W	2472.0	E 3	175.9	0.4	MultiCorer	MUC	at sea bottom	GE 52.2 2449 m
PS62/005-1	02.07.02	19:30	62° 15.31' N	37° 18.47' W	2465.0	E 4	261.5	0.3	HydroSweep/ParaSound profile	HS_PS	continue the profile	
PS62/005-1	02.07.02	23:38	62° 47.27' N	37° 43.74' W	2164.0	ENE 4	121.6	6.6	HydroSweep/ParaSound profile	HS_PS	profile end	
PS62/007-1	03.07.02	00:53	62° 42.91' N	37° 40.28' W	2162.0	E 4	186.6	0.3	Large Box Corer	GKG	at sea bottom	2145 m ausgesteckt
PS62/007-2	03.07.02	02:49	62° 42.82' N	37° 40.30' W	2161.0	E 4	234.7	0.1	Piston corer	PC	at sea bottom	2121 m ausgesteckt
PS62/008-1	03.07.02	08:10	63° 30.01' N	36° 49.05' W	1934.0	SE 4	30.0	9.7	HydroSweep/ParaSound profile	HS_PS	start track	
PS62/009-1	03.07.02	10:06	63° 42.35' N	36° 27.52' W	1777.0	S 2	51.7	12.2	HydroSweep/ParaSound profile	HS_PS	start track	
PS62/008-1	03.07.02	11:42	63° 54.97' N	35° 53.51' W	1907.0	WSW 1	51.1	12.6	HydroSweep/ParaSound profile	HS_PS	profile end	
PS62/009-1	03.07.02	20:46	65° 1.13' N	32° 46.86' W	1728.3	WSW 7	224.8	8.2	HydroSweep/ParaSound profile	HS_PS	profile end	
PS62/010-1	03.07.02	21:50	64° 59.76' N	32° 54.49' W	1697.0	SW 6	106.1	0.1	Large Box Corer	GKG	at sea bottom	1705 m ausgesteckt
PS62/010-2	03.07.02	23:16	64° 59.68' N	32° 54.35' W	1701.0	WSW 5	209.4	0.6	Large Box Corer	GKG	at sea bottom	1701 m ausgesteckt
PS62/011-1	04.07.02	00:25	64° 57.81' N	32° 59.74' W	1714.0	W 4	133.9	6.6	HydroSweep/ParaSound profile	HS_PS	start track	
PS62/011-1	04.07.02	06:03	64° 32.10' N	31° 21.22' W	2495.0	WSW 3	122.5	9.1	HydroSweep/ParaSound profile	HS_PS	profile end	
PS62/012-1	04.07.02	08:14	64° 37.39' N	31° 41.64' W	2430.0	SSE 2	84.6	0.7	CTD/rosette water sampler	CTD/RO	at depth	2408 m ausgesteckt
PS62/012-2	04.07.02	09:56	64° 37.46' N	31° 41.60' W	2431.0	SW 1	39.2	0.3	Large Box Corer	GKG	at sea bottom	
PS62/012-3	04.07.02	12:19	64° 37.45' N	31° 41.68' W	2432.0	SSE 3	58.7	0.2	Piston corer	PC	at sea bottom	2395 m ausgesteckt
PS62/012-4	04.07.02	13:44	64° 37.88' N	31° 40.12' W	2428.0	SSE 5	15.3	0.3	CTD/rosette water sampler	CTD/RO	at depth	197 m ausgesteckt
PS62/013-1	04.07.02	15:51	64° 37.09' N	30° 45.95' W	2403.0	S 6	29.2	12.3	HydroSweep/ParaSound profile	HS_PS	start track	
PS62/013-1	04.07.02	21:44	65° 25.23' N	29° 48.03' W	971.5	SSE 5	26.8	8.9	HydroSweep/ParaSound profile	HS_PS	profile end	
PS62/014-1	05.07.02	21:06	67° 55.99' N	25° 24.12' W	1039.0	ESE 3	77.8	7.1	HydroSweep/ParaSound profile	HS_PS	start track	
PS62/014-1	05.07.02	21:37	67° 57.57' N	25° 18.07' W	1100.0	ENE 3	239.1	4.4	HydroSweep/ParaSound profile	HS_PS	profile end	
PS62/015-1	05.07.02	23:02	67° 55.89' N	25° 25.41' W	1021.0	ESE 5	232.6	0.0	Large Box Corer	GKG	at sea bottom	
PS62/015-2	05.07.02	23:38	67° 55.89' N	25° 25.46' W	1018.0	ESE 3	37.9	0.3	Large Box Corer	GKG	at sea bottom	
PS62/015-3	06.07.02	00:44	67° 55.85' N	25° 25.59' W	1013.0	E 4	243.4	0.0	Piston corer	PC	at sea bottom	963 m ausgesteckt
PS62/015-4	06.07.02	01:49	67° 55.84' N	25° 25.74' W	1013.0	E 4	233.1	0.0	Large Box Corer	GKG	at sea bottom	985 m ausgesteckt
PS62/016-1	06.07.02	02:20	67° 55.64' N	25° 25.94' W	0.0	ENE 6	94.9	4.3	HydroSweep/ParaSound profile	HS_PS	start track	
PS62/016-1	06.07.02	05:15	67° 51.07' N	24° 35.59' W	1499.0	NE 7	108.4	5.3	HydroSweep/ParaSound profile	HS_PS	profile end	
PS62/017-1	06.07.02	06:13	67° 51.05' N	24° 34.92' W	1502.0	NE 6	41.2	0.0	Large Box Corer	GKG	at sea bottom	GE 52.2 1462 m
PS62/017-2	06.07.02	07:42	67° 51.05' N	24° 34.71' W	1503.0	NE 6	11.3	0.0	Piston corer	PC	at sea bottom	GE 52.2 1441 m
PS62/017-3	06.07.02	09:13	67° 51.31' N	24° 34.96' W	1501.0	NE 6	60.7	0.6	CTD	CTD	at depth	1456 m ausgesteckt
PS62/017-4	06.07.02	10:32	67° 51.02' N	24° 35.10' W	1502.0	NNE 7	213.7	0.2	Piston corer	PC	at sea bottom	
PS62/018-1	06.07.02	11:18	67° 50.49' N	24° 35.16' W	1502.0	NE 8	140.9	4.7	HydroSweep/ParaSound profile	HS_PS	start track	
PS62/018-2	06.07.02	13:22	67° 57.63' N	24° 13.81' W	1512.0	NNE 6	154.4	0.8	Eisfischen	EF		1.Hol

Station	Date	Time	PositionLat	PositionLon	Depth [m]	Windstrength [m/s]	Course [°]	Speed [kn]	Gear	Gear Abbreviation	Action	Comment
PS62/018-2	06.07.02	14:01	67° 57.24' N	24° 14.22' W	1513.0	NE 7	231.2	0.6	Eisfischen	EF		
PS62/018-1	07.07.02	04:07	68° 55.26' N	20° 53.27' W	1449.0	NNE 6	343.5	8.5	HydroSweep/ParaSound profile	HS_PS	start track	
PS62/018-1	07.07.02	05:34	69° 4.78' N	21° 11.41' W	634.5	NE 4	179.0	5.0	HydroSweep/ParaSound profile	HS_PS	alter course	107°
PS62/018-1	07.07.02	06:50	69° 1.89' N	20° 44.17' W	1186.0	NNE 6	95.2	8.2	HydroSweep/ParaSound profile	HS_PS	profile end	
PS62/019-1	07.07.02	09:19	69° 16.19' N	20° 56.57' W	411.1	NE 4	29.7	0.0	CTD	CTD	at depth	
PS62/020-1	08.07.02	06:44	70° 59.94' N	18° 54.90' W	1374.0	NNE 6	349.9	0.0	MultiCorer	MUC	at sea bottom	1342 m GE 52.2
PS62/021-1	08.07.02	13:44	71° 30.15' N	16° 50.23' W	1754.0	ESE 1	22.5	0.4	MultiCorer	MUC	at sea bottom	1714 m ausgesteckt
PS62/022-1	08.07.02	22:09	72° 29.45' N	12° 36.15' W	525.7	SSW 2	347.6	0.5	CTD	CTD	at depth	
PS62/022-2	08.07.02	22:37	72° 29.47' N	12° 36.20' W	527.0	SSW 2	222.1	0.7	Large Box Corer	GKG	at sea bottom	
PS62/022-3	08.07.02	23:13	72° 29.44' N	12° 36.38' W	527.2	SW 2	65.2	0.2	Large Box Corer	GKG	at sea bottom	
PS62/022-4	08.07.02	23:58	72° 28.60' N	12° 37.89' W	513.8	WSW 2	65.2	0.1	Large Box Corer	GKG	at sea bottom	
PS62/023-1	09.07.02	07:07	73° 27.82' N	9° 16.05' W	778.7	SSW 5	277.3	0.2	Large Box Corer	GKG	at sea bottom	780 m
PS62/023-2	09.07.02	08:07	73° 27.78' N	9° 16.09' W	842.4	SW 5	182.1	0.6	Large Box Corer	GKG	at sea bottom	
PS62/023-3	09.07.02	08:52	73° 27.84' N	9° 15.88' W	765.1	SSW 5	45.9	0.3	Large Box Corer	GKG	at sea bottom	
PS62/023-4	09.07.02	09:32	73° 27.82' N	9° 15.85' W	762.1	SSW 6	61.3	0.1	Large Box Corer	GKG	at sea bottom	
PS62/024-1	09.07.02	11:04	73° 31.76' N	9° 6.96' W	157.5	SSW 6	191.7	1.6	Large Box Corer	GKG	at sea bottom	
PS62/024-2	09.07.02	11:37	73° 31.64' N	9° 7.12' W	142.8	SW 6	147.1	0.7	Large Box Corer	GKG	at sea bottom	
PS62/024-3	09.07.02	12:10	73° 31.66' N	9° 7.40' W	153.9	SSW 7	228.3	1.0	Large Box Corer	GKG	at sea bottom	155 m ausgesteckt
PS62/024-4	09.07.02	12:21	73° 31.56' N	9° 7.70' W	156.4	SSW 7	249.8	0.3	Large Box Corer	GKG	at sea bottom	157 m ausgesteckt
PS62/024-5	09.07.02	12:48	73° 31.67' N	9° 7.16' W	156.9	SW 6	216.4	0.8	Large Box Corer	GKG	at sea bottom	173 m ausgesteckt
PS62/024-6	09.07.02	13:00	73° 31.60' N	9° 7.39' W	161.3	SW 7	240.2	0.3	Large Box Corer	GKG	at sea bottom	161 m ausgesteckt
PS62/024-7	09.07.02	13:28	73° 31.78' N	9° 7.64' W	151.3	SW 7	217.8	0.3	Large Box Corer	GKG	at sea bottom	157 m ausgesteckt
PS62/024-8	09.07.02	14:00	73° 31.63' N	9° 7.28' W	152.0	SW 7	64.2	0.2	Large Box Corer	GKG	at sea bottom	153 m ausgesteckt
PS62/024-9	09.07.02	14:28	73° 31.76' N	9° 6.80' W	168.8	SW 8	54.2	0.8	Large Box Corer	GKG	at sea bottom	177 m ausgesteckt
PS62/025-1	09.07.02	15:41	73° 35.59' N	9° 2.01' W	1668.0	SSW 7	27.9	0.2	CTD/rosette water sampler	CTD/RO	at depth	1576 m ausgesteckt; Missweisung 15,3°W
PS62/025-2	09.07.02	16:47	73° 35.56' N	9° 1.98' W	1651.0	SSW 8	45.1	0.0	Large Box Corer	GKG	at sea bottom	1574 m
PS62/025-3	09.07.02	17:49	73° 35.58' N	9° 1.91' W	1654.0	SSW 8	44.8	0.0	Large Box Corer	GKG	at sea bottom	1592 m
PS62/025-4	09.07.02	19:06	73° 34.97' N	9° 2.26' W	1366.0	SSW 9	79.1	0.4	Large Box Corer	GKG	at sea bottom	1364 m
PS62/025-5	09.07.02	20:10	73° 34.97' N	9° 1.81' W	1270.0	SSW 10	234.2	0.0	Large Box Corer	GKG	at sea bottom	1256 m
PS62/026-1	10.07.02	06:07	74° 20.12' N	8° 13.03' W	3340.0	SSW 12	143.9	0.3	CTD/rosette water sampler	CTD/RO	surface	
PS62/026-2	10.07.02	06:51	74° 19.99' N	8° 12.90' W	3340.0	SSW 12	207.6	0.0	CTD/rosette water sampler	CTD/RO	surface	
PS62/026-3	10.07.02	08:13	74° 19.94' N	8° 12.77' W	3341.0	SSW 11	203.0	0.0	MultiCorer	MUC	at sea bottom	3278 m ausgesteckt
PS62/027-1	10.07.02	14:57	74° 49.45' N	7° 0.47' W	3510.0	SSW 12	9.6	0.3	MultiCorer	MUC	at sea bottom	3455 m ausgesteckt
PS62/028-1	10.07.02	22:06	74° 50.95' N	6° 54.92' W	3477.0	S 11	227.7	0.2	MultiCorer	MUC	at sea bottom	3415 m ausgesteckt
PS62/029-1	11.07.02	01:55	74° 50.97' N	6° 54.87' W	3477.0	S 8	295.3	0.2	Ocean Floor Observ. System	OFOS	at depth	3405 m ausgesteckt
PS62/029-1	11.07.02	02:00	74° 50.95' N	6° 55.05' W	3478.0	S 8	235.2	0.8	Ocean Floor Observ. System	OFOS	action	Beginn des OFOS-Profils
PS62/029-1	11.07.02	07:43	74° 48.61' N	7° 2.90' W	3471.0	S 9	226.2	0.4	Ocean Floor Observ. System	OFOS	Start Hoisting	
PS62/029-1	11.07.02	08:47	74° 48.12' N	7° 4.21' W	3470.0	S 9	209.3	0.8	Ocean Floor Observ. System	OFOS	on deck	
PS62/029-2	11.07.02	10:06	74° 47.92' N	7° 5.01' W	3471.0	S 10	61.8	0.2	MultiCorer	MUC	at sea bottom	ausgesteckt 3408 m
PS62/029-3	11.07.02	12:16	74° 47.79' N	7° 5.16' W	3473.0	S 6	174.9	0.3	Large Box Corer	GKG	at sea bottom	3413 m ausgesteckt
PS62/029-4	11.07.02	14:06	74° 47.90' N	7° 4.76' W	3473.0	S 6	163.1	0.6	Gravity corer	GC	at sea bottom	3417 m ausgesteckt
PS62/030-1	12.07.02	07:59	74° 55.17' N	4° 38.13' W	3621.0	SE 6	88.3	0.3	Mooring	MOR	action	Jojo CTD an Deck
PS62/030-2	12.07.02	10:30	74° 55.02' N	4° 38.03' W	3622.0	ESE 8	279.9	0.7	Mooring	MOR	at depth	Verankerung auf Grund und ausgelöst
PS62/031-1	12.07.02	14:22	75° 5.04' N	3° 27.53' W	3676.0	ESE 6	202.1	0.2	Mooring	MOR	on deck	Verankerung komplett geborgen
PS62/031-2	12.07.02	16:11	75° 5.00' N	3° 27.39' W	3676.0	ESE 7	6.6	0.0	Mooring	MOR	at depth	auf Grund gefiert
PS62/032-1	13.07.02	07:11	74° 49.97' N	2° 30.50' W	3704.0	SE 7	173.8	0.2	Mooring	MOR	on deck	JoJo , Kugelkorb. Auslöser an Deck
PS62/032-2	13.07.02	09:53	74° 49.99' N	2° 30.23' W	3703.0	SSW 6	309.5	0.8	Mooring	MOR	at depth	Verankerung auf grund und ausgelöst

Station	Date	Time	PositionLat	PositionLon	Depth [m]	Windstrength [m/s]	Course [°]	Speed [kn]	Gear	Gear Abbreviation	Action	Comment
PS62/032-3	13.07.02	10:37	74° 49.92' N	2° 37.26' W	3701.0	SSW 6	347.3	0.6	CTD	CTD	at depth	399 m ausgesteckt
PS62/033-1	13.07.02	12:57	74° 52.21' N	3° 5.37' W	3692.0	SW 8	19.6	0.3	Large Box Corer	GKG	at sea bottom	3628 m ausgesteckt
PS62/033-2	13.07.02	14:51	74° 52.17' N	3° 5.34' W	3691.0	SW 6	192.3	0.7	Gravity corer	GC	at sea bottom	3647 m ausgesteckt
PS62/034-1	13.07.02	16:54	74° 50.57' N	3° 16.27' W	3688.0	SSW 4	270.2	0.3	Gravity corer	GC	at sea bottom	3636 m
PS62/034-2	13.07.02	18:53	74° 50.53' N	3° 16.09' W	3691.0	SSW 5	189.8	0.1	Large Box Corer	GKG	at sea bottom	3632 m
PS62/035-1	13.07.02	21:15	74° 49.96' N	3° 13.82' W	3687.0	SSW 6	85.9	0.7	MultiCorer	MUC	at sea bottom	3635 m ausgesteckt
PS62/036-1	13.07.02	23:35	74° 50.02' N	3° 14.17' W	3686.0	S 6	180.2	0.3	Ocean Floor Observ. System	OFOS	at depth	Abstandsgewicht hat Grundberührung 3608m
PS62/036-1	14.07.02	07:40	74° 46.79' N	3° 3.62' W	3646.0	SSE 4	102.8	0.6	Ocean Floor Observ. System	OFOS	Start Hoisting	
PS62/037-1	14.07.02	09:08	74° 47.49' N	3° 6.02' W	3521.0	SSE 5	285.9	9.4	HydroSweep/ParaSound profile	HS_PS	start track	
PS62/037-1	14.07.02	19:57	74° 44.87' N	5° 1.78' W	3601.0	ESE 8	179.0	8.1	HydroSweep/ParaSound profile	HS_PS	profile end	
PS62/038-1	14.07.02	21:34	74° 46.01' N	5° 1.55' W	3603.0	SE 10	156.3	0.5	MultiCorer	MUC	at sea bottom	3539 m ausgesteckt
PS62/039-1	15.07.02	00:02	74° 45.85' N	5° 0.36' W	3610.0	SE 9	161.4	0.4	Ocean Floor Observ. System	OFOS	at depth	OFOS bei 3528 m am Grund
PS62/039-1	15.07.02	00:03	74° 45.84' N	5° 0.36' W	3608.0	SE 9	200.1	0.8	Ocean Floor Observ. System	OFOS	action	Beginn der Profilfahrt/v=0.5 kn
PS62/039-1	15.07.02	02:45	74° 44.04' N	5° 0.81' W	3603.0	ESE 10	194.7	1.0	Ocean Floor Observ. System	OFOS	Start Hoisting	
PS62/040-1	15.07.02	05:33	74° 41.02' N	5° 1.05' W	3602.0	SE 13	206.7	0.4	Ocean Floor Observ. System	OFOS	at depth	
PS62/040-1	15.07.02	08:21	74° 39.66' N	5° 1.13' W	3603.0	SE 11	209.4	0.5	Ocean Floor Observ. System	OFOS	action	Aktion abgeschlossen, beginnen mit hieven
PS62/040-1	15.07.02	08:36	74° 39.56' N	5° 1.16' W	3602.0	SE 11	215.7	0.3	Ocean Floor Observ. System	OFOS	Start Hoisting	
PS62/041-1	15.07.02	11:08	74° 41.06' N	5° 0.70' W	3602.0	SE 10	1.3	0.4	MultiCorer	MUC	at sea bottom	3538 m ausgesteckt
PS62/042-1	15.07.02	13:50	74° 40.24' N	5° 1.19' W	3604.0	SE 8	179.4	2.5	Agassiz trawl	AGT	AGT on ground	
PS62/042-1	15.07.02	14:21	74° 39.15' N	5° 1.36' W	3605.0	ESE 7	182.9	2.0	Agassiz trawl	AGT	start trawl	5500 m ausgesteckt
PS62/042-1	15.07.02	14:31	74° 38.99' N	5° 1.54' W	3602.0	SE 7	163.6	0.8	Agassiz trawl	AGT	Stop Trawl	
PS62/042-1	15.07.02	15:35	74° 38.66' N	5° 3.06' W	3596.0	ESE 7	246.7	0.4	Agassiz trawl	AGT	AGT off ground	
PS62/042-2	15.07.02	17:29	74° 38.34' N	5° 2.82' W	3593.0	ESE 8	44.9	0.4	CTD/rosette water sampler	CTD/RO	at depth	396m EL 31
PS62/043-1	15.07.02	18:14	74° 41.49' N	5° 11.92' W	3593.0	ESE 8	334.6	8.1	HydroSweep/ParaSound profile	HS_PS	start track	
PS62/043-1	15.07.02	19:44	74° 53.31' N	5° 12.02' W	3594.0	ESE 9	356.4	7.8	HydroSweep/ParaSound profile	HS_PS	alter course	
PS62/043-1	15.07.02	20:10	74° 52.93' N	5° 22.80' W	3587.0	ESE 9	183.3	6.4	HydroSweep/ParaSound profile	HS_PS	alter course	
PS62/043-1	15.07.02	21:39	74° 41.63' N	5° 22.83' W	3581.0	ESE 8	181.8	8.6	HydroSweep/ParaSound profile	HS_PS	alter course	
PS62/043-1	15.07.02	21:55	74° 41.50' N	5° 31.27' W	3564.0	ESE 8	273.3	8.6	HydroSweep/ParaSound profile	HS_PS	alter course	
PS62/043-1	15.07.02	23:41	74° 56.02' N	5° 32.68' W	3578.0	ESE 8	284.9	6.1	HydroSweep/ParaSound profile	HS_PS	alter course	
PS62/043-1	15.07.02	23:59	74° 55.99' N	5° 41.55' W	3568.0	ESE 9	251.0	7.8	HydroSweep/ParaSound profile	HS_PS	alter course	
PS62/043-1	16.07.02	01:07	74° 47.62' N	5° 41.99' W	3556.0	SE 8	175.0	3.3	HydroSweep/ParaSound profile	HS_PS	profile end	
PS62/044-1	16.07.02	02:02	74° 47.41' N	5° 41.62' W	3558.0	SE 8	187.2	0.2	Large Box Corer	GKG	at sea bottom	3492 m ausgesteckt
PS62/044-2	16.07.02	03:54	74° 47.41' N	5° 41.51' W	3552.0	ESE 7	337.8	0.7	Gravity corer	GC	at sea bottom	3503 m ausgesteckt
PS62/045-1	16.07.02	05:00	74° 46.53' N	5° 41.91' W	3569.0	SE 8	191.7	8.1	HydroSweep/ParaSound profile	HS_PS	start track	
PS62/045-1	16.07.02	05:28	74° 42.98' N	5° 43.00' W	3569.0	SE 8	271.5	7.8	HydroSweep/ParaSound profile	HS_PS	alter course	
PS62/045-1	16.07.02	08:16	74° 43.01' N	7° 8.57' W	3473.0	ESE 7	270.0	8.0	HydroSweep/ParaSound profile	HS_PS	alter course	
PS62/045-1	16.07.02	09:51	74° 46.40' N	7° 54.60' W	3420.0	ESE 6	286.9	8.1	HydroSweep/ParaSound profile	HS_PS	alter course	
PS62/045-1	16.07.02	10:52	74° 54.05' N	7° 48.41' W	3416.0	SE 6	14.6	7.9	HydroSweep/ParaSound profile	HS_PS	alter course	
PS62/045-1	16.07.02	11:16	74° 55.23' N	7° 58.19' W	3402.0	ESE 6	285.2	8.0	HydroSweep/ParaSound profile	HS_PS	alter course	
PS62/045-1	16.07.02	12:58	74° 45.52' N	8° 9.08' W	3399.0	E 5	179.2	8.0	HydroSweep/ParaSound profile	HS_PS	profile end	
PS62/046-1	16.07.02	14:05	74° 48.56' N	8° 8.89' W	3396.0	E 5	81.0	0.5	Gravity corer	GC	at sea bottom	3340 m ausgesteckt
PS62/046-2	16.07.02	15:54	74° 48.43' N	8° 8.75' W	3394.0	E 5	145.9	0.5	Large Box Corer	GKG	at sea bottom	3331 m ausgesteckt
PS62/046-3	16.07.02	17:51	74° 48.50' N	8° 9.11' W	3395.0	E 6	27.5	0.1	MultiCorer	MUC	at sea bottom	3334 m
PS62/047-1	16.07.02	20:27	74° 51.29' N	8° 9.09' W	3391.0	ESE 5	160.4	0.6	CTD/rosette water sampler	CTD/RO	at depth	Missweisung 15,2 W, ausgesteckt 3326 m
PS62/047-1	16.07.02	20:30	74° 51.27' N	8° 9.03' W	3392.0	ESE 5	172.9	0.4	CTD/rosette water sampler	CTD/RO	at depth	Beginn Schleppen mit o,5 kn

Station	Date	Time	PositionLat	PositionLon	Depth [m]	Windstrength [m/s]	Course [°]	Speed [kn]	Gear	Gear Abbreviation	Action	Comment
PS62/047-1	16.07.02	23:20	74° 49.14' N	8° 9.03' W	3392.0	E 5	207.7	0.6	CTD/rosette water sampler	CTD/RO	at depth	Schleppen beendet
PS62/048-1	17.07.02	01:34	74° 50.48' N	8° 8.54' W	3458.0	ESE 6	131.5	0.2	MultiCorer	MUC	at sea bottom	3396 m ausgesteckt
PS62/049-1	17.07.02	04:06	74° 51.85' N	8° 9.17' W	3390.0	ESE 4	166.1	0.5	Ocean Floor Observ. System	OFOS	at depth	
PS62/049-1	17.07.02	10:28	74° 48.85' N	8° 8.88' W	3388.0	E 4	178.0	0.6	Ocean Floor Observ. System	OFOS	Start Hoisting	
PS62/050-1	17.07.02	13:02	74° 52.04' N	8° 9.26' W	3383.0	E 3	270.0	0.1	MultiCorer	MUC	at sea bottom	3326 m ausgesteckt
PS62/051-1	17.07.02	14:12	74° 51.97' N	8° 8.80' W	3384.0	ENE 4	205.0	6.9	HydroSweep/ParaSound profile	HS_PS	start track	
PS62/051-1	17.07.02	14:54	74° 46.70' N	8° 15.76' W	3384.0	ENE 3	198.8	7.9	HydroSweep/ParaSound profile	HS_PS	alter course	
PS62/051-1	17.07.02	16:06	74° 39.22' N	8° 37.65' W	3347.0	ENE 3	150.4	7.1	HydroSweep/ParaSound profile	HS_PS	alter course	
PS62/051-1	17.07.02	18:02	74° 43.33' N	7° 42.14' W	3431.0	NNE 2	71.9	8.1	HydroSweep/ParaSound profile	HS_PS	alter course	
PS62/051-1	17.07.02	18:40	74° 44.39' N	7° 57.55' W	3414.0	ENE 2	251.6	8.0	HydroSweep/ParaSound profile	HS_PS	alter course	
PS62/051-1	17.07.02	20:32	74° 41.67' N	8° 50.78' W	3322.0	NNE 2	309.5	8.0	HydroSweep/ParaSound profile	HS_PS	alter course	
PS62/051-1	17.07.02	21:08	74° 44.74' N	9° 3.75' W	3314.0	NNE 3	312.9	8.5	HydroSweep/ParaSound profile	HS_PS	profile end	
PS62/052-1	17.07.02	23:07	74° 46.73' N	8° 58.38' W	3381.0	N 4	61.4	1.7	Agassiz trawl	AGT	AGT on ground	5500 m ausgesteckt, Beginn Schleppen mit v=o,5-1 kn
PS62/052-1	17.07.02	23:19	74° 46.80' N	8° 57.67' W	3385.0	NNW 3	62.9	0.9	Agassiz trawl	AGT	Start hoisting	
PS62/052-1	18.07.02	00:29	74° 47.03' N	8° 54.70' W	3390.0	NW 3	86.0	0.3	Agassiz trawl	AGT	AGT off ground	
PS62/053-1	18.07.02	01:56	74° 47.17' N	8° 51.31' W	3375.0	NW 4	45.5	6.0	HydroSweep/ParaSound profile	HS_PS	start track	
PS62/053-1	18.07.02	02:19	74° 48.94' N	8° 41.63' W	3408.0	NW 4	69.0	8.4	HydroSweep/ParaSound profile	HS_PS	alter course	
PS62/053-1	18.07.02	02:52	74° 48.07' N	8° 25.26' W	3364.0	NW 5	102.9	7.8	HydroSweep/ParaSound profile	HS_PS	alter course	
PS62/053-1	18.07.02	06:09	74° 26.18' N	9° 27.75' W	3246.0	NW 4	219.3	7.6	HydroSweep/ParaSound profile	HS_PS	alter course	
PS62/053-1	18.07.02	08:12	74° 26.07' N	10° 24.81' W	3176.0	NW 3	231.2	0.5	HydroSweep/ParaSound profile	HS_PS	profile end	
PS62/054-1	18.07.02	08:59	74° 26.08' N	10° 24.83' W	3174.0	WNW 4	310.4	0.0	Large Box Corer	GKG	at sea bottom	3118 m ausgesteckt
PS62/054-2	18.07.02	10:50	74° 26.07' N	10° 24.89' W	3174.0	WNW 5	353.0	0.2	Piston corer	PC	at sea bottom	
PS62/054-3	18.07.02	12:58	74° 26.13' N	10° 24.83' W	3174.0	WNW 4	305.6	0.0	MultiCorer	MUC	at sea bottom	3120 m ausgesteckt
PS62/055-1	18.07.02	15:38	74° 22.32' N	10° 22.33' W	3125.0	W 4	341.5	0.3	CTD/rosette water sampler	CTD/RO	at depth	3056 m ausgesteckt, Missweisung 16,7°W
PS62/055-1	18.07.02	16:02	74° 22.52' N	10° 22.56' W	3125.0	WSW 3	344.6	0.7	CTD/rosette water sampler	CTD/RO	at depth	3070 m
PS62/055-1	18.07.02	16:25	74° 22.70' N	10° 22.73' W	3129.0	WSW 4	357.2	0.3	CTD/rosette water sampler	CTD/RO	at depth	3081 m
PS62/055-1	18.07.02	16:47	74° 22.87' N	10° 22.91' W	3131.0	WSW 4	348.5	0.4	CTD/rosette water sampler	CTD/RO	at depth	3085 m
PS62/055-1	18.07.02	17:11	74° 23.07' N	10° 23.00' W	3139.0	WSW 4	1.7	0.5	CTD/rosette water sampler	CTD/RO	at depth	3088 m
PS62/055-1	18.07.02	17:34	74° 23.26' N	10° 23.11' W	3152.0	SW 3	350.9	0.6	CTD/rosette water sampler	CTD/RO	at depth	3103 m
PS62/055-1	18.07.02	17:56	74° 23.46' N	10° 23.24' W	3172.0	SW 3	344.9	0.8	CTD/rosette water sampler	CTD/RO	at depth	
PS62/055-1	18.07.02	20:44	74° 24.90' N	10° 23.29' W	3191.0	SSW 5	9.6	0.5	CTD/rosette water sampler	CTD/RO	at depth	2681 m
PS62/055-1	18.07.02	22:35	74° 25.25' N	10° 21.82' W	3181.0	S 8	102.8	0.4	CTD/rosette water sampler	CTD/RO	on deck	
PS62/056-1	18.07.02	23:55	74° 22.00' N	10° 22.79' W	3132.0	S 8	240.9	0.0	MultiCorer	MUC	at sea bottom	3065 m ausgesteckt
PS62/057-1	19.07.02	02:15	74° 25.02' N	10° 23.59' W	3185.0	S 9	94.9	0.1	Ocean Floor Observ. System	OFOS	at depth	3115 m ausgesteckt
PS62/057-1	19.07.02	02:16	74° 25.02' N	10° 23.58' W	3185.0	S 9	171.5	0.2	Ocean Floor Observ. System	OFOS	action	Beginn der Profilfahrt mit v=0,5 kn
PS62/057-1	19.07.02	08:41	74° 21.60' N	10° 23.57' W	3129.0	SSW 8	159.6	0.6	Ocean Floor Observ. System	OFOS	Start Hoisting	
PS62/058-1	19.07.02	11:07	74° 23.80' N	10° 23.80' W	3199.0	S 5	265.2	0.8	MultiCorer	MUC	at sea bottom	3144 m ausgesteckt
PS62/059-1	19.07.02	12:27	74° 23.95' N	10° 25.51' W	3200.0	S 5	139.1	0.4	CTD/rosette water sampler	CTD/RO	at depth	400 m ausgesteckt
PS62/060-1	19.07.02	14:46	74° 30.67' N	11° 4.02' W	3121.0	SSE 4	301.3	1.8	Agassiz trawl	AGT	AGT on ground	
PS62/060-1	19.07.02	15:13	74° 31.11' N	11° 6.72' W	3113.0	SSE 4	302.6	1.3	Agassiz trawl	AGT	start trawl	5000 m ausgesteckt
PS62/060-1	19.07.02	15:23	74° 31.15' N	11° 7.03' W	3112.0	SSE 4	305.4	0.1	Agassiz trawl	AGT	Stop Trawl	Beginn Hieven mit 0,5 m/s
PS62/060-1	19.07.02	16:28	74° 31.23' N	11° 7.41' W	3114.0	S 3	309.7	0.0	Agassiz trawl	AGT	AGT off ground	
PS62/061-1	19.07.02	18:30	74° 33.95' N	11° 23.70' W	3053.0	SW 3	252.6	0.6	Eisfischen	EF		
PS62/062-1	20.07.02	06:24	74° 59.89' N	16° 25.25' W	334.4	S 2	174.3	0.0	CTD/rosette water sampler	CTD/RO	at depth	314 m EL 31
PS62/063-1	20.07.02	07:50	75° 0.13' N	15° 39.67' W	200.6	S 1	178.7	0.3	CTD/rosette water sampler	CTD/RO	at depth	EL 31 182 m

Station	Date	Time	PositionLat	PositionLon	Depth [m]	Windstrength [m/s]	Course [°]	Speed [kn]	Gear	Gear Abbreviation	Action	Comment
PS62/064-1	20.07.02	09:15	74° 59.96' N	15° 2.28' W	119.2	SSE 2	137.7	0.2	CTD	CTD	at depth	102 m ausgesteckt, Missweisung 20,7 W
PS62/065-1	20.07.02	11:23	74° 59.98' N	14° 20.75' W	160.0	ESE 4	256.1	0.2	CTD	CTD	at depth	144m ausgesteckt, MW 20,1 W
PS62/066-1	20.07.02	13:14	74° 59.98' N	13° 39.75' W	200.6	ESE 2	132.5	0.4	CTD/rosette water sampler	CTD/RO	at depth	179 m ausgesteckt
PS62/067-1	20.07.02	14:58	75° 0.02' N	13° 9.71' W	237.6	ENE 2	214.8	0.5	CTD/rosette water sampler	CTD/RO	at depth	220 m ausgesteckt; Mw. 19,2°W
PS62/068-1	20.07.02	16:30	75° 0.00' N	12° 44.89' W	592.5	ESE 3	276.4	0.9	CTD/rosette water sampler	CTD/RO	at depth	568 m
PS62/069-1	20.07.02	17:42	74° 59.81' N	12° 31.81' W	1016.0	E 5	97.1	0.0	CTD/rosette water sampler	CTD/RO	at depth	980 m
PS62/070-1	20.07.02	19:06	74° 59.85' N	12° 22.35' W	1250.0	ENE 4	4.6	0.1	CTD/rosette water sampler	CTD/RO	at depth	1208 m
PS62/071-1	20.07.02	20:45	75° 0.07' N	12° 9.32' W	1540.0	ENE 4	281.8	0.5	CTD	CTD	at depth	1494 m ausgesteckt, MW 18,4 W
PS62/072-1	20.07.02	22:48	75° 0.06' N	11° 53.11' W	1883.0	NE 5	317.8	0.4	CTD	CTD	at depth	1839 m ausgesteckt, MW 18,2 W
PS62/073-1	21.07.02	01:25	74° 59.82' N	11° 28.98' W	2327.0	NE 6	30.2	0.0	CTD/rosette water sampler	CTD/RO	at depth	2283 m ausgesteckt; Mw.17,8°W
PS62/074-1	21.07.02	04:10	74° 59.86' N	11° 2.76' W	2737.0	NNE 6	239.2	0.3	CTD/rosette water sampler	CTD/RO	at depth	MW (-)17,5 Grad W 2683 m ausgesteckt
PS62/075-1	21.07.02	07:06	74° 59.86' N	10° 36.79' W	3079.0	NE 6	211.6	0.1	CTD/rosette water sampler	CTD/RO	at depth	MW -17,2 West; EL 31-1: 3026 m Draht ausgesteckt
PS62/076-1	21.07.02	10:58	74° 59.98' N	9° 57.08' W	3225.0	NE 5	211.3	0.4	CTD	CTD	at depth	Missweisung 16,2 W, ausgesteckt 3170m
PS62/077-1	21.07.02	14:08	75° 0.14' N	9° 18.13' W	3308.0	NE 6	41.3	0.1	CTD/rosette water sampler	CTD/RO	at depth	3246 m ausgesteckt; Mw. 16,1°W
PS62/078-1	21.07.02	17:06	75° 0.05' N	8° 39.59' W	3367.0	NE 4	268.3	0.2	CTD/rosette water sampler	CTD/RO	at depth	3305 m
PS62/079-1	21.07.02	20:19	75° 0.21' N	8° 0.86' W	3406.0	E 4	10.8	0.2	CTD/rosette water sampler	CTD/RO	at depth	3348 m ausgesteckt, Missweisung 15,1 W
PS62/080-1	21.07.02	23:25	75° 0.66' N	7° 22.09' W	3445.0	NE 2	320.6	0.5	CTD/rosette water sampler	CTD/RO	at depth	3403 m ausgesteckt, MW 14,6 W
PS62/081-1	22.07.02	02:28	75° 0.33' N	6° 42.84' W	3491.0	NNE 4	226.2	0.1	CTD/rosette water sampler	CTD/RO	at depth	3425 m ausgesteckt; Mw.14,1°W
PS62/082-1	22.07.02	05:37	75° 0.16' N	6° 4.61' W	3530.0	N 5	327.5	0.1	CTD/rosette water sampler	CTD/RO	at depth	3470 m
PS62/083-1	22.07.02	08:57	75° 0.05' N	5° 24.88' W	3580.0	NNW 5	24.4	0.5	CTD/rosette water sampler	CTD/RO	at depth	ausgesteckt 3530 m, MW 13,1 W
PS62/084-1	22.07.02	12:14	75° 0.07' N	4° 46.89' W	3617.0	NNW 6	103.5	0.4	CTD/rosette water sampler	CTD/RO	at depth	3559 m ausgesteckt; Mw.12,6°W
PS62/085-1	22.07.02	15:36	75° 0.10' N	4° 8.84' W	3643.0	NNE 5	255.3	0.2	CTD/rosette water sampler	CTD/RO	at depth	3586 m ausgesteckt; Mw.12,1°W
PS62/086-1	22.07.02	19:01	75° 0.11' N	3° 30.35' W	3671.0	NNE 3	14.2	0.4	CTD/rosette water sampler	CTD/RO	at depth	3612 m
PS62/087-1	22.07.02	22:18	74° 59.96' N	2° 50.58' W	3695.0	N 4	108.4	0.0	CTD/rosette water sampler	CTD/RO	at depth	ausgesteckt 3628 m, Missweisung 11,1 W
PS62/088-1	23.07.02	01:30	75° 0.02' N	2° 12.18' W	3634.0	NNW 3	111.4	0.6	CTD/rosette water sampler	CTD/RO	at depth	3577 m ausgesteckt; Mw.10,6°W
PS62/089-1	23.07.02	04:41	75° 0.22' N	1° 35.38' W	3736.0	NNE 2	317.2	0.2	CTD/rosette water sampler	CTD/RO	at depth	3677 m
PS62/090-1	23.07.02	08:01	75° 0.06' N	0° 56.71' W	3693.0	NNE 2	17.9	0.9	CTD/rosette water sampler	CTD/RO	at depth	3623 m
PS62/091-1	23.07.02	11:19	74° 59.79' N	0° 18.45' W	3775.0	W 1	220.8	0.8	CTD/rosette water sampler	CTD/RO	at depth	ausgesteckt 3710 m, MW 9,1 W
PS62/092-1	23.07.02	14:29	74° 59.90' N	0° 46.44' W	3761.0	NNE 1	30.8	0.4	CTD/rosette water sampler	CTD/RO	at depth	3720 m ausgesteckt; Mw.9,5°W
PS62/093-1	23.07.02	17:22	75° 2.26' N	0° 55.86' W	3754.0	NNW 0	164.9	0.4	CTD/rosette water sampler	CTD/RO	at depth	3743 m
PS62/094-1	23.07.02	20:07	75° 2.55' N	0° 47.59' W	3759.0	N 0	182.5	0.3	CTD/rosette water sampler	CTD/RO	at depth	3712 m ausgesteckt, MW 9,5 W
PS62/095-1	23.07.02	22:52	75° 2.16' N	0° 36.32' W	3763.0	SW 1	109.4	1.0	CTD/rosette water sampler	CTD/RO	at depth	ausgesteckt 3711 m, MW 9,4 W
PS62/096-1	24.07.02	01:25	75° 0.10' N	0° 37.88' W	3764.0	SW 2	76.8	0.5	CTD/rosette water sampler	CTD/RO	at depth	3733 m ausgesteckt; Mw.9,4°W

Station	Date	Time	PositionLat	PositionLon	Depth [m]	Windstrength [m/s]	Course [°]	Speed [kn]	Gear	Gear Abbreviation	Action	Comment
PS62/097-1	24.07.02	04:06	74° 57.47' N	0° 37.47' W	3764.0	SW 1	298.5	0.4	CTD/rosette water sampler	CTD/RO	at depth	3763 m
PS62/098-1	24.07.02	06:44	74° 57.49' N	0° 47.57' W	3761.0	SSE 2	249.9	0.0	CTD/rosette water sampler	CTD/RO	at depth	3715 m
PS62/099-1	24.07.02	09:22	74° 57.65' N	0° 57.86' W	3765.0	SSE 3	282.6	0.3	CTD/rosette water sampler	CTD/RO	at depth	3708 m ausgesteckt, MW 9,6 W
PS62/100-1	24.07.02	12:08	75° 0.54' N	0° 46.44' W	3763.0	S 2	293.9	0.2	CTD/rosette water sampler	CTD/RO	at depth	3702 m ausgesteckt; Mw 9,5°W
PS62/101-1	24.07.02	15:24	74° 55.15' N	0° 47.22' W	3765.0	ESE 3	282.5	0.9	CTD/rosette water sampler	CTD/RO	at depth	3712 m ausgesteckt; Mw 9,5°W
PS62/102-1	24.07.02	18:01	74° 53.15' N	0° 47.57' W	3769.0	SE 2	276.1	0.3	CTD/rosette water sampler	CTD/RO	at depth	EL 31: 3704 m ausgesteckt
PS62/103-1	24.07.02	20:53	74° 55.24' N	1° 5.87' W	3765.0	S 4	313.6	1.1	CTD/rosette water sampler	CTD/RO	at depth	3706 m ausgesteckt, MW 9,7 W
PS62/104-1	24.07.02	23:44	74° 59.98' N	1° 5.75' W	3567.0	SSW 2	34.5	0.1	CTD/rosette water sampler	CTD/RO	at depth	MW 9,7 W ausgesteckt 3552 m
PS62/105-1	25.07.02	02:15	75° 0.19' N	1° 13.00' W	3641.0	S 3	206.6	0.6	CTD/rosette water sampler	CTD/RO	at depth	3597 m ausgesteckt; Mw 9,8°W
PS62/106-1	25.07.02	05:01	75° 5.10' N	1° 4.44' W	3749.0	S 2	62.6	0.5	CTD/rosette water sampler	CTD/RO	at depth	3681 m
PS62/107-1	25.07.02	07:42	75° 4.67' N	0° 45.97' W	3757.0	SSE 4	108.4	0.8	CTD/rosette water sampler	CTD/RO	at depth	3720 m
PS62/108-1	25.07.02	10:34	75° 7.12' N	0° 44.95' W	3755.0	SE 4	80.4	0.3	CTD/rosette water sampler	CTD/RO	at depth	Missweisung 9,5 W ausgesteckt 3700 m
PS62/109-1	25.07.02	13:21	75° 4.78' N	0° 26.55' W	3767.0	ESE 5	263.5	0.7	CTD/rosette water sampler	CTD/RO	at depth	3713 m ausgesteckt; Mw 9,3°W
PS62/110-1	25.07.02	16:16	74° 59.73' N	0° 30.40' W	3767.0	ESE 4	221.4	0.4	CTD/rosette water sampler	CTD/RO	at depth	3739 m
PS62/111-1	25.07.02	19:02	74° 55.82' N	0° 24.94' W	3770.0	ESE 6	209.6	0.1	CTD/rosette water sampler	CTD/RO	at depth	3710 m
PS62/112-1	26.07.02	01:48	74° 59.81' N	0° 1.09' W	3779.0	ESE 9	88.4	0.4	CTD/rosette water sampler	CTD/RO	at depth	3718 m ausgesteckt; Mw 8,9°W
PS62/113-1	26.07.02	04:36	75° 0.08' N	0° 21.60' E	3781.0	ESE 8	351.7	0.2	CTD/rosette water sampler	CTD/RO	at depth	3718 m
PS62/114-1	26.07.02	07:54	75° 0.09' N	0° 59.32' E	3783.0	E 8	103.0	0.0	CTD/rosette water sampler	CTD/RO	at depth	3717 m
PS62/115-1	26.07.02	11:07	74° 59.99' N	1° 38.28' E	3139.0	E 10	135.5	0.6	CTD/rosette water sampler	CTD/RO	at depth	ausgesteckt 3138 m,Missweisung 7,7 W
PS62/115-2	26.07.02	12:30	74° 59.98' N	1° 38.09' E	3146.0	E 12	133.8	0.3	Rosette water sampler	RO	at depth	10 m ausgesteckt
PS62/116-1	26.07.02	14:39	75° 0.17' N	2° 17.63' E	2935.0	ENE 12	138.3	0.4	CTD/rosette water sampler	CTD/RO	at depth	2888 m ausgesteckt; Mw 7,1°W
PS62/117-1	26.07.02	17:42	75° 0.04' N	2° 56.03' E	2525.0	E 12	287.3	0.1	CTD/rosette water sampler	CTD/RO	at depth	2466 m
PS62/118-1	26.07.02	20:42	74° 59.97' N	3° 35.18' E	3485.0	E 13	120.4	0.4	CTD/rosette water sampler	CTD/RO	at depth	ausgesteckt 3425 m Missweisung 6,2 W
PS62/119-1	26.07.02	23:39	75° 0.26' N	4° 14.60' E	3077.0	E 15	208.6	0.3	CTD/rosette water sampler	CTD/RO	at depth	3060 m ausgesteckt, MW 5,7 W
PS62/120-1	27.07.02	02:41	74° 59.99' N	4° 51.87' E	3248.0	E 17	72.5	0.1	CTD/rosette water sampler	CTD/RO	at depth	3198 m ausgesteckt; Mw 5,2°W
PS62/121-1	27.07.02	06:00	75° 0.40' N	5° 28.55' E	3155.0	E 16	298.4	1.0	CTD/rosette water sampler	CTD/RO	at depth	3098 m
PS62/122-1	27.07.02	09:28	75° 0.57' N	6° 8.88' E	2789.0	E 13	252.3	0.5	CTD/rosette water sampler	CTD/RO	at depth	ausgestecxkt 2776 m
PS62/123-1	27.07.02	12:23	75° 0.13' N	6° 47.47' E	2249.0	ESE 12	139.7	0.4	CTD/rosette water sampler	CTD/RO	at depth	2220 m ausgesteckt; Mw 3,7°W
PS62/124-1	27.07.02	15:03	74° 59.93' N	7° 26.26' E	2484.0	ESE 10	317.3	0.4	CTD/rosette water sampler	CTD/RO	at depth	2436 m ausgesteckt; Mw 3,3°W
PS62/125-1	27.07.02	18:00	75° 0.10' N	8° 5.27' E	3540.0	S 4	109.7	0.1	CTD/rosette water sampler	CTD/RO	at depth	EL 31: 3486 m ausgesteckt
PS62/126-1	27.07.02	20:57	75° 0.02' N	8° 44.24' E	2671.0	SE 5	216.7	0.9	CTD/rosette water sampler	CTD/RO	at depth	ausgesteckt 2611 m,Missweisung 3,7 W
PS62/127-1	27.07.02	23:35	74° 59.92' N	9° 21.14' E	2609.0	SSE 7	46.7	0.7	CTD/rosette water sampler	CTD/RO	at depth	2556 m ausgesteckt, MW=1,8 W
PS62/128-1	28.07.02	02:08	74° 59.75' N	10° 0.17' E	2586.0	SSW 8	253.0	0.3	CTD/rosette water sampler	CTD/RO	at depth	2532 m ausgesteckt; Mw 1,3°W
PS62/129-1	28.07.02	04:37	74° 59.93' N	10° 39.71' E	2540.0	S 8	26.0	0.5	CTD/rosette water sampler	CTD/RO	at depth	2487m

Station	Date	Time	PositionLat	PositionLon	Depth [m]	Windstrength [m/s]	Course [°]	Speed [kn]	Gear	Gear Abbreviation	Action	Comment
PS62/130-1	28.07.02	07:02	74° 59.98' N	11° 17.98' E	2458.0	S 9	357.2	0.4	CTD/rosette water sampler	CTD/RO	at depth	2407 m
PS62/131-1	28.07.02	09:27	74° 59.91' N	11° 55.07' E	2340.0	S 8	197.8	0.3	CTD/rosette water sampler	CTD/RO	at depth	Missweisung 0,1 E,Ausgesteckt 2275 m
PS62/132-1	28.07.02	12:21	74° 59.61' N	12° 35.09' E	2192.0	S 9	350.1	0.9	CTD/rosette water sampler	CTD/RO	at depth	2141 m ausgesteckt; Mw.0.6°E
PS62/133-1	28.07.02	14:57	74° 59.87' N	13° 13.35' E	2017.0	S 8	219.3	0.4	CTD/rosette water sampler	CTD/RO	at depth	1966 m ausgesteckt; Mw.1.0°E
PS62/134-1	28.07.02	17:13	75° 0.12' N	13° 51.76' E	1802.0	S 8	215.4	0.5	CTD/rosette water sampler	CTD/RO	at depth	1753 m
PS62/135-1	28.07.02	19:32	74° 59.81' N	14° 31.65' E	1434.0	SSE 7	191.9	0.6	CTD/rosette water sampler	CTD/RO	at depth	1404 m
PS62/136-1	28.07.02	21:25	75° 0.12' N	15° 10.01' E	1024.0	SE 6	222.4	0.8	CTD/rosette water sampler	CTD/RO	at depth	ausgesteckt 1008m, Missweisung 2,6 E
PS62/137-1	28.07.02	22:51	74° 59.97' N	15° 49.53' E	275.1	SE 6	108.9	0.8	CTD/rosette water sampler	CTD/RO	at depth	Missweisung 2,9 E ausgesteckt 262 m
PS62/138-1	29.07.02	00:22	75° 0.06' N	16° 29.17' E	265.7	ENE 5	291.1	0.4	CTD/rosette water sampler	CTD/RO	at depth	250 m ausgesteckt; Mw.3.4°E
PS62/139-1	29.07.02	01:52	75° 0.30' N	17° 6.26' E	169.6	SE 3	18.5	0.7	CTD/rosette water sampler	CTD/RO	at depth	149 m ausgesteckt; 3.9°E
PS62/139-1	29.07.02	01:56	75° 0.32' N	17° 6.40' E	170.0	SE 4	76.9	1.1	CTD/rosette water sampler	CTD/RO	on deck	
ARK 18-1/b												
PS62/140-1	31.07.02	11:30	78° 49.94' N	8° 36.69' E	384.5	N 10	197.1	1.4	Mooring (year)	MOORY	on deck	Geräte an Deck
PS62/140-2	31.07.02	11:55	78° 49.81' N	8° 35.12' E	449.0	NNW 8	250.7	0.9	CTD/rosette water sampler	CTD/RO	at depth	436 m ausgesteckt
PS62/141-1	31.07.02	12:56	78° 50.27' N	8° 18.57' E	814.4	NNW 10	168.5	2.0	Mooring (year)	MOORY	action	Toppboje an Deck
PS62/141-1	31.07.02	13:05	78° 50.10' N	8° 18.46' E	816.1	N 10	263.3	0.4	Mooring (year)	MOORY	action	Rest der Verankerung abgerissen und verloren
PS62/141-2	31.07.02	14:02	78° 50.58' N	8° 17.73' E	824.7	NNW 9	330.3	0.5	CTD/rosette water sampler	CTD/RO	at depth	801 m ausgesteckt
PS62/142-1	31.07.02	15:37	78° 49.98' N	7° 55.92' E	1061.0	N 10	202.6	1.1	Mooring (year)	MOORY	action	Verankerung nicht aufgetaucht; gilt als verloren nach Bergen der Toppeinheit durch RV "Lance"
PS62/142-2	31.07.02	16:07	78° 50.12' N	7° 55.05' E	1065.0	NNW 11	331.2	0.7	CTD/rosette water sampler	CTD/RO	at depth	1039 m
PS62/143-1	31.07.02	18:41	78° 50.42' N	6° 55.03' E	1560.0	NNW 9	330.1	0.7	Mooring (year)	MOORY	on deck	
PS62/143-2	31.07.02	19:22	78° 50.15' N	6° 56.24' E	1530.0	NW 9	64.4	0.2	CTD/rosette water sampler	CTD/RO	at depth	1492 m
PS62/144-1	31.07.02	20:49	78° 50.08' N	7° 8.97' E	1369.0	NW 9	328.7	0.3	MultiCorer	MUC	at sea bottom	
PS62/144-1	31.07.02	20:53	78° 50.12' N	7° 8.86' E	1369.0	NW 10	324.5	0.5	MultiCorer	MUC	at sea bottom	1330 m ausgesteckt
PS62/144-1	31.07.02	20:56	78° 50.16' N	7° 8.76' E	1371.0	NW 10	323.3	0.6	MultiCorer	MUC	at sea bottom	
PS62/144-2	31.07.02	22:29	78° 50.18' N	7° 9.36' E	1367.0	NW 9	312.8	0.8	CTD/rosette water sampler	CTD/RO	at depth	1326 m ausgesteckt, MW 4.3 W
PS62/145-1	01.08.02	00:19	78° 49.96' N	6° 30.31' E	1983.0	WNW 12	121.6	0.3	CTD/rosette water sampler	CTD/RO	at depth	1931 m ausgesteckt
PS62/146-1	01.08.02	02:05	78° 49.63' N	6° 9.21' E	2386.0	WNW 12	228.6	0.5	CTD/rosette water sampler	CTD/RO	at depth	2339 m ausgesteckt
PS62/147-1	01.08.02	04:13	78° 49.92' N	5° 39.74' E	2584.0	WNW 10	306.8	0.0	CTD/rosette water sampler	CTD/RO	at depth	2533 m
PS62/148-1	01.08.02	06:07	78° 49.69' N	5° 20.18' E	2627.0	WNW 10	197.5	0.3	CTD/rosette water sampler	CTD/RO	at depth	2590 m
PS62/149-1	01.08.02	08:46	78° 58.07' N	6° 43.06' E	1410.0	NW 10	280.9	1.5	Mooring	MOR	action	Hydrophon zu Wasser
PS62/149-1	01.08.02	08:50	78° 58.06' N	6° 42.75' E	1416.0	NW 9	258.5	0.5	Mooring	MOR	action	Lander ausgelöst
PS62/149-1	01.08.02	09:33	78° 57.87' N	6° 41.63' E	1462.0	NW 10	264.5	0.5	Mooring	MOR	action	DREDGE WIRD GEFIERT
PS62/149-1	01.08.02	14:02	78° 58.63' N	6° 36.32' E	1448.0	NW 7	234.0	0.4	Mooring	MOR	action	Dredge vom Grund
PS62/149-1	01.08.02	14:52	78° 58.89' N	6° 34.05' E	1460.0	NNW 7	326.5	1.5	Mooring	MOR	action	Letzter Draggen an Deck/Kein Erfolg
PS62/150-1	01.08.02	17:16	78° 52.96' N	7° 57.18' E	1074.0	NNW 7	352.5	0.3	Mooring (year)	MOORY	action	Hydrophone zu Wasser
PS62/150-1	01.08.02	17:18	78° 52.96' N	7° 57.18' E	1075.0	NNW 6	308.9	0.0	Mooring (year)	MOORY	action	Signal ~2100m
PS62/150-1	01.08.02	17:30	78° 52.93' N	7° 57.55' E	1071.0	NNW 7	115.0	0.6	Mooring (year)	MOORY	action	Wellen ausgekuppelt
PS62/150-1	01.08.02	17:41	78° 52.86' N	7° 58.00' E	1066.0	NNW 7	145.1	0.6	Mooring (year)	MOORY	action	Transponder Kontakt
PS62/150-1	01.08.02	17:58	78° 51.93' N	7° 57.07' E	1075.0	N 8	223.8	0.3	Mooring (year)	MOORY	action	Hydrophone z. W. ruhiges Schiff

Station	Date	Time	PositionLat	PositionLon	Depth [m]	Windstrength [m/s]	Course [°]	Speed [kn]	Gear	Gear Abbreviation	Action	Comment
PS62/150-1	01.08.02	18:54	78° 51.25' N	7° 55.71' E	1077.0	NNW 8	199.7	0.9	Mooring (year)	MOORY	action	ausgelöst
PS62/150-1	01.08.02	18:55	78° 51.24' N	7° 55.67' E	1077.0	NNW 8	200.6	0.8	Mooring (year)	MOORY	action	Hubschrauber in der Luft
PS62/150-1	01.08.02	19:30	78° 49.96' N	8° 0.34' E	1027.0	NNW 9	204.3	1.6	Mooring (year)	MOORY	action	
PS62/150-1	01.08.02	19:31	78° 49.94' N	8° 0.25' E	1029.0	NNW 9	232.6	1.9	Mooring (year)	MOORY	action	Hubschrauber zurück
PS62/151-1	01.08.02	20:24	78° 50.00' N	7° 59.71' E	1035.0	NNW 8	339.3	0.0	Mooring (year)	MOORY	action	Toppeinheit mit Auslöser zu Wasser
PS62/151-1	01.08.02	21:06	78° 50.01' N	7° 59.72' E	1035.0	NNW 10	352.9	0.0	Mooring (year)	MOORY	action	Verankerung ausgelöst
PS62/152-1	01.08.02	21:36	78° 50.07' N	7° 54.40' E	1068.0	NNW 8	255.7	1.1	CTD	CTD	at depth	
PS62/153-1	01.08.02	23:00	78° 50.20' N	7° 28.99' E	1182.0	NNW 8	333.6	0.6	CTD	CTD	at depth	1148 m ausgesteckz
PS62/154-1	02.08.02	00:35	78° 50.06' N	8° 9.14' E	947.3	NNW 9	317.6	0.7	CTD/rosette water sampler	CTD/RO	at depth	927 m ausgesteckt
PS62/155-1	02.08.02	01:35	78° 50.16' N	8° 29.73' E	592.2	NNW 10	280.1	0.3	CTD/rosette water sampler	CTD/RO	at depth	570 m ausgesteckt
PS62/156-1	02.08.02	02:24	78° 50.05' N	8° 50.21' E	238.2	N 9	282.6	0.4	CTD/rosette water sampler	CTD/RO	at depth	228 m ausgesteckt
PS62/157-1	02.08.02	02:56	78° 50.08' N	8° 59.60' E	217.1	N 10	272.8	0.2	CTD/rosette water sampler	CTD/RO	at depth	207 m ausgesteckt
PS62/157-2	02.08.02	03:14	78° 50.08' N	8° 59.34' E	216.7	N 11	338.6	0.5	MultiCorer	MUC	at sea bottom	214 m ausgesteckt
PS62/158-1	02.08.02	06:29	78° 49.96' N	8° 39.90' E	248.3	N 11	2.6	0.0	Mooring (year)	MOORY	surface	mit 44 m Geodraht auf den Boden gefiert und ausgelöst
PS62/159-1	02.08.02	09:03	78° 50.02' N	8° 19.78' E	795.7	N 10	315.4	0.2	Mooring (year)	MOORY	at depth	Toppkugeln mit Sender zu Wasser, Verankerung ausgelöst
PS62/160-1	02.08.02	13:08	78° 49.66' N	5° 48.89' E	2538.0	NNE 9	223.3	0.9	Mooring (year)	MOORY	action	Verankerung komplett geborgen
PS62/160-2	02.08.02	14:12	78° 50.31' N	5° 50.66' E	2536.0	NNE 11	299.1	0.3	CTD/rosette water sampler	CTD/RO	at depth	2485 m ausgesteckt
PS62/161-1	02.08.02	18:57	79° 3.88' N	4° 10.74' E	2476.0	NNE 10	34.1	0.0	Bottom water sampler	BWS	at sea bottom	
PS62/161-2	02.08.02	21:16	79° 3.90' N	4° 10.93' E	2469.0	NNE 10	318.0	0.2	Sequentieller Multiple Corer	S-MUC	on the bottom	2417 m ausgesteckt
PS62/161-3	03.08.02	00:31	79° 2.00' N	4° 9.94' E	2634.0	NNW 9	188.8	0.4	Ocean Floor Observ. System	OFOS	at depth	
PS62/161-3	03.08.02	05:02	79° 3.86' N	4° 17.25' E	2416.0	NNE 8	33.3	0.6	Ocean Floor Observ. System	OFOS	Start Hoisting	
PS62/161-4	03.08.02	06:15	79° 4.43' N	4° 8.42' E	2494.0	NE 7	332.7	0.6	Bottom lander, profile	BL_P	into the water	MIC Mikroprofiler
PS62/161-5	03.08.02	07:25	79° 4.50' N	4° 7.59' E	2497.0	NNE 6	210.9	0.1	Bottom lander, chamber	BL_C	lander into water	UKW Sendertest 159,475 o.K. 1 kammer arbeitet nicht
PS62/162-1	03.08.02	08:59	79° 6.53' N	4° 36.09' E	1918.0	NNE 8	245.0	0.5	Bottom water sampler	BWS	at sea bottom	
PS62/162-1	03.08.02	09:06	79° 6.52' N	4° 35.90' E	1920.0	NNE 9	34.0	0.3	Bottom water sampler	BWS	off bottom	
PS62/162-2	03.08.02	10:47	79° 6.51' N	4° 36.40' E	1928.0	NNE 6	59.0	0.1	MultiCorer	MUC	at sea bottom	1866 m ausgesteckt
PS62/161-4	03.08.02	13:18	79° 4.07' N	4° 8.39' E	2499.0	NE 5	187.4	0.6	Bottom lander, profile	BL_P	released	Nochmals ausgelöst, Lander steigt auf
PS62/163-1	03.08.02	16:24	79° 4.78' N	3° 36.09' E	3306.0	NE 5	2.1	0.0	Bottom water sampler	BWS	at sea bottom	3235 m
PS62/163-1	03.08.02	16:32	79° 4.77' N	3° 36.06' E	3310.0	NE 5	209.8	0.2	Bottom water sampler	BWS	off bottom	
PS62/163-2	03.08.02	19:09	79° 5.10' N	3° 32.40' E	3640.0	ENE 1	353.1	0.0	Sequentieller Multiple Corer	S-MUC	on the bottom	3591 m
PS62/163-2	03.08.02	19:15	79° 5.10' N	3° 32.45' E	3638.0	ENE 1	113.4	0.2	Sequentieller Multiple Corer	S-MUC	on the bottom	2. mal
PS62/163-2	03.08.02	19:21	79° 5.10' N	3° 32.54' E	3636.0	ENE 1	66.4	0.3	Sequentieller Multiple Corer	S-MUC	on the bottom	3.mal
PS62/163-2	03.08.02	19:25	79° 5.11' N	3° 32.59' E	3627.0	E 1	27.4	0.2	Sequentieller Multiple Corer	S-MUC	off bottom	
PS62/163-3	03.08.02	22:34	79° 3.00' N	3° 30.97' E	3958.0	E 2	97.8	1.4	Ocean Floor Observ. System	OFOS	at depth	4128 m ausgesteckt
PS62/163-3	04.08.02	03:37	79° 2.99' N	3° 42.04' E	2903.0	SSE 4	100.0	0.0	Ocean Floor Observ. System	OFOS	Start Hoisting	
PS62/163-4	04.08.02	05:08	79° 5.24' N	3° 33.11' E	3613.0	SSE 5	230.0	0.5	Bottom lander, profile	BL_P	into the water	
PS62/161-5	04.08.02	06:09	79° 4.55' N	4° 8.22' E	2491.0	SSE 5	259.1	0.0	Bottom lander, chamber	BL_C	Lander released	
PS62/161-5	04.08.02	06:47	79° 4.54' N	4° 8.32' E	2493.0	SSE 4	84.6	0.6	Bottom lander, chamber	BL_C	lander afloat	
PS62/164-1	04.08.02	11:58	78° 49.96' N	7° 0.18' E	1471.0	SSE 3	123.0	0.0	Mooring	MOR	action	Ankerstein u. Doppel-releaser zu Wasser
PS62/164-1	04.08.02	13:14	78° 49.95' N	7° 0.03' E	1472.0	S 3	311.6	0.3	Mooring	MOR	released	

Station	Date	Time	PositionLat	PositionLon	Depth [m]	Windstrength [m/s]	Course [°]	Speed [kn]	Gear	Gear Abbreviation	Action	Comment
PS62/165-1	04.08.02	14:40	78° 49.81' N	5° 59.58' E	2477.0	S 2	123.6	0.4	Mooring	MOR	action	Ankerstein, Doppel-releaser, 5 Benthos + Strömungsmesser zu Wasser
PS62/165-1	04.08.02	16:03	78° 49.96' N	6° 0.16' E	2477.0	SSW 3	195.1	0.0	Mooring	MOR	released	
PS62/166-1	04.08.02	19:00	78° 49.89' N	5° 5.13' E	2675.0	WSW 1	44.5	1.2	Mooring (year)	MOORY	on deck	
PS62/166-2	04.08.02	20:03	78° 50.09' N	5° 4.33' E	2687.0	W 3	85.8	0.9	CTD/rosette water sampler	CTD/RO	at depth	2639 m
PS62/167-1	04.08.02	22:26	78° 49.96' N	4° 40.04' E	2592.0	SW 2	254.8	0.5	CTD/rosette water sampler	CTD/RO	at depth	2570 m ausgesteckt
PS62/168-1	05.08.02	00:17	78° 50.23' N	4° 19.72' E	2402.0	SSW 3	292.3	0.3	CTD/rosette water sampler	CTD/RO	at depth	2353 m ausgesteckt
PS62/169-1	05.08.02	03:40	79° 3.83' N	3° 42.64' E	2936.0	SSW 4	293.5	0.5	Bottom water sampler	BWS	at sea bottom	2884 m ausgesteckt
PS62/169-1	05.08.02	03:47	79° 3.89' N	3° 42.76' E	2945.0	SW 4	39.0	0.8	Bottom water sampler	BWS	off bottom	
PS62/169-2	05.08.02	05:58	79° 3.99' N	3° 43.45' E	2899.0	SW 6	207.1	0.0	Sequentieller Multiple Corer	S-MUC	on the bottom	
PS62/169-2	05.08.02	06:16	79° 3.99' N	3° 43.35' E	2910.0	SW 6	207.1	0.0	Sequentieller Multiple Corer	S-MUC	off bottom	max 2838 m
PS62/163-4	05.08.02	07:50	79° 5.32' N	3° 32.51' E	3727.0	SW 5	326.6	0.3	Bottom lander, profile	BL_P	released	Releaser hat geant-wortet, Lander steigt
PS62/163-4	05.08.02	09:12	79° 5.47' N	3° 33.79' E	3553.0	SW 4	65.1	1.0	Bottom lander, profile	BL_P	on deck	
PS62/170-1	05.08.02	11:39	79° 7.83' N	4° 53.86' E	1560.0	SSW 3	148.8	0.8	Bottom water sampler	BWS	at sea bottom	
PS62/170-2	05.08.02	13:00	79° 7.84' N	4° 53.91' E	1559.0	S 2	330.0	0.0	Sequentieller Multiple Corer	S-MUC	on the bottom	1517 m ausgesteckt
PS62/170-3	05.08.02	14:43	79° 6.90' N	4° 50.65' E	1701.0	S 3	25.1	0.0	Ocean Floor Observ. System	OFOS	at depth	
PS62/170-3	05.08.02	19:41	79° 9.14' N	4° 59.68' E	1405.0	SE 5	38.9	0.5	Ocean Floor Observ. System	OFOS	Start Hoisting	
PS62/170-4	05.08.02	20:45	79° 7.78' N	4° 53.36' E	1581.0	SE 4	264.6	0.3	Bottom lander, profile	BL_P	into the water	
PS62/171-1	05.08.02	23:04	79° 8.44' N	6° 6.37' E	1292.0	SE 6	4.5	0.3	Bottom water sampler	BWS	at sea bottom	
PS62/171-2	06.08.02	00:16	79° 8.44' N	6° 5.49' E	1292.0	ESE 7	140.3	0.0	Sequentieller Multiple Corer	S-MUC	on the bottom	1266 m ausgesteckt
PS62/172-1	06.08.02	00:58	79° 8.24' N	6° 4.55' E	1288.0	ESE 7	263.7	5.2	HydroSweep/ParaSound profile	HS_PS	start track	
PS62/172-1	06.08.02	04:11	79° 7.79' N	4° 54.61' E	1551.0	ESE 6	269.7	3.8	HydroSweep/ParaSound profile	HS_PS	alter course	
PS62/172-1	06.08.02	05:09	79° 6.45' N	4° 35.79' E	1932.0	ESE 7	242.6	4.0	HydroSweep/ParaSound profile	HS_PS	alter course	
PS62/172-1	06.08.02	06:26	79° 3.98' N	4° 11.89' E	2451.0	E 10	240.3	4.2	HydroSweep/ParaSound profile	HS_PS	alter course	
PS62/172-1	06.08.02	07:48	79° 3.89' N	3° 41.65' E	3003.0	E 9	270.3	4.4	HydroSweep/ParaSound profile	HS_PS	profile end	
PS62/170-4	06.08.02	09:45	79° 7.73' N	4° 53.31' E	1577.0	ESE 9	166.5	0.2	Bottom lander, profile	BL_P	released	
PS62/173-1	06.08.02	12:30	78° 49.99' N	5° 0.36' E	2708.0	SE 12	295.0	0.1	Mooring (year)	MOORY	surface	Ankerstein, Doppelreleaser, Strömungsmesser+5 Benthos zu Wasser
PS62/173-1	06.08.02	13:22	78° 50.03' N	5° 0.52' E	2704.0	ESE 11	201.9	0.4	Mooring (year)	MOORY	action	ausgelöst
PS62/174-1	06.08.02	14:46	78° 49.98' N	4° 2.32' E	2372.0	SE 12	345.6	1.3	Mooring	MOR	released	
PS62/174-1	06.08.02	16:17	78° 50.97' N	4° 4.45' E	2406.0	SE 13	136.0	0.0	Mooring	MOR	on deck	alles an Deck
PS62/174-2	06.08.02	17:14	78° 50.14' N	4° 3.68' E	2378.0	SE 13	79.0	0.5	CTD/rosette water sampler	CTD/RO	at depth	2328 m
PS62/174-3	06.08.02	20:08	78° 50.00' N	4° 0.01' E	2348.0	SE 14	359.4	0.2	Mooring (year)	MOORY	at depth	Ankerstein mit 55 m Geodraht abgesetzt
PS62/175-1	06.08.02	21:35	79° 3.50' N	3° 50.31' E	2738.0	SE 11	351.4	9.6	HydroSweep/ParaSound profile	HS_PS	start track	
PS62/175-1	06.08.02	21:52	79° 3.90' N	3° 43.41' E	2874.0	ESE 12	276.6	5.2	HydroSweep/ParaSound profile	HS_PS	alter course	
PS62/175-1	06.08.02	22:45	79° 4.48' N	3° 22.05' E	4817.0	SE 12	277.2	4.4	HydroSweep/ParaSound profile	HS_PS	alter course	
PS62/175-1	07.08.02	00:11	79° 8.13' N	2° 54.41' E	5576.0	SE 11	305.9	4.0	HydroSweep/ParaSound profile	HS_PS	profile end	
PS62/176-1	07.08.02	02:20	79° 8.44' N	4° 5.60' E	2072.0	SE 11	291.3	0.3	MultiCorer	MUC	at sea bottom	2032 m ausgesteckt
PS62/177-1	07.08.02	04:14	79° 7.27' N	4° 39.95' E	1844.0	SE 12	288.5	0.2	MultiCorer	MUC	at sea bottom	1804 m
PS62/178-1	07.08.02	06:13	79° 4.50' N	4° 7.95' E	2498.0	SE 10	300.5	0.4	Bottom lander, chamber	BL_C	lander into water	Sendertest 159,475 i. O.
PS62/179-1	07.08.02	07:50	79° 1.84' N	4° 20.63' E	2549.0	SE 10	52.6	0.4	Mooring	MOR	action	Toppeinheit an Deck
PS62/179-1	07.08.02	09:03	79° 2.25' N	4° 22.25' E	2512.0	SE 9	309.2	0.3	Mooring	MOR	releaser on deck	
PS62/179-2	07.08.02	09:59	79° 1.04' N	4° 19.53' E	2597.0	SE 8	291.9	0.4	Mooring (year)	MOORY	surface	Ankerstein zu wasser
PS62/179-2	07.08.02	11:26	79° 1.03' N	4° 19.82' E	2593.0	SE 8	180.0	0.0	Mooring (year)	MOORY	action	Releaser mit Topkugeln zu wasser

Station	Date	Time	PositionLat	PositionLon	Depth [m]	Windstrength [m/s]	Course [°]	Speed [kn]	Gear	Gear Abbreviation	Action	Comment
PS62/179-2	07.08.02	11:29	79° 1.04' N	4° 19.77' E	2593.0	SE 8	329.1	0.5	Mooring (year)	MOORY	at depth	
PS62/180-1	07.08.02	13:42	79° 6.18' N	4° 20.08' E	2335.0	SSE 8	103.3	2.3	Agassiz trawl	AGT	AGT on ground	
PS62/180-1	07.08.02	13:51	79° 6.16' N	4° 21.50' E	2337.0	SSE 7	97.1	1.9	Agassiz trawl	AGT	start trawl	3400 m ausgesteckt
PS62/180-1	07.08.02	14:10	79° 6.11' N	4° 22.98' E	2338.0	SSE 6	110.9	0.7	Agassiz trawl	AGT	Stop Trawl	Beginn Hieven mit 0,5 m/s
PS62/180-1	07.08.02	14:53	79° 6.06' N	4° 24.53' E	2343.0	WNW 3	113.7	0.5	Agassiz trawl	AGT	AGT off ground	
PS62/181-1	07.08.02	18:10	79° 4.52' N	4° 9.82' E	2469.0	WNW 3	334.1	0.0	Sequentieller Multiple Corer	S-MUC	on the bottom	72.1 : 2409 m ausgesteckt
PS62/181-1	07.08.02	18:18	79° 4.52' N	4° 9.82' E	2465.0	WNW 2	17.4	0.2	Sequentieller Multiple Corer	S-MUC	off bottom	
PS62/182-1	07.08.02	20:38	79° 6.20' N	4° 20.03' E	2336.0	NW 3	95.7	1.9	Agassiz trawl	AGT	AGT on ground	
PS62/182-1	07.08.02	20:49	79° 6.17' N	4° 21.65' E	2337.0	NW 3	85.2	1.1	Agassiz trawl	AGT	start trawl	
PS62/182-1	07.08.02	20:59	79° 6.15' N	4° 22.44' E	2336.0	NW 3	84.4	0.8	Agassiz trawl	AGT	Stop Trawl	
PS62/182-1	07.08.02	21:00	79° 6.15' N	4° 22.50' E	2335.0	NW 3	86.4	0.4	Agassiz trawl	AGT	Start hoisting	
PS62/182-1	07.08.02	21:46	79° 6.24' N	4° 19.48' E	2337.0	NW 3	279.8	0.7	Agassiz trawl	AGT	AGT off ground	
PS62/178-1	08.08.02	00:04	79° 4.47' N	4° 7.71' E	2499.0	N 2	284.6	0.2	Bottom lander, chamber	BL_C	Lander released	
PS62/178-1	08.08.02	00:42	79° 4.11' N	4° 8.21' E	2507.0	NNW 3	118.7	0.3	Bottom lander, chamber	BL_C	lander afloat	
PS62/183-1	08.08.02	03:29	79° 3.63' N	3° 28.20' E	4093.0	ENE 2	270.3	0.0	Bottom water sampler	BWS	at sea bottom	
PS62/183-1	08.08.02	03:37	79° 3.63' N	3° 28.11' E	4095.0	NE 2	327.8	0.1	Bottom water sampler	BWS	off bottom	72.1: 4073 m ausgesteckt
PS62/183-2	08.08.02	06:45	79° 3.60' N	3° 28.87' E	4039.0	N 1	281.5	0.0	Sequentieller Multiple Corer	S-MUC	on the bottom	4003 m
PS62/183-2	08.08.02	07:01	79° 3.63' N	3° 28.78' E	4057.0	NNE 1	12.0	0.1	Sequentieller Multiple Corer	S-MUC	off bottom	
PS62/184-1	08.08.02	11:18	79° 7.89' N	2° 55.29' E	5571.0	ESE 1	99.6	0.1	Bottom water sampler	BWS	at sea bottom	32.1: 5558 m ausgesteckt
PS62/184-1	08.08.02	11:59	79° 7.83' N	2° 56.24' E	5569.0	W 2	277.5	0.2	Bottom water sampler	BWS	off bottom	
PS62/184-2	08.08.02	15:46	79° 8.21' N	2° 51.22' E	5582.0	NNE 2	290.7	0.9	Sequentieller Multiple Corer	S-MUC	on the bottom	5545 m ausgesteckt
PS62/184-2	08.08.02	16:03	79° 8.20' N	2° 51.46' E	5581.0	NNW 3	113.0	0.2	Sequentieller Multiple Corer	S-MUC	off bottom	
PS62/184-3	08.08.02	20:51	79° 8.14' N	2° 51.71' E	5579.0	NNW 2	306.8	0.0	Bottom lander, profile	BL_P	released	Gerät im Grund, ausgesteckt 5568 m, Beginn Messen
PS62/184-3	08.08.02	22:51	79° 8.14' N	2° 51.69' E	5584.0	NNW 3	339.5	0.0	Bottom lander, profile	BL_P	released	Beginn Hieven Tiefe:5573 m
PS62/185-1	09.08.02	03:19	79° 4.57' N	3° 21.31' E	5047.0	N 4	51.8	0.2	Bottom water sampler	BWS	at sea bottom	5051 m ausgesteckt
PS62/185-1	09.08.02	03:26	79° 4.56' N	3° 21.20' E	5086.0	N 4	241.7	0.4	Bottom water sampler	BWS	off bottom	
PS62/185-2	09.08.02	06:51	79° 4.54' N	3° 21.06' E	5128.0	N 6	43.8	0.1	CTD/rosette water sampler	CTD/RO	at depth	5163 m
PS62/185-3	09.08.02	11:10	79° 4.52' N	3° 19.63' E	5231.0	N 3	276.1	0.5	Sequentieller Multiple Corer	S-MUC	on the bottom	5089 m ausgesteckt
PS62/185-3	09.08.02	11:29	79° 4.51' N	3° 19.80' E	5230.0	N 5	46.2	0.4	Sequentieller Multiple Corer	S-MUC	off bottom	
PS62/186-1	09.08.02	14:40	78° 49.92' N	2° 32.39' E	2531.0	N 4	227.3	0.7	Mooring	MOR	released	
PS62/186-1	09.08.02	16:20	78° 49.29' N	2° 29.33' E	2539.0	N 3	204.7	1.1	Mooring	MOR	on deck	letzte Paket an Deck
PS62/186-2	09.08.02	17:27	78° 50.12' N	2° 32.75' E	2527.0	NW 3	300.0	0.3	CTD/rosette water sampler	CTD/RO	at depth	2478 m
PS62/186-3	09.08.02	18:34	78° 49.87' N	2° 48.97' E	2491.0	NW 4	305.5	0.5	Mooring (year)	MOORY	surface	Ankerstein& 2 Releaser
PS62/186-3	09.08.02	20:24	78° 50.00' N	2° 48.15' E	2495.0	NNW 3	319.9	0.6	Mooring (year)	MOORY	action	Toppboje zu Wasser, Ausgelöst
PS62/186-4	09.08.02	21:38	78° 49.47' N	2° 48.15' E	2505.0	NNW 3	245.5	0.3	CTD	CTD	at depth	2453 m ausgesteckt
PS62/187-1	09.08.02	23:45	78° 50.02' N	3° 24.73' E	2373.0	NNE 5	152.4	0.2	CTD	CTD	at depth	2323 m ausgesteckt
PS62/188-1	10.08.02	01:28	78° 50.19' N	3° 39.49' E	2309.0	N 3	248.7	0.2	CTD/rosette water sampler	CTD/RO	at depth	2258 m ausgesteckt
PS62/188-1	10.08.02	01:28	78° 50.19' N	3° 39.49' E	2309.0	N 3	248.7	0.2	CTD/rosette water sampler	CTD/RO	at depth	2258 m ausgesteckt
PS62/189-1	10.08.02	05:12	78° 34.93' N	5° 4.05' E	2343.0	NNE 5	235.0	0.2	Bottom water sampler	BWS	at sea bottom	2293 m
PS62/189-1	10.08.02	05:20	78° 34.94' N	5° 4.08' E	2346.0	NNE 4	54.7	0.0	Bottom water sampler	BWS	off bottom	
PS62/189-2	10.08.02	07:01	78° 34.96' N	5° 4.21' E	2343.0	NNW 5	55.4	0.0	Sequentieller Multiple Corer	S-MUC	on the bottom	2290 m
PS62/189-2	10.08.02	07:14	78° 34.97' N	5° 4.21' E	2344.0	NNW 5	258.8	0.3	Sequentieller Multiple Corer	S-MUC	off bottom	
PS62/189-3	10.08.02	08:55	78° 34.98' N	5° 5.00' E	2340.0	NNW 6	97.8	0.2	Bottom water sampler	BWS	at sea bottom	2292 m ausgesteckt
PS62/189-3	10.08.02	09:00	78° 34.98' N	5° 5.08' E	2339.0	NNW 4	122.3	0.1	Bottom water sampler	BWS	off bottom	

Station	Date	Time	PositionLat	PositionLon	Depth [m]	Windstrength [m/s]	Course [°]	Speed [kn]	Gear	Gear Abbreviation	Action	Comment
PS62/190-1	10.08.02	12:52	78° 50.00' N	6° 29.24' E	2006.0	NNW 9	223.5	0.2	CTD/rosette water sampler	CTD/RO	at depth	1949 m ausgesteckt
PS62/191-1	10.08.02	16:14	79° 8.08' N	5° 59.66' E	1299.0	N 6	306.5	0.7	Ocean Floor Observ. System	OFOS	at depth	
PS62/191-1	10.08.02	20:39	79° 8.03' N	5° 46.52' E	1325.0	NNW 7	276.3	0.8	Ocean Floor Observ. System	OFOS	Start Hoisting	
PS62/191-2	10.08.02	22:00	79° 7.99' N	5° 48.11' E	1314.0	N 8	88.0	1.4	Agassiz trawl	AGT	AGT on ground	
PS62/191-2	10.08.02	22:06	79° 7.98' N	5° 48.83' E	1314.0	NNE 8	88.6	1.1	Agassiz trawl	AGT	start trawl	
PS62/191-2	10.08.02	22:21	79° 7.95' N	5° 49.97' E	1315.0	N 7	99.3	1.0	Agassiz trawl	AGT	Stop Trawl	
PS62/191-2	10.08.02	22:26	79° 7.92' N	5° 50.19' E	1316.0	N 8	186.1	0.6	Agassiz trawl	AGT	Start hoisting	
PS62/191-2	10.08.02	22:42	79° 7.77' N	5° 49.24' E	1308.0	NNE 6	245.8	0.8	Agassiz trawl	AGT	AGT off ground	
PS62/192-1	11.08.02	03:16	79° 35.06' N	5° 15.60' E	2670.0	NNE 6	161.5	0.2	Bottom water sampler	BWS	at sea bottom	2631 m ausgesteckt
PS62/192-1	11.08.02	03:22	79° 35.06' N	5° 15.63' E	2667.0	N 7	27.6	0.1	Bottom water sampler	BWS	off bottom	
PS62/192-2	11.08.02	05:22	79° 35.02' N	5° 15.33' E	2668.0	N 7	331.5	0.1	Sequentieller Multiple Corer	S-MUC	on the bottom	
PS62/192-2	11.08.02	05:43	79° 35.12' N	5° 15.08' E	2694.0	NNE 7	333.3	0.2	Sequentieller Multiple Corer	S-MUC	off bottom	
PS62/193-1	11.08.02	10:58	79° 4.34' N	4° 9.19' E	2484.0	N 8	190.2	0.3	Sequentieller Multiple Corer	S-MUC	on the bottom	2419 m ausgesteckt
PS62/193-1	11.08.02	11:13	79° 4.26' N	4° 9.12' E	2493.0	N 8	180.8	0.4	Sequentieller Multiple Corer	S-MUC	off bottom	
PS62/193-2	11.08.02	12:11	79° 4.19' N	4° 8.87' E	2499.0	N 8	189.1	0.2	Bottom lander	LANDER	surface	Bleibt für ein Jahr am Grund
PS62/194-1	11.08.02	13:32	78° 58.82' N	3° 16.12' E	2594.0	NNE 6	249.8	0.5	Eisfischen	EF		
PS62/194-1	11.08.02	13:47	78° 58.69' N	3° 16.03' E	2515.0	N 6	162.0	0.4	Eisfischen	EF		
PS62/195-1	11.08.02	17:10	78° 50.12' N	1° 32.81' E	2549.0	N 5	296.8	0.9	CTD/rosette water sampler	CTD/RO	at depth	2515 m
PS62/195-2	11.08.02	18:05	78° 49.89' N	1° 38.32' E	2552.0	N 5	336.6	0.7	Mooring (year)	MOORY	surface	Ankerstein
PS62/195-2	11.08.02	19:12	78° 49.96' N	1° 36.72' E	2554.0	N 5	359.3	0.0	Mooring (year)	MOORY	at depth	69m auf Grund gefiert&ausgelöäst
PS62/196-1	11.08.02	21:01	78° 49.99' N	2° 12.41' E	2547.0	NNW 5	225.8	0.8	CTD/rosette water sampler	CTD/RO	at depth	2498 m ausgesteckt
PS62/197-1	11.08.02	22:57	78° 49.95' N	1° 54.98' E	2563.0	N 4	279.4	0.3	CTD	CTD	at depth	2509 m ausgesteckt
PS62/198-1	12.08.02	01:11	78° 50.06' N	1° 18.85' E	2524.0	NNW 4	248.8	0.2	CTD/rosette water sampler	CTD/RO	at depth	2474 m ausgesteckt
PS62/199-1	12.08.02	02:59	78° 50.08' N	0° 59.89' E	2499.0	N 4	318.6	0.4	CTD/rosette water sampler	CTD/RO	at depth	2446 m ausgesteckt
PS62/200-1	12.08.02	04:49	78° 50.05' N	0° 42.53' E	2468.0	N 3	89.1	0.3	CTD/rosette water sampler	CTD/RO	at depth	2432 m
PS62/201-1	12.08.02	06:42	78° 50.09' N	0° 22.60' E	2592.0	NNW 3	49.9	0.0	CTD/rosette water sampler	CTD/RO	at depth	2539 m
PS62/201-2	12.08.02	07:43	78° 50.00' N	0° 24.16' E	2586.0	NW 4	244.2	0.1	Mooring (year)	MOORY	surface	Ankerstein und Mooring
PS62/201-2	12.08.02	08:43	78° 50.07' N	0° 24.19' E	2587.0	NNW 4	344.8	0.4	Mooring (year)	MOORY	surface	Releaser und Toppeinheit
PS62/201-2	12.08.02	08:49	78° 50.10' N	0° 23.99' E	2587.0	NNW 4	263.4	0.7	Mooring (year)	MOORY	at depth	Mooring slipped
PS62/202-1	12.08.02	10:14	78° 56.48' N	0° 22.59' W	2503.0	WNW 1	299.4	1.1	Mooring	MOR	released	
PS62/202-1	12.08.02	11:54	78° 56.23' N	0° 24.93' W	2625.0	NW 2	265.2	0.3	Mooring	MOR	mooring on deck	
PS62/203-1	12.08.02	13:37	78° 49.66' N	0° 48.12' W	2663.0	WNW 2	171.7	0.3	CTD/rosette water sampler	CTD/RO	at depth	2612 m ausgesteckt
PS62/203-2	12.08.02	16:04	78° 49.95' N	0° 48.28' W	2665.0	W 0	88.7	0.1	Mooring (year)	MOORY	surface	Toppeinheit mit Strömungsmesser und Transponder
PS62/203-2	12.08.02	17:10	78° 50.04' N	0° 48.13' W	2666.0	SW 2	79.9	0.0	Mooring (year)	MOORY	action	45 m auf Grund gefiert und ausgelöst
PS62/204-1	12.08.02	19:15	78° 50.26' N	0° 5.73' E	2633.0	WNW 2	325.1	0.3	CTD/rosette water sampler	CTD/RO	at depth	2582 m
PS62/205-1	12.08.02	21:19	78° 50.00' N	0° 12.09' W	2648.0	NE 0	276.0	0.1	CTD/rosette water sampler	CTD/RO	at depth	2596 m ausgesteckt
PS62/206-1	12.08.02	23:14	78° 49.88' N	0° 30.11' W	2693.0	N 0	200.3	0.2	CTD/rosette water sampler	CTD/RO	at depth	2641 m ausgesteckt
PS62/207-1	13.08.02	01:28	78° 49.46' N	1° 6.74' W	2644.0	SSE 1	141.2	0.4	CTD/rosette water sampler	CTD/RO	at depth	2594 m ausgesteckt
PS62/208-1	13.08.02	03:29	78° 50.21' N	1° 24.41' W	2690.0	SE 0	200.2	0.0	CTD/rosette water sampler	CTD/RO	at depth	2641 m ausgesteckt
PS62/209-1	13.08.02	05:27	78° 49.90' N	1° 42.21' W	2716.0	ESE 2	11.1	0.0	CTD/rosette water sampler	CTD/RO	at depth	2665 m
PS62/210-1	13.08.02	07:53	79° 1.37' N	2° 1.33' W	2628.0	SE 4	210.6	0.4	Mooring	MOR	released	
PS62/210-1	13.08.02	09:34	79° 1.99' N	2° 4.48' W	2612.0	SE 5	12.6	0.2	Mooring	MOR	mooring on deck	
PS62/211-1	13.08.02	12:57	78° 49.88' N	1° 59.72' W	2722.0	SSE 5	249.1	0.0	CTD/rosette water sampler	CTD/RO	at depth	2670 m ausgesteckt

Station	Date	Time	PositionLat	PositionLon	Depth [m]	Windstrength [m/s]	Course [°]	Speed [kn]	Gear	Gear Abbreviation	Action	Comment
PS62/211-2	13.08.02	14:03	78° 50.23' N	2° 1.03' W	2717.0	S 3	303.6	0.4	Mooring (year)	MOORY	surface	Ankerstein, Deppel-releaser, Strömungs-messer+4 Benthos
PS62/211-2	13.08.02	16:16	78° 49.89' N	1° 59.94' W	2721.0	SSE 2	345.1	0.0	Mooring (year)	MOORY	surface	mit 50 m Geodraht auf Grund gefiert und ausgelöst
PS62/212-1	13.08.02	17:57	78° 49.91' N	2° 19.43' W	2679.0	SSE 3	11.6	0.0	CTD/rosette water sampler	CTD/RO	at depth	2628 m
PS62/213-1	13.08.02	20:32	78° 49.85' N	2° 39.07' W	2622.0	ESE 2	235.4	0.1	CTD/rosette water sampler	CTD/RO	at depth	2570 ausgesteckt
PS62/214-1	13.08.02	23:18	78° 49.35' N	2° 55.46' W	2563.0	SE 1	188.1	0.8	CTD/rosette water sampler	CTD/RO	at depth	2515 m ausgesteckt
PS62/215-1	14.08.02	01:46	78° 48.45' N	3° 18.25' W	2419.0	E 1	158.8	0.5	CTD/rosette water sampler	CTD/RO	at depth	2376 m ausgesteckt
PS62/216-1	14.08.02	04:07	78° 50.20' N	3° 38.58' W	2219.0	E 2	309.4	0.0	CTD/rosette water sampler	CTD/RO	at depth	2174 m
PS62/216-1	14.08.02	04:33	78° 50.02' N	3° 37.29' W	2220.0	ENE 1	120.4	0.5	CTD/rosette water sampler	CTD/RO	on deck	
PS62/217-1	14.08.02	05:49	78° 49.87' N	3° 58.60' W	1951.0	ENE 2	352.0	0.0	CTD/rosette water sampler	CTD/RO	at depth	1901 m starker Oberflächenstrom nach Osten
PS62/218-1	14.08.02	07:17	78° 49.89' N	4° 18.87' W	1675.0	ENE 3	266.0	0.0	CTD/rosette water sampler	CTD/RO	at depth	1633m starker Oberflächenstrom nach Südost
PS62/219-1	14.08.02	08:41	78° 49.97' N	4° 39.27' W	1373.0	NE 4	279.8	0.0	CTD/rosette water sampler	CTD/RO	at depth	1268 m ausgesteckt
PS62/220-1	14.08.02	10:04	78° 50.01' N	4° 59.16' W	1060.0	NE 4	275.9	0.0	CTD/rosette water sampler	CTD/RO	at depth	1030 m ausgesteckt
PS62/221-1	14.08.02	11:08	78° 49.96' N	5° 20.10' W	709.5	NE 4	158.8	0.3	CTD/rosette water sampler	CTD/RO	at depth	689 m ausgesteckt
PS62/221-2	14.08.02	11:27	78° 49.88' N	5° 20.34' W	697.8	NE 5	240.7	0.5	Hand net	HN	surface	
PS62/221-2	14.08.02	11:59	78° 49.81' N	5° 20.92' W	684.8	ENE 5	268.6	0.0	Hand net	HN	on deck	
PS62/221-3	14.08.02	12:05	78° 49.80' N	5° 20.93' W	689.1	ENE 5	268.7	0.0	CTD/rosette water sampler	CTD/RO	on deck	30 m waren ausgesteckt
PS62/222-1	14.08.02	12:57	78° 50.03' N	5° 39.84' W	448.4	NE 8	201.9	0.6	CTD/rosette water sampler	CTD/RO	at depth	426 m ausgesteckt
PS62/223-1	14.08.02	13:55	78° 49.96' N	6° 0.45' W	353.4	NE 7	251.3	0.6	CTD/rosette water sampler	CTD/RO	at depth	333 m ausgesteckt
PS62/224-1	14.08.02	15:06	78° 50.03' N	6° 30.15' W	286.2	NE 7	260.2	0.6	CTD/rosette water sampler	CTD/RO	at depth	269 m ausgesteckt
PS62/225-1	14.08.02	16:15	78° 50.04' N	7° 0.46' W	249.7	NE 8	276.2	0.7	CTD/rosette water sampler	CTD/RO	at depth	242 m
PS62/226-1	14.08.02	17:14	78° 50.02' N	7° 30.13' W	188.3	NE 7	319.8	0.7	CTD/rosette water sampler	CTD/RO	at depth	174 m
PS62/227-1	14.08.02	18:15	78° 49.92' N	7° 59.93' W	194.7	NNE 8	185.4	0.4	CTD/rosette water sampler	CTD/RO	at depth	EL : 183 m ausgesteckt
PS62/228-1	14.08.02	19:16	78° 49.92' N	8° 30.02' W	285.0	NNE 9	9.6	0.1	CTD/rosette water sampler	CTD/RO	at depth	268 m
PS62/229-1	14.08.02	20:12	78° 49.94' N	8° 59.29' W	250.6	NNE 9	97.6	0.3	CTD/rosette water sampler	CTD/RO	at depth	236 m
PS62/230-1	14.08.02	21:31	78° 50.00' N	9° 28.79' W	190.8	NNE 10	166.0	0.6	CTD/rosette water sampler	CTD/RO	at depth	177 m ausgesteckt
PS62/231-1	14.08.02	22:52	78° 49.99' N	9° 59.40' W	292.4	N 10	198.4	0.5	CTD/rosette water sampler	CTD/RO	at depth	276 m ausgesteckt
PS62/232-1	15.08.02	00:04	78° 49.81' N	10° 29.94' W	384.7	NNE 10	201.4	0.7	CTD/rosette water sampler	CTD/RO	at depth	367 m ausgesteckt
PS62/233-1	15.08.02	01:25	78° 49.88' N	11° 0.11' W	338.6	N 10	261.0	0.5	CTD/rosette water sampler	CTD/RO	at depth	320 m ausgesteckt
PS62/234-1	15.08.02	02:36	78° 50.17' N	11° 29.76' W	244.1	N 12	315.3	0.2	CTD/rosette water sampler	CTD/RO	at depth	231 m ausgesteckt
PS62/235-1	15.08.02	03:48	78° 50.22' N	11° 59.25' W	200.4	N 11	294.0	0.4	CTD/rosette water sampler	CTD/RO	at depth	187 m ausgesteckt
PS62/236-1	15.08.02	04:48	78° 50.08' N	12° 29.59' W	188.4	N 10	279.9	0.7	CTD/rosette water sampler	CTD/RO	at depth	175 m
PS62/237-1	15.08.02	06:11	78° 49.89' N	13° 0.08' W	202.1	NNE 11	328.8	0.3	CTD/rosette water sampler	CTD/RO	at depth	185 m
PS62/238-1	15.08.02	07:16	78° 49.71' N	13° 30.70' W	145.4	NNE 11	222.8	0.5	CTD/rosette water sampler	CTD/RO	at depth	134 m
PS62/239-1	15.08.02	08:36	78° 50.00' N	13° 59.86' W	120.7	N 12	222.4	0.4	CTD/rosette water sampler	CTD/RO	at depth	95 m ausgesteckt
PS62/240-1	15.08.02	10:10	78° 50.06' N	14° 30.46' W	218.8	NNE 12	195.7	0.5	CTD/rosette water sampler	CTD/RO	at depth	92 m ausgesteckt
PS62/241-1	15.08.02	11:25	78° 50.50' N	14° 59.69' W	149.8	NNE 11	268.4	0.7	CTD/rosette water sampler	CTD/RO	at depth	68 m ausgesteckt
PS62/242-1	15.08.02	12:44	78° 50.01' N	15° 30.42' W	60.5	NNE 10	268.7	0.4	CTD/rosette water sampler	CTD/RO	at depth	67 m ausgesteckt
PS62/243-1	15.08.02	14:05	78° 50.03' N	16° 0.75' W	218.0	NNE 10	276.4	0.6	CTD/rosette water sampler	CTD/RO	at depth	219 m ausgesteckt
PS62/244-1	15.08.02	15:37	78° 50.38' N	16° 28.57' W	327.6	NNE 8	280.8	0.8	CTD/rosette water sampler	CTD/RO	at depth	311 m ausgesteckt
PS62/245-1	15.08.02	17:06	78° 50.23' N	16° 58.65' W	398.8	NNE 10	306.0	0.7	CTD/rosette water sampler	CTD/RO	at depth	383 m
PS62/246-1	15.08.02	18:30	78° 50.09' N	17° 28.96' W	567.2	N 7	204.8	0.4	CTD/rosette water sampler	CTD/RO	at depth	EL31: 546 m ausgesteckt
PS62/247-1	17.08.02	12:52	79° 17.97' N	5° 41.63' E	1801.0	N 0	19.7	7.7	HydroSweep/ParaSound profile	HS_PS	start track	
PS62/247-1	17.08.02	15:30	79° 31.85' N	5° 13.94' E	2703.0	SSE 13	44.4	5.7	HydroSweep/ParaSound profile	HS_PS	alter course	
PS62/247-1	17.08.02	18:00	79° 16.47' N	5° 59.80' E	1638.0	SSE 13	160.1	8.0	HydroSweep/ParaSound profile	HS_PS	profile end	
PS62/248-1	18.08.02	03:21	78° 0.21' N	8° 20.57' E	1996.0	SSE 14	218.8	0.2	CTD/rosette water sampler	CTD/RO	at depth	1950 m ausgesteckt
PS62/249-1	18.08.02	04:44	78° 0.10' N	8° 29.97' E	1801.0	S 13	4.4	0.5	CTD/rosette water sampler	CTD/RO	at depth	1759 m

Station	Date	Time	PositionLat	PositionLon	Depth [m]	Windstrength [m/s]	Course [°]	Speed [kn]	Gear	Gear Abbreviation	Action	Comment
PS62/250-1	18.08.02	06:04	78° 0.25' N	8° 40.07' E	1601.0	S 13	289.5	0.1	CTD/rosette water sampler	CTD/RO	at depth	1560 m
PS62/251-1	18.08.02	07:15	78° 0.35' N	8° 51.50' E	1391.0	S 12	352.6	1.0	CTD/rosette water sampler	CTD/RO	at depth	1354 m
PS62/252-1	18.08.02	08:17	78° 0.46' N	8° 45.40' E	1505.0	S 12	17.1	0.8	CTD/rosette water sampler	CTD/RO	at depth	1469 m ausgesteckt
PS62/253-1	18.08.02	09:33	78° 0.36' N	9° 1.13' E	1208.0	S 9	22.0	0.3	CTD/rosette water sampler	CTD/RO	at depth	1177 m ausgesteckt
PS62/254-1	18.08.02	10:32	78° 0.54' N	9° 9.92' E	1000.0	SSW 11	38.7	0.8	CTD/rosette water sampler	CTD/RO	at depth	982 m ausgesteckt
PS62/255-1	18.08.02	11:23	77° 59.96' N	9° 17.20' E	830.1	S 9	234.3	0.2	CTD/rosette water sampler	CTD/RO	at depth	808 m ausgesteckt
PS62/256-1	18.08.02	19:21	76° 59.74' N	12° 0.21' E	800.1	SSW 4	53.6	0.2	CTD/rosette water sampler	CTD/RO	at depth	786 m
PS62/257-1	18.08.02	20:17	76° 57.79' N	11° 51.66' E	998.1	SSW 3	346.5	0.2	CTD/rosette water sampler	CTD/RO	at depth	975 m ausgesteckt
PS62/258-1	18.08.02	21:33	76° 55.10' N	11° 40.26' E	1221.0	SW 2	269.0	0.8	CTD/rosette water sampler	CTD/RO	at depth	1197 m ausgesteckt
PS62/259-1	18.08.02	22:49	76° 51.45' N	11° 29.88' E	1420.0	W 3	234.6	0.8	CTD/rosette water sampler	CTD/RO	at depth	
PS62/260-1	19.08.02	00:10	76° 48.33' N	11° 20.70' E	1616.0	WSW 4	256.2	0.2	CTD/rosette water sampler	CTD/RO	at depth	1565 m ausgesteckt
PS62/261-1	19.08.02	01:40	76° 45.14' N	11° 11.86' E	1817.0	WSW 4	130.0	0.2	CTD/rosette water sampler	CTD/RO	at depth	1770 m ausgesteckt
PS62/262-1	19.08.02	03:17	76° 41.61' N	11° 1.44' E	2015.0	WSW 3	168.8	0.5	CTD/rosette water sampler	CTD/RO	at depth	1967 m ausgesteckt
PS62/263-1	20.08.02	03:55	72° 0.04' N	14° 43.50' E	1291.0	S 9	78.2	0.3	Sequentieller Multiple Corer	S-MUC	on the bottom	1264 m ausgesteckt
PS62/263-1	20.08.02	04:14	72° 0.02' N	14° 43.92' E	1296.0	S 9	115.9	0.4	Sequentieller Multiple Corer	S-MUC	off bottom	
PS62/263-2	20.08.02	05:17	71° 59.81' N	14° 43.68' E	1293.0	S 9	197.4	0.1	CTD/rosette water sampler	CTD/RO	at depth	1241 m
PS62/263-3	20.08.02	06:05	72° 0.12' N	14° 43.53' E	1289.0	S 8	68.7	0.2	Bottom lander, profile	BL_P	into the water	wird mit 1000m Geodraht gefiert & dann ausgelöst
PS62/263-3	20.08.02	06:57	72° 0.12' N	14° 43.52' E	1291.0	S 8	32.8	0.3	Bottom lander, profile	BL_P	released	684 m gefiert, kein Releaser gehört, Absinken auf Fischlot beobachtet
PS62/263-4	20.08.02	08:05	72° 0.50' N	14° 43.82' E	1273.0	S 8	301.4	0.3	Fischereilotsurvey	FLS	Start Track	
PS62/263-4	20.08.02	09:28	72° 0.15' N	14° 43.54' E	1271.0	S 7	160.7	0.8	Fischereilotsurvey	FLS	End of Track	
PS62/264-1	20.08.02	10:12	72° 0.14' N	14° 43.61' E	1289.0	SSE 9	200.9	0.4	Bottom water sampler	BWS	action	Gerät auf Tiefe 1266m
PS62/264-1	20.08.02	10:19	72° 0.11' N	14° 43.60' E	1272.0	SSE 9	181.1	0.0	Bottom water sampler	BWS	off bottom	
PS62/264-1	20.08.02	10:27	72° 0.11' N	14° 43.59' E	1292.0	SSE 8	53.7	0.4	Bottom water sampler	BWS	action	Korrektur: Gerät vom Grund10.26 Uhr
PS62/264-2	20.08.02	11:25	72° 0.11' N	14° 43.57' E	1290.0	S 9	129.8	0.2	CTD/rosette water sampler	CTD/RO	at depth	1258 m ausgesteckt
PS62/265-1	20.08.02	12:31	72° 0.20' N	14° 43.68' E	1290.0	S 8	45.0	0.3	Bottom water sampler	BWS	at sea bottom	1260 m ausgesteckt
PS62/265-1	20.08.02	12:38	72° 0.19' N	14° 43.69' E	1289.0	S 7	5.7	0.2	Bottom water sampler	BWS	off bottom	
PS62/265-2	20.08.02	13:41	72° 0.18' N	14° 43.64' E	1289.0	SSE 8	116.1	0.3	CTD/rosette water sampler	CTD/RO	at depth	1259 m ausgesteckt
PS62/266-1	20.08.02	15:00	72° 0.30' N	14° 43.76' E	1288.0	SSE 8	88.8	0.7	Bottom water sampler	BWS	at sea bottom	1257 m ausgesteckt
PS62/266-1	20.08.02	15:06	72° 0.32' N	14° 43.80' E	1288.0	SSE 7	188.3	0.0	Bottom water sampler	BWS	off bottom	
PS62/266-2	20.08.02	16:06	72° 0.28' N	14° 43.82' E	1290.0	SSW 7	48.0	0.2	CTD/rosette water sampler	CTD/RO	at depth	1255 m
PS62/267-1	20.08.02	17:27	72° 0.40' N	14° 43.78' E	1287.0	WSW 7	238.5	0.2	Bottom water sampler	BWS	at sea bottom	1253 m
PS62/267-1	20.08.02	17:35	72° 0.40' N	14° 43.79' E	302.0	WSW 7	356.1	0.1	Bottom water sampler	BWS	off bottom	
PS62/267-2	20.08.02	18:35	72° 0.41' N	14° 43.82' E	1292.0	WSW 5	90.2	0.2	CTD/rosette water sampler	CTD/RO	at depth	1254 m
PS62/263-3	20.08.02	19:25	72° 0.22' N	14° 43.67' E	277.0	WSW 5	44.8	0.8	Bottom lander, profile	BL_P	released	Signal 1260 m , Auslösen erfolgreich.
PS62/263-3	20.08.02	20:05	72° 0.35' N	14° 44.13' E	1270.0	WSW 5	67.5	0.6	Bottom lander, profile	BL_P	on deck	
PS62/268-1	20.08.02	20:50	72° 0.37' N	14° 43.84' E	1288.0	WSW 5	56.9	0.7	CTD/rosette water sampler	CTD/RO	at depth	1256 m ausgersteckt
PS62/268-2	20.08.02	21:52	72° 0.34' N	14° 43.56' E	1288.0	SW 7	354.0	0.3	Bottom water sampler	BWS	at sea bottom	1255 m
PS62/269-1	20.08.02	23:00	72° 0.47' N	14° 43.86' E	1287.0	W 4	47.6	0.4	Bottom water sampler	BWS	at sea bottom	
PS62/269-2	21.08.02	00:02	72° 0.53' N	14° 43.89' E	1294.0	WNW 4	31.0	0.5	CTD/rosette water sampler	CTD/RO	at depth	1260 m ausgesteckt
PS62/270-1	21.08.02	01:11	72° 0.26' N	14° 43.85' E	1289.0	W 3	101.8	0.3	Sequentieller Multiple Corer	S-MUC	on the bottom	
PS62/270-1	21.08.02	01:19	72° 0.33' N	14° 43.72' E	1287.0	W 3	310.9	0.9	Sequentieller Multiple Corer	S-MUC	off bottom	
PS62/271-1	21.08.02	02:33	72° 0.69' N	14° 44.26' E	1288.0	W 3	67.0	0.4	Ocean Floor Observ. System	OFOS	at depth	1270 m ausgesteckt
PS62/271-1	21.08.02	04:17	71° 59.85' N	14° 43.56' E	1295.0	SW 2	219.0	0.7	Ocean Floor Observ. System	OFOS	Start Hoisting	
PS62/272-1	21.08.02	05:12	72° 0.26' N	14° 43.76' E	1287.0	SSE 1	312.7	0.1	Bottom lander, profile	BL_P	into the water	wird zum Grund gefiert
PS62/272-1	21.08.02	05:59	72° 0.31' N	14° 43.79' E	1288.0	SSE 1	163.5	0.4	Bottom lander, profile	BL_P	released	1100 m Draht, Auslöseerfolg nicht zu beobachten

Station	Date	Time	PositionLat	PositionLon	Depth [m]	Windstrength [m/s]	Course [°]	Speed [kn]	Gear	Gear Abbreviation	Action	Comment
PS62/272-1	21.08.02	06:08	72° 0.35' N	14° 43.77' E	1288.0	SE 1	335.5	0.6	Bottom lander, profile	BL_P	released	Wellen ausgekuppelt, erfolgreich ausgelöst, Releasersignal, Lastschreiber, Fischlot
PS62/272-2	21.08.02	07:17	72° 0.29' N	14° 43.77' E	1288.0	SE 2	178.3	0.5	Sequentieller Multiple Corer	S-MUC	on the bottom	
PS62/272-2	21.08.02	07:23	72° 0.23' N	14° 43.72' E	1288.0	ESE 2	181.3	0.5	Sequentieller Multiple Corer	S-MUC	off bottom	
PS62/273-1	21.08.02	08:42	72° 0.43' N	14° 41.21' E	1310.0	E 2	128.3	1.0	Ocean Floor Observ. System	OFOS	at depth	1280 m ausgesteckt, Beginn Track
PS62/273-1	21.08.02	10:56	72° 0.22' N	14° 45.35' E	1282.0	E 6	179.3	0.2	Ocean Floor Observ. System	OFOS	Start Hoisting	
PS62/274-1	21.08.02	12:10	72° 0.10' N	14° 45.89' E	1278.0	E 7	359.7	0.3	Sequentieller Multiple Corer	S-MUC	on the bottom	1291 m ausgesteckt
PS62/274-1	21.08.02	12:20	72° 0.12' N	14° 45.57' E	1280.0	E 7	260.2	0.6	Sequentieller Multiple Corer	S-MUC	off bottom	
PS62/275-1	21.08.02	13:54	71° 59.86' N	14° 42.12' E	1306.0	ESE 9	7.4	0.5	Sequentieller Multiple Corer	S-MUC	on the bottom	1274 m ausgesteckt
PS62/275-1	21.08.02	14:05	71° 59.98' N	14° 42.52' E	1297.0	ESE 9	79.2	0.7	Sequentieller Multiple Corer	S-MUC	off bottom	
PS62/275-2	21.08.02	15:19	71° 59.89' N	14° 42.58' E	1305.0	SE 7	60.7	0.5	Bottom water sampler	BWS	at sea bottom	1270 m ausgesteckt
PS62/275-2	21.08.02	15:25	71° 59.89' N	14° 42.65' E	1300.0	SE 7	142.6	0.3	Bottom water sampler	BWS	off bottom	
PS62/276-1	21.08.02	16:53	72° 0.25' N	14° 43.53' E	1287.0	SSE 8	157.0	0.0	Bottom water sampler	BWS	at sea bottom	1255 m
PS62/276-1	21.08.02	17:01	72° 0.25' N	14° 43.55' E	1289.0	SSE 8	23.7	0.2	Bottom water sampler	BWS	off bottom	
PS62/272-1	21.08.02	17:41	72° 0.44' N	14° 43.67' E	1286.0	S 7	337.2	1.2	Bottom lander, profile	BL_P	released	Wellen ausgekuppelt, Lote aus
PS62/272-1	21.08.02	18:15	72° 0.47' N	14° 43.66' E	1288.0	SSW 6	346.2	0.7	Bottom lander, profile	BL_P	on deck	
PS62/277-1	21.08.02	18:54	72° 0.01' N	14° 38.90' E	1338.0	SSW 4	61.2	8.6	HydroSweep/ParaSound profile	HS_PS	start track	
PS62/277-1	21.08.02	19:22	72° 2.11' N	14° 47.62' E	1242.0	SSW 5	66.2	6.9	HydroSweep/ParaSound profile	HS_PS	alter course	auf 231 °
PS62/277-1	21.08.02	19:58	71° 59.35' N	14° 39.74' E	1332.0	S 5	213.7	7.1	HydroSweep/ParaSound profile	HS_PS	alter course	auf 51 °
PS62/277-1	21.08.02	20:26	72° 0.84' N	14° 48.66' E	1243.0	SSW 6	48.5	8.0	HydroSweep/ParaSound profile	HS_PS	alter course	
PS62/277-1	21.08.02	21:27	71° 56.40' N	14° 34.25' E	1412.0	SW 5	229.6	8.3	HydroSweep/ParaSound profile	HS_PS	alter course	
PS62/277-1	21.08.02	22:43	71° 59.20' N	14° 50.47' E	1242.0	SSW 6	224.3	6.2	HydroSweep/ParaSound profile	HS_PS	alter course	
PS62/277-1	21.08.02	23:31	71° 55.55' N	14° 37.01' E	1402.0	SW 6	228.8	7.2	HydroSweep/ParaSound profile	HS_PS	alter course	
PS62/277-1	22.08.02	00:30	71° 59.51' N	14° 55.18' E	1179.0	SW 5	48.9	7.4	HydroSweep/ParaSound profile	HS_PS	alter course	
PS62/277-1	22.08.02	00:35	71° 59.51' N	14° 56.65' E	1164.0	WSW 5	144.0	6.8	HydroSweep/ParaSound profile	HS_PS	alter course	
PS62/277-1	22.08.02	01:47	71° 54.21' N	14° 37.90' E	1351.0	W 6	231.9	7.0	HydroSweep/ParaSound profile	HS_PS	alter course	
PS62/277-1	22.08.02	01:52	71° 53.79' N	14° 38.76' E	1338.0	W 6	128.2	8.5	HydroSweep/ParaSound profile	HS_PS	alter course	
PS62/277-1	22.08.02	02:53	71° 58.42' N	14° 57.23' E	1152.0	W 6	50.3	7.0	HydroSweep/ParaSound profile	HS_PS	profile end	
PS62/278-1	22.08.02	03:41	72° 0.21' N	14° 43.64' E	1290.0	NW 6	277.1	0.0	Bottom lander, profile	BL_P	into the water	
PS62/279-1	22.08.02	04:01	71° 59.85' N	14° 43.62' E	1294.0	NW 6	8.7	0.5	CTD/rosette water sampler	CTD/RO	at depth	30 m
PS62/280-1	22.08.02	04:53	72° 0.78' N	14° 42.96' E	1295.0	WNW 6	103.4	0.5	Sequentieller Multiple Corer	S-MUC	on the bottom	
PS62/280-1	22.08.02	05:25	72° 1.03' N	14° 42.97' E	1293.0	WNW 6	2.2	0.7	Sequentieller Multiple Corer	S-MUC	off bottom	1277m
PS62/281-1	22.08.02	06:49	71° 58.64' N	14° 48.89' E	1215.0	W 3	71.0	0.6	CTD/rosette water sampler	CTD/RO	at depth	1180 m
PS62/281-2	22.08.02	07:54	71° 58.58' N	14° 48.52' E	1214.0	WNW 4	264.3	0.6	Bottom water sampler	BWS	at sea bottom	1177 m ausgesteckt
PS62/281-2	22.08.02	08:02	71° 58.59' N	14° 48.49' E	1228.0	WNW 3	295.8	0.3	Bottom water sampler	BWS	off bottom	
PS62/281-3	22.08.02	09:12	71° 58.61' N	14° 48.75' E	1206.0	W 6	102.1	0.6	Sequentieller Multiple Corer	S-MUC	on the bottom	
PS62/281-3	22.08.02	09:43	71° 58.60' N	14° 49.16' E	1223.0	W 6	317.3	0.7	Sequentieller Multiple Corer	S-MUC	off bottom	
PS62/282-1	22.08.02	11:19	71° 55.56' N	14° 38.78' E	1358.0	W 6	337.6	0.2	Ocean Floor Observ. System	OFOS	at depth	1321 m ausgesteckt
PS62/282-1	22.08.02	11:50	71° 55.92' N	14° 39.73' E	1335.0	W 5	19.1	1.0	Ocean Floor Observ. System	OFOS	Start Hoisting	
PS62/282-2	22.08.02	12:59	71° 57.24' N	14° 40.32' E	1355.0	WNW 5	93.4	0.3	Ocean Floor Observ. System	OFOS	at depth	1321 m ausgesteckt
PS62/282-2	22.08.02	15:40	71° 55.90' N	14° 39.21' E	1342.0	W 4	216.8	0.6	Ocean Floor Observ. System	OFOS	Start Hoisting	
PS62/278-1	22.08.02	16:43	72° 0.28' N	14° 43.93' E	1288.0	W 4	44.8	0.4	Bottom lander, profile	BL_P	released	
PS62/278-1	22.08.02	17:15	72° 0.31' N	14° 43.54' E	1290.0	WSW 3	34.3	0.7	Bottom lander, profile	BL_P	on deck	
PS62/283-1	22.08.02	17:55	72° 0.19' N	14° 43.17' E	1288.0	WSW 5	123.2	0.1	CTD/rosette water sampler	CTD/RO	at depth	1254 m
PS62/283-2	22.08.02	19:09	72° 0.10' N	14° 43.12' E	1289.0	SW 6	225.1	0.3	Bottom water sampler	BWS	at sea bottom	1258 m ausgesteckt
PS62/283-2	22.08.02	19:12	72° 0.09' N	14° 43.07' E	1288.0	SW 6	214.0	0.3	Bottom water sampler	BWS	off bottom	
PS62/283-3	22.08.02	19:48	72° 0.10' N	14° 43.08' E	1289.0	SSW 6	116.5	0.1	Bottom water sampler	BWS	action	2. Aussetzen,da Gerät nicht ausgelöst hatte!

Station	Date	Time	PositionLat	PositionLon	Depth [m]	Windstrength [m/s]	Course [°]	Speed [kn]	Gear	Gear Abbreviation	Action	Comment
PS62/283-3	22.08.02	20:22	72° 0.09' N	14° 43.02' E	1291.0	S 6	136.0	0.1	Bottom water sampler	BWS	at sea bottom	1256 m ausgesteckt
PS62/283-3	22.08.02	20:29	72° 0.09' N	14° 43.04' E	1291.0	SSW 7	346.7	0.3	Bottom water sampler	BWS	off bottom	
PS62/283-4	22.08.02	21:30	72° 0.03' N	14° 43.20' E	1290.0	SW 7	200.0	0.0	Sequentieller Multiple Corer	S-MUC	on the bottom	1253 m ausgesteckt
PS62/283-4	22.08.02	22:29	72° 0.01' N	14° 44.22' E	1293.0	SSW 7	199.5	0.0	Sequentieller Multiple Corer	S-MUC	off bottom	
PS62/284-1	22.08.02	23:44	72° 0.27' N	14° 41.79' E	1304.0	SW 9	98.5	0.3	Ocean Floor Observ. System	OFOS	at depth	1271 m ausgesteckt
PS62/284-1	23.08.02	01:17	71° 59.83' N	14° 45.91' E	1283.0	SW 10	101.9	1.3	Ocean Floor Observ. System	OFOS	Start Hoisting	
PS62/284-1	23.08.02	01:53	71° 60.00' N	14° 44.86' E	1289.0	SSW 12	286.9	0.7	Ocean Floor Observ. System	OFOS	on deck	

Appendix 2: Marine sediment cores in the Denmark Strait region

PS 62/002-2

Position

Latitude: 61°47,744 N
Longitude: 39°22,351 W
Water depth: 1888 m

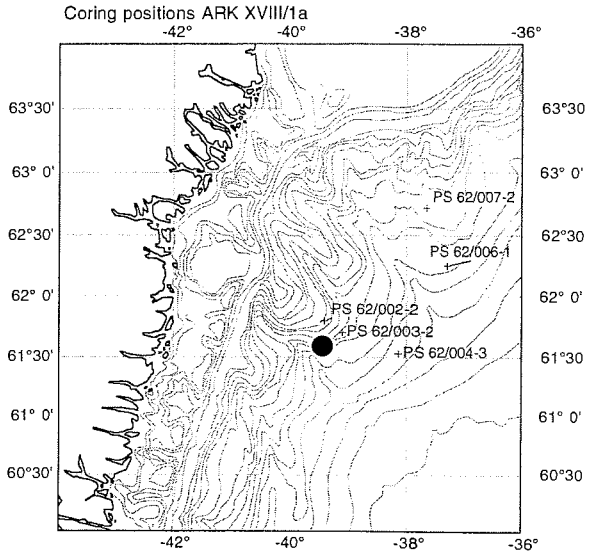

Parasound profile

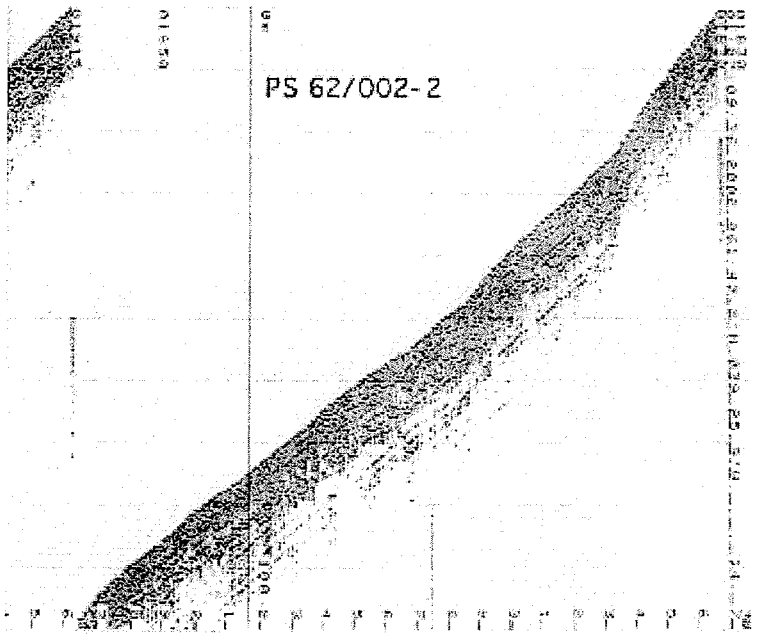

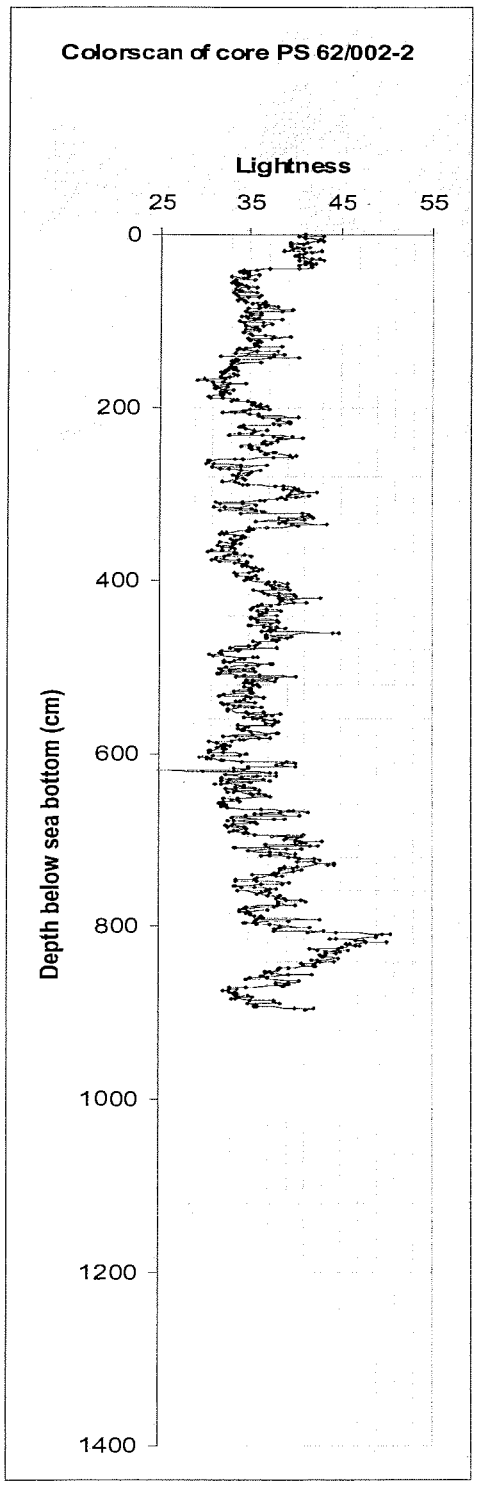
Colorscan of core PS 62/002-2
Lightness
25
35
45
55
0
200
400
600
800
1000
1200
1400
Depth below sea bottom (cm)

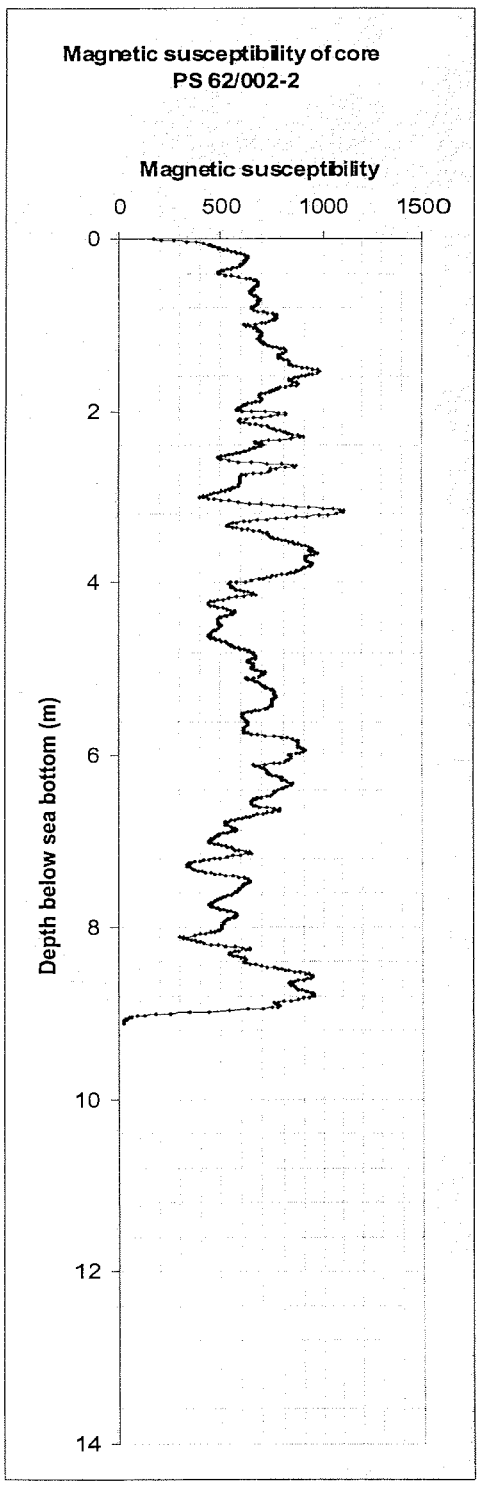
Magnetic susceptibility of core
PS 62/002-2
Magnetic susceptibility
0
500
1000
1500
0
2
4
6
8
10
12
14
Depth below sea bottom (m)

PS 62/003-2

Position

Latitude: 61°42,003 N
Longitude: 39°04,041 W
Water depth: 2159 m

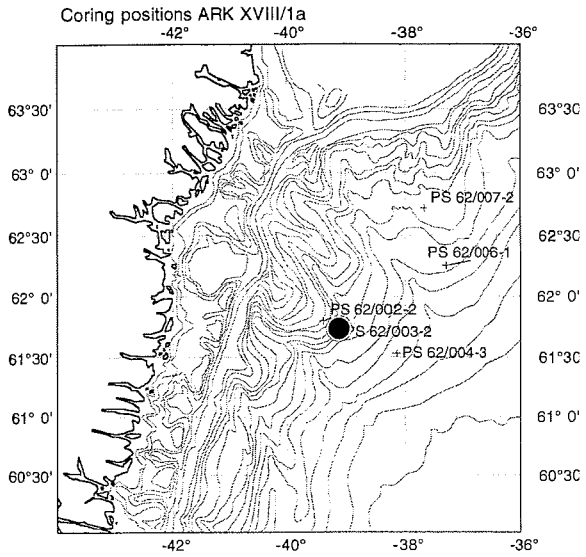

Parasound profile

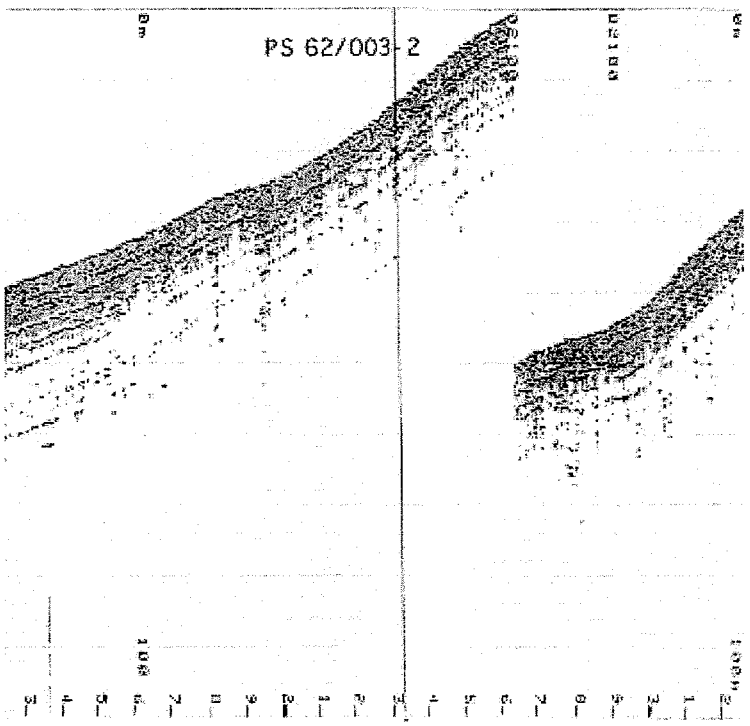

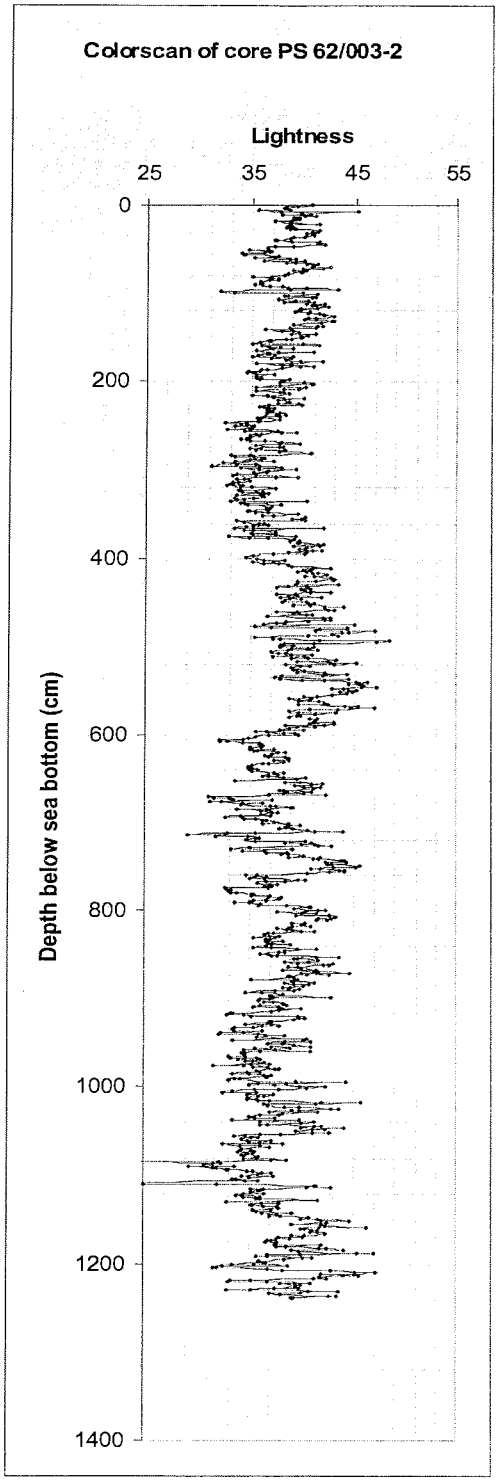
Colorscan of core PS 62/003-2
Lightness
25
35
45
55
0
200
400
600
800
1000
1200
1400
Depth below sea bottom (cm)

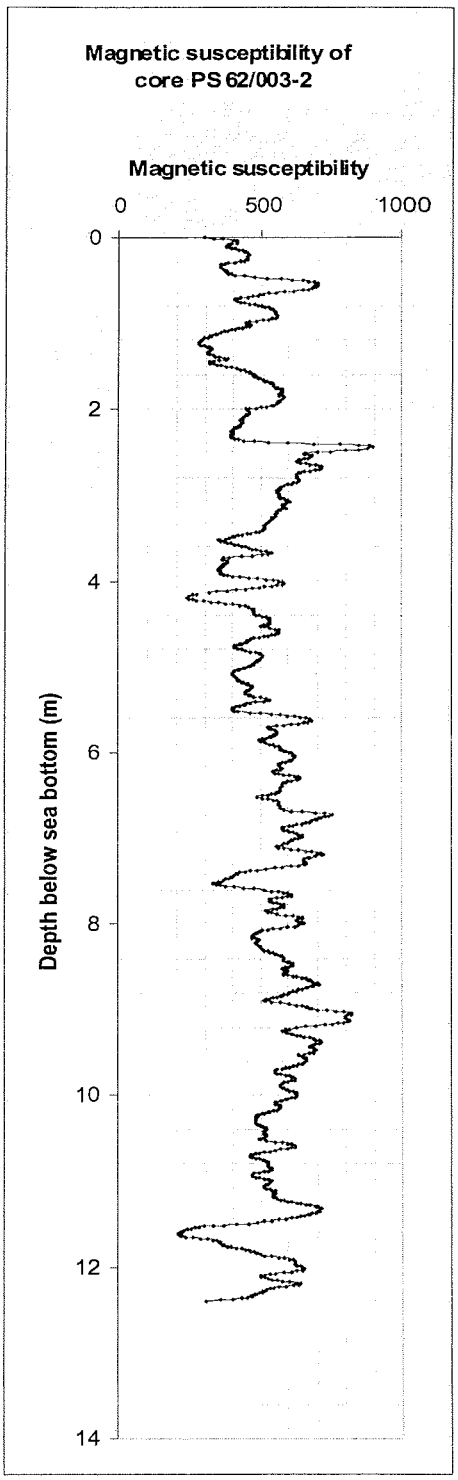
Magnetic susceptibility of core PS 62/003-2
Magnetic susceptibility
0
500
1000
0
2
4
6
8
10
12
14
Depth below sea bottom (m)

PS 62/004-3

Position

Latitude: 61°31,544 N
Longitude: 38°97,387 W
Water depth: 2565 m

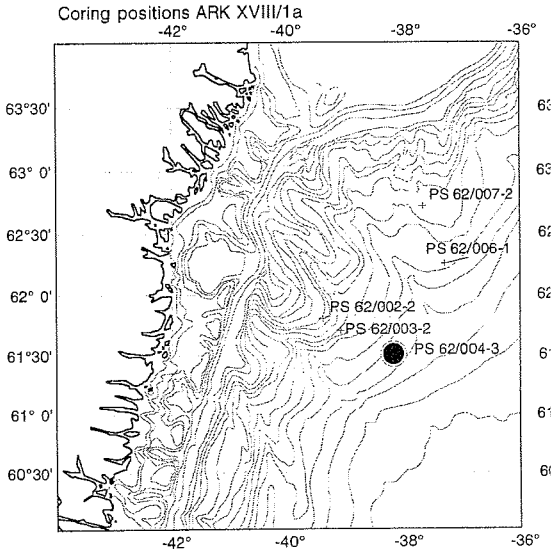

Parasound profile

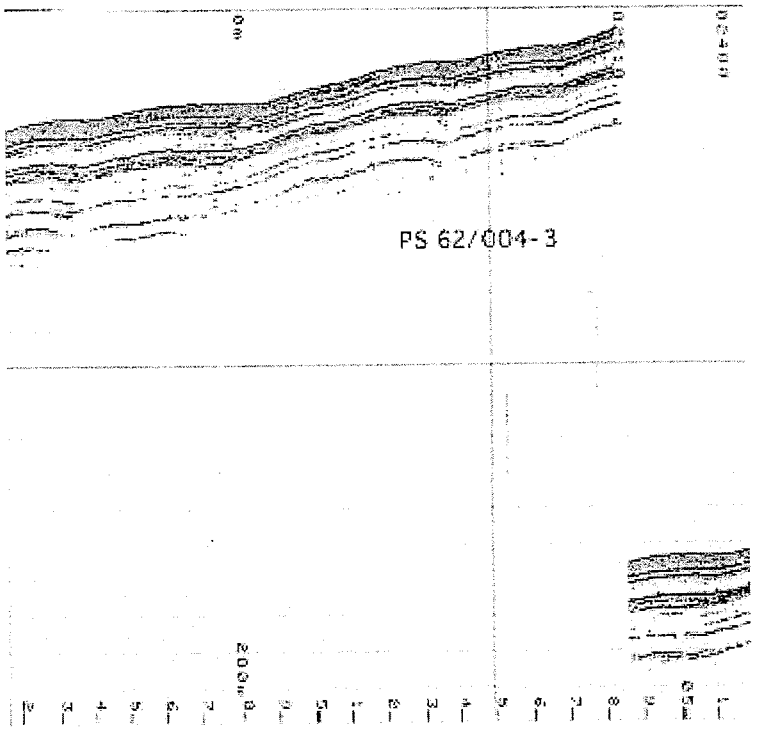

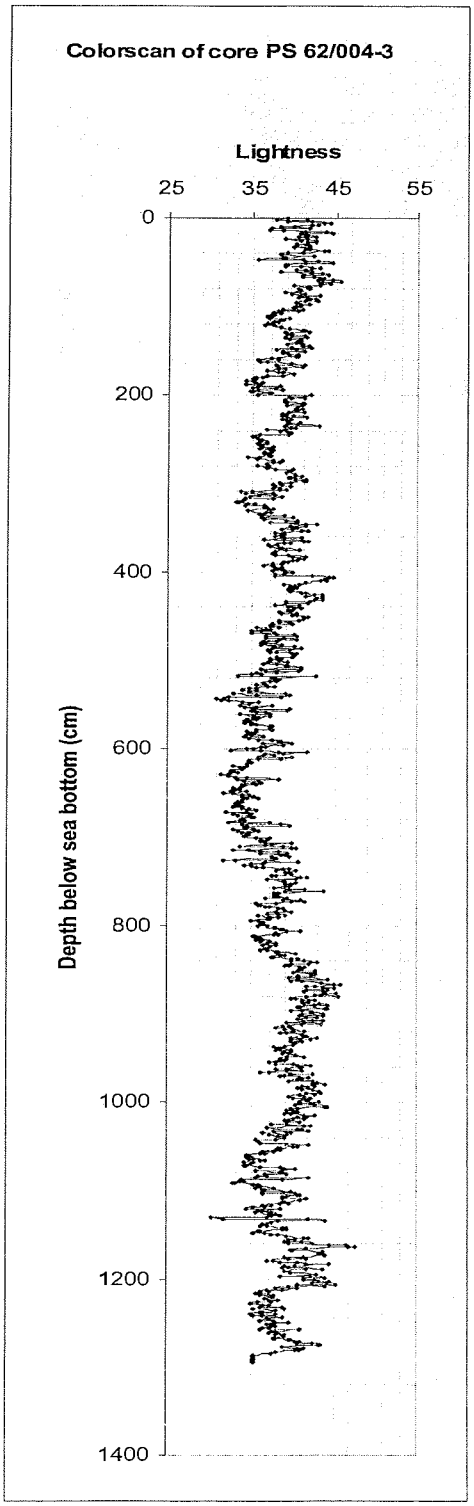
Colorscan of core PS 62/004-3
Lightness
25
35
45
55
0
200
400
600
800
1000
1200
1400
Depth below sea bottom (cm)

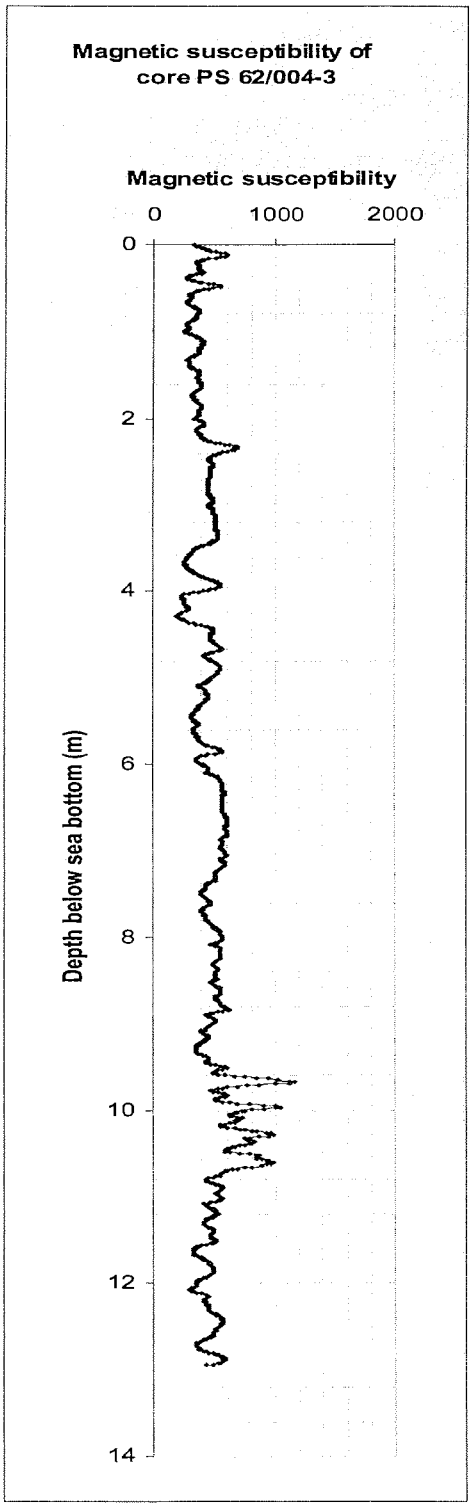
Magnetic susceptibility of core PS 62/004-3
Magnetic susceptibility
0
1000
2000
0
2
4
6
8
10
12
14
Depth below sea bottom (m)

PS 62/006-1

Position

Latitude: 62°15,053 N
Longitude: 37°18,403 W
Water depth: 2436 m

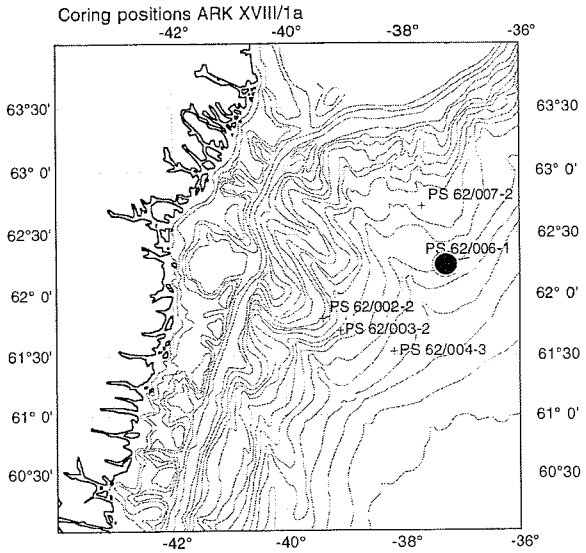

Parasound profile

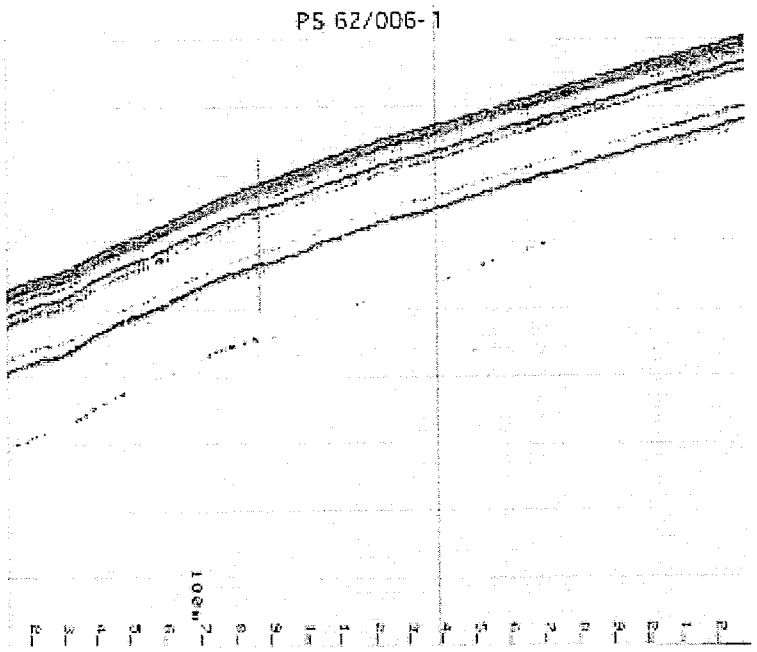

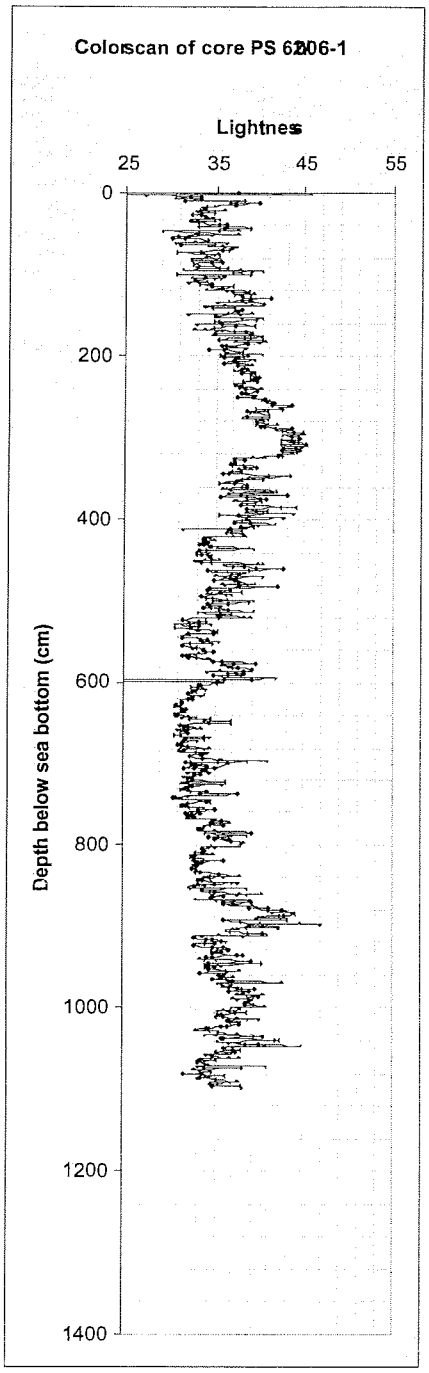
Colorscan of core PS 62/006-1
Lightness
25
35
45
55
0
200
400
600
800
1000
1200
1400
Depth below sea bottom (cm)

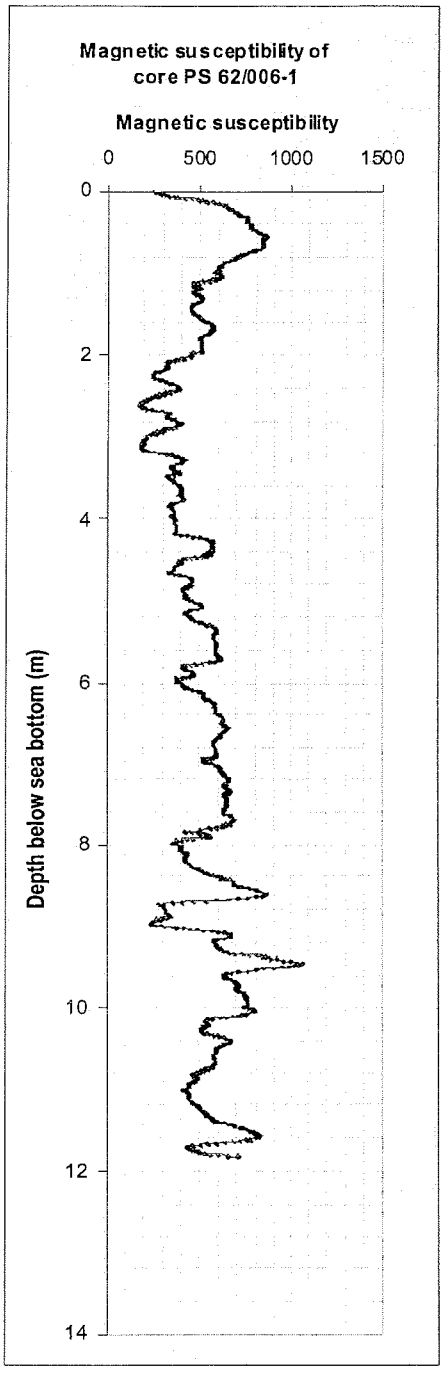
Magnetic susceptibility of core PS 62/006-1
Magnetic susceptibility
0
500
1000
1500
0
2
4
6
8
10
12
14
Depth below sea bottom (m)

PS 62/007-2

Position

Latitude: 62°42,827 N
Longitude: 37°49,307 W

Water depth: 2131 m

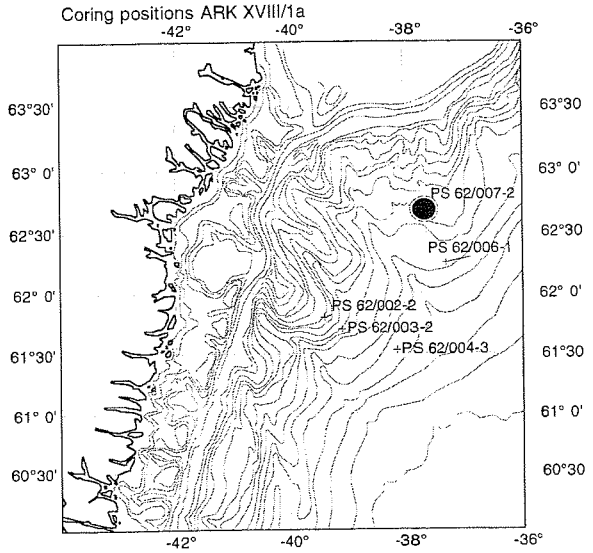

Parasound profile

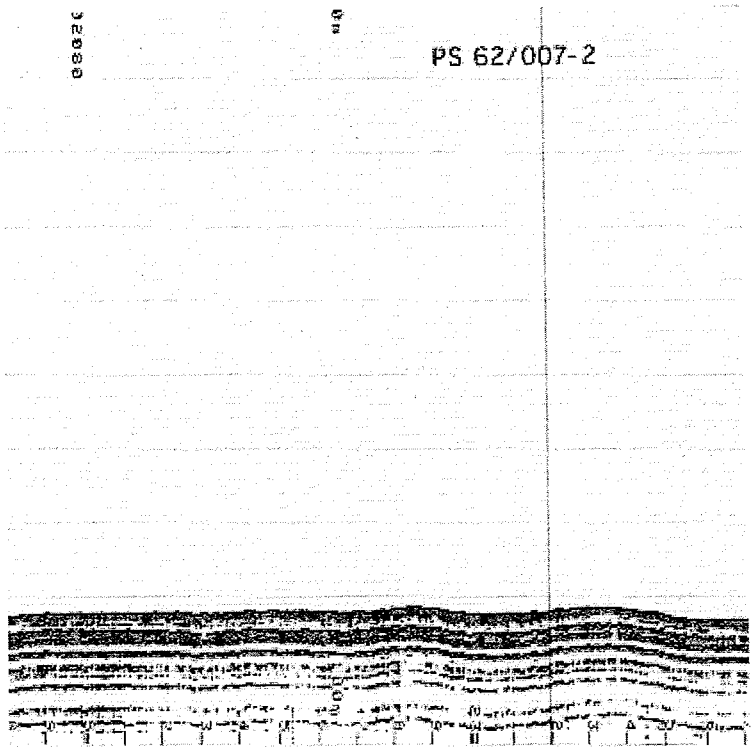

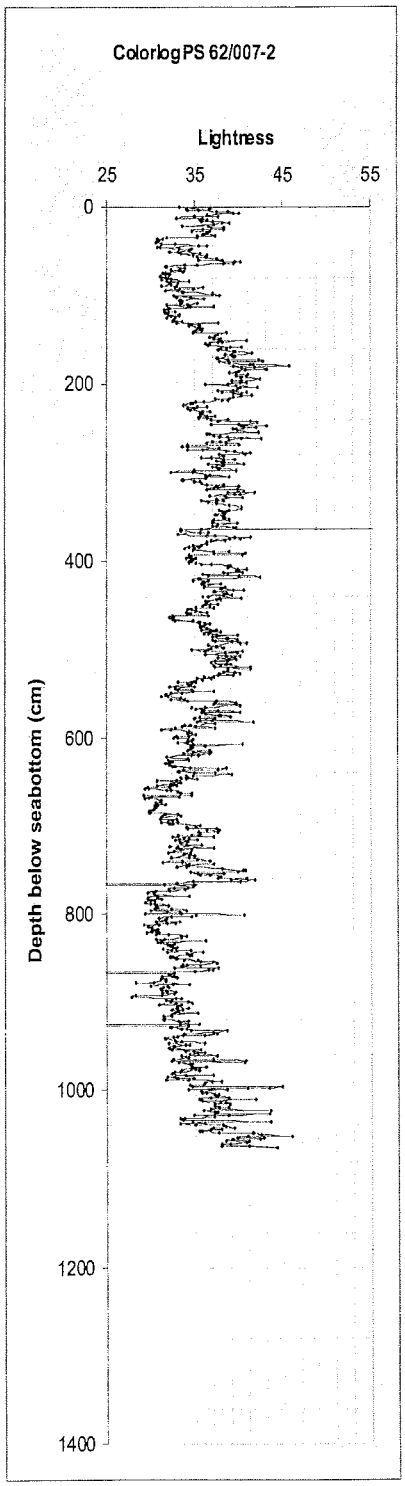
ColorlogPS 62/007-2
Lightness
25
35
45
55
0
200
400
600
800
1000
1200
1400
Depth below seabottom (cm)

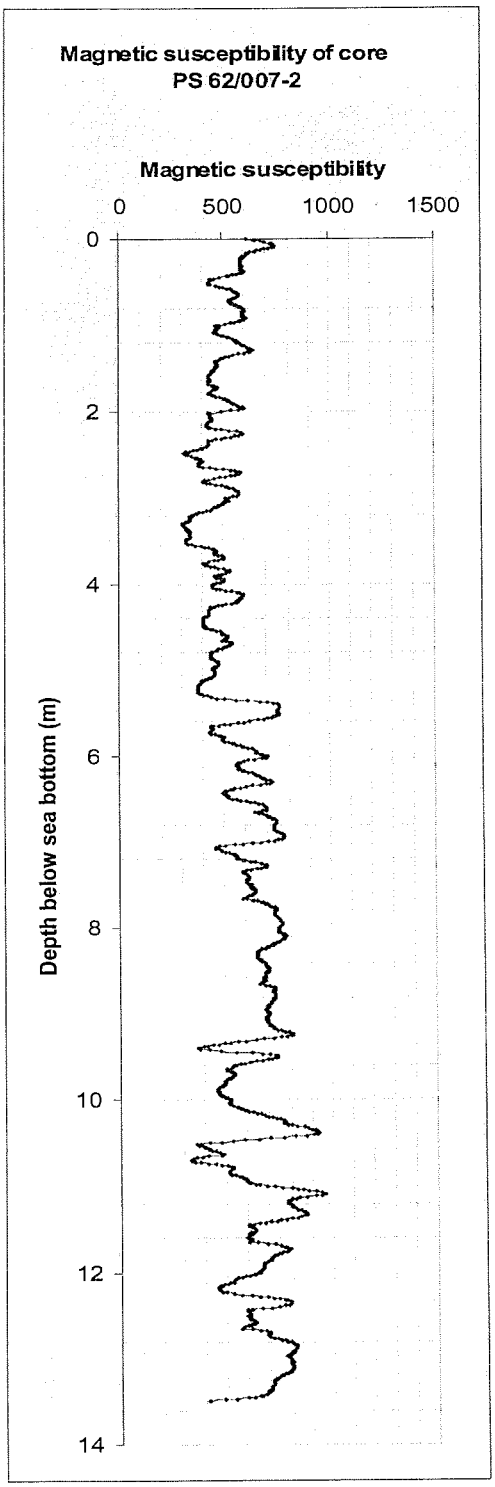
Magnetic susceptibility of core
PS 62/007-2
Magnetic susceptibility
0
500
1000
1500
0
2
4
6
8
10
12
14
Depth below sea bottom (m)

PS 62/012-3

Position

Latitude: 64°37,449' N
Longitude: 31°41,679' W
Water depth: 2404 m

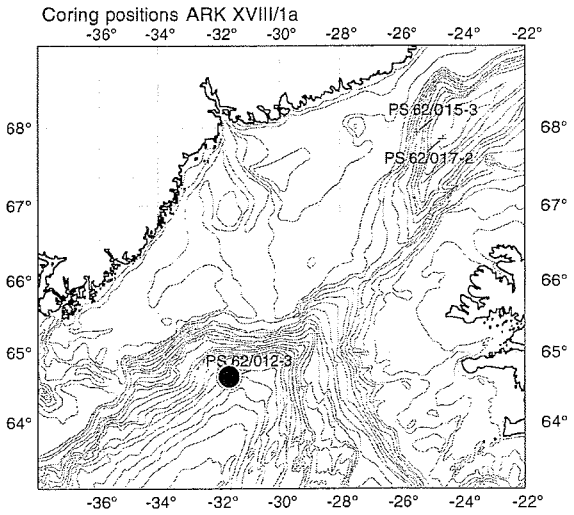

Parasound profile

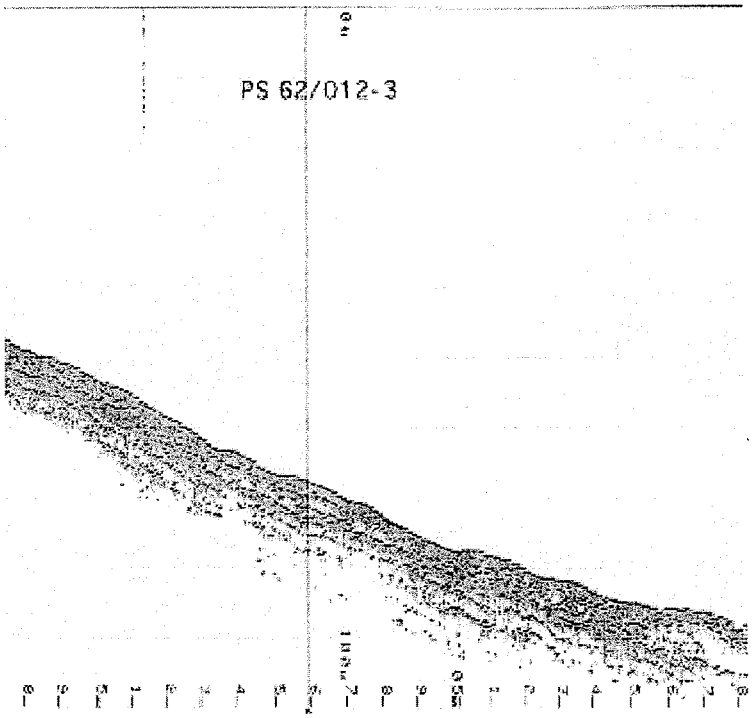

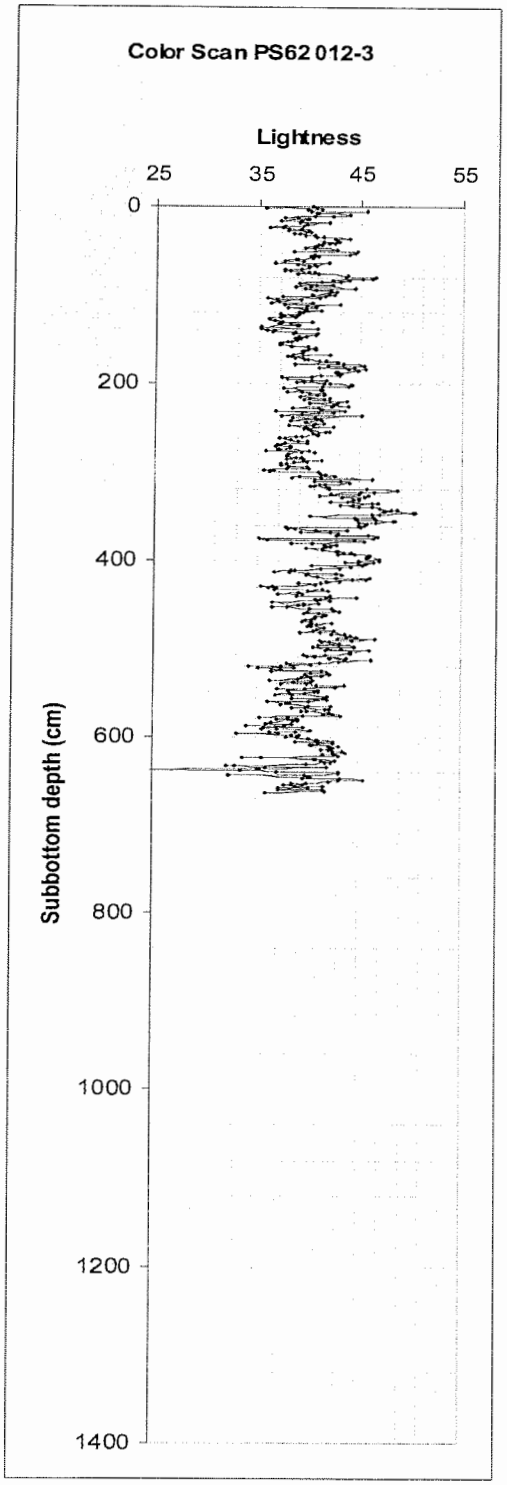
Color Scan PS62 012-3
Lightness
25
35
45
55
0
200
400
600
800
1000
1200
1400
Subbottom depth (cm)

PS 62/015-3

Position

Latitude: 67°55.855' N
Longitude: 25°25.414' W

Water depth: 980.2 m

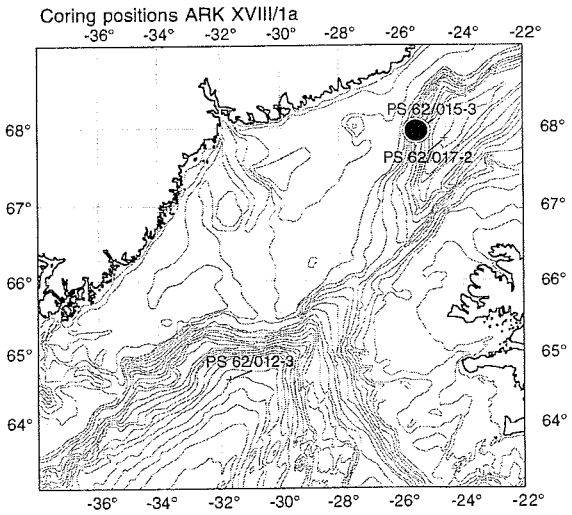

Parasound profile

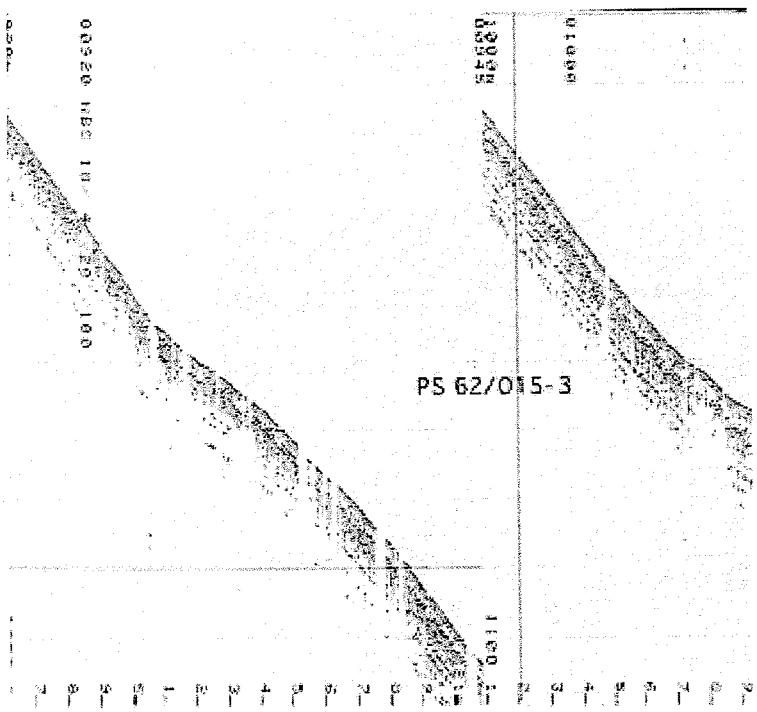

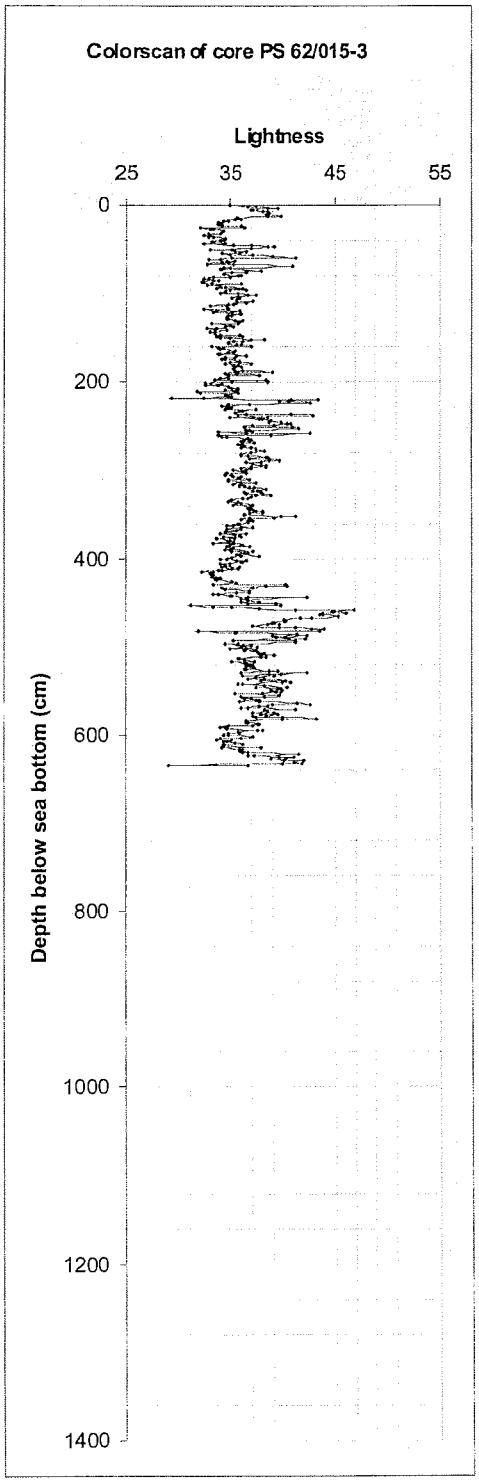
Colorscan of core PS 62/015-3
Lightness
25
35
45
55
0
200
400
600
800
1000
1200
1400
Depth below sea bottom (cm)

PS 62/017-2

Position

Latitude: 67°51,045' N
Longitude: 24°34,714' W
Water depth: 1452 m

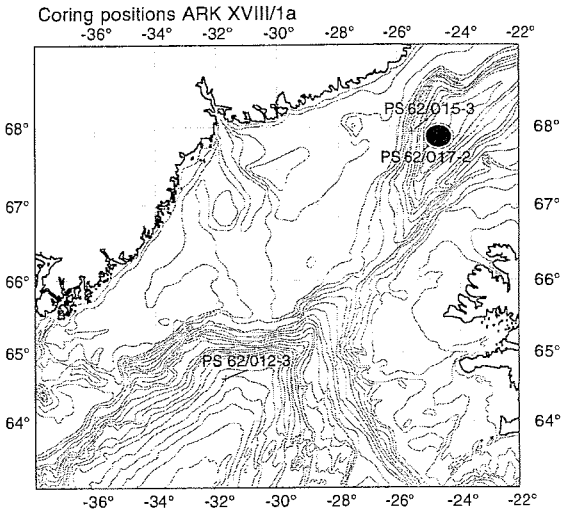

Parasound profile

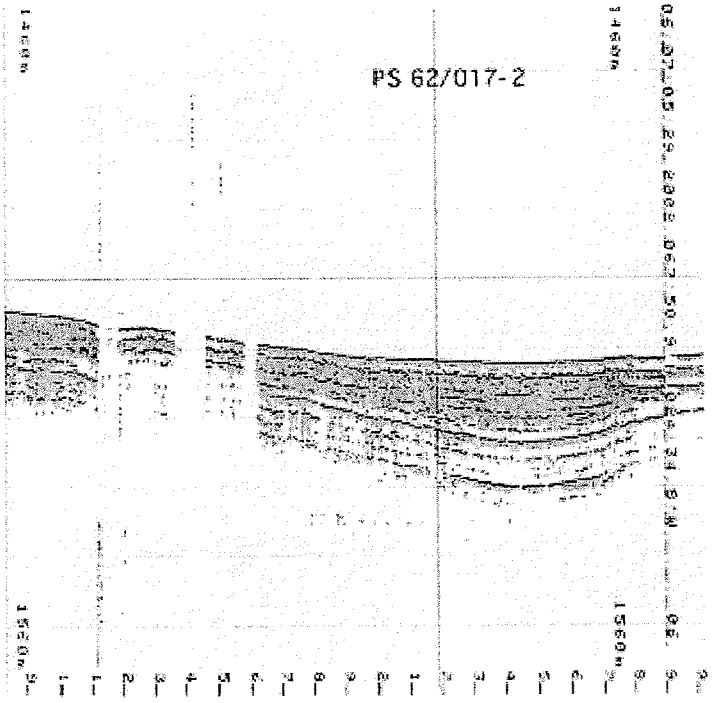

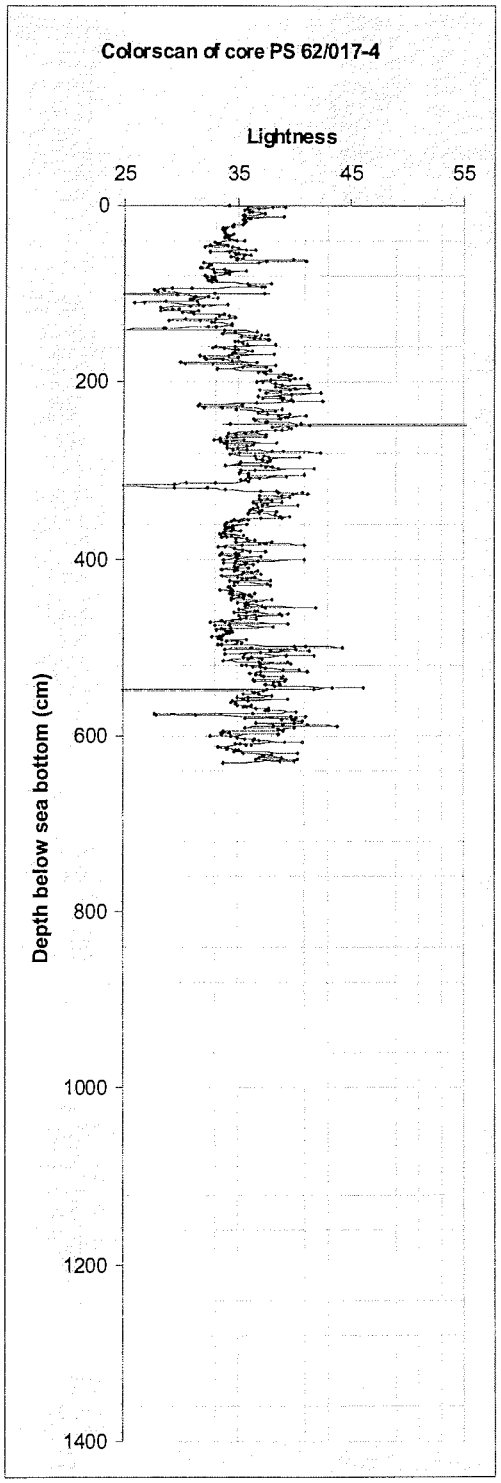
Colorscan of core PS 62/017-4
Lightness
25
35
45
55
0
200
400
600
800
1000
1200
1400
Depth below sea bottom (cm)

Appendix 3 : Mooring array along 78° 50'N

Recovered Moorings

Mooring	Latitude Longitude	Date & Time (UTC) of first record	Water Depth	Type	SN	Instrument Depth
FRAM STRAIT						
F1-4	78° 50.33 N 08° 38.55 E	31 Jul 2002 12:00	258 m	FSI Microcat BB-ADCP UP RCM7	#1551 # 211 #1561 #9401	45 m 46 m 95 m 202 m
F2-5	78° 50.35 N 08° 18.30 E	31 Jul 2002 14:00	794 m	ACM/CTD SBE 37	#1471 #449 V	55 m 56 m
	Line torn *Attempt to locate remaining instruments unsuccessful*			RCM7 SBE 37 RCM8 SBE26	#8418 #219 #10495 #226	261 m 782 m 788 m 794 m
F4-4	78° 49.95 N 06° 56.60 E	31 Jul 2002 18:00	1481 m	FSI Microcat RCM7 Seacat RCM8	#1560 #214 #8367 #2420 #9770	43 m 44 m 233 m 1469 m 1470 m
F5-4	78° 50.38 N 05° 50.86 E	02 Aug 2002 12:00	2470 m	FSI Microcat RCM8 RCM8 RCM8	#1561 #215 #10004 #10503 #10498	57 m 58 m 247 m 1503 m 2459 m
F6-5	78° 49.95 N 05° 02.55 E	04 Aug 2002 18:00	2636 m	ACM/CTD SBE37 RCM7 RCM8 RCM8 SBE26	#1449A #445 #8400 #12326 #12330 #259	53 m 54 m 258 m 1514 m 2630 m 2636 m
F7-3	78° 50.60 N 04° 03.07 E	06 Aug 2002 16:00	2319 m	FSI Microcat RCM8 RCM8 RCM8	#1563 #220 #11887 #9783 #9390	76 m 77 m 266 m 1512 m 2308 m
F8-4	78° 50.05 N 02° 33.83 E	09 Aug 2002 16:00	2470 m	RCM SBE37 RCM7 RCM7 RCM7 RCM8 RCM8 SBE26	#10005 #446 #8401 #8402 #8396 #12328 #10532 #261	59 m 61 m 145 m 251 m 752 m 1508 m 2464 m 2470 m

F9-3	78° 56.60 N 00° 22.50 W	12 Aug 2002 12:00	2444 m	FSI Microcat RCM8 RCM8 RCM8 RCM8 RCM8 SBE26	#1566 #222 #9201 #11890 #10491 #9995 #9184 #257	59 m 60 m 184 m 270 m 771 m 1527 m 2433 m 2444 m
F10-4	79° 01.48 N 02° 01.57 W	13 Aug 2002 08:00	2554 m	FSI Microcat NB-ADCP UP RCM8 RCM8 RCM8	#1568 #223 #378 #11892 #12324 #9188	74 m 75 m 254 m 511 m 1517 m 2543 m

Deployed Moorings

Mooring	Latitude Longitude	Date & Time (UTC) of first record	Water Depth	Type	SN	Instrument Depth
FRAM STRAIT						
F1-5	78° 49.96 N 08° 39.90 E	02 Aug 2002 08:00	239 m	ACM Coastal SBE37 RCM7	#1557 #212 #8048	58 m 59 m 228 m
F2-6	78° 50.02 N 08° 19.78 E	02 Aug 2002 10:00	763 m	ACM Coastal SBE37 RCM7 SBE37 ACM/CTD SBE26	#1562 #217 #9402 #221 #1504 #258	57 m 58 m 231 m 751 m 758 m 763 m
F3-5	78° 50.01 N 07° 59.72 E	01 Aug 2002 22:00	990 m	ACM Coastal SBE37 RCM7 ACM	#1564 #246 #8417 #1317	53 m 54 m 223 m 980 m
F4-5	78° 49.95 N 07° 00.03 E	04 Aug 2002 14:00	1413 m	SBE37 ADCP RCM7 3D ACM ACM/CTD	#437 #1368 #8050 #1404 #1453	54 m 78 m 195 m 697 m 1403 m
F5-5	78° 49.96 N 06° 00.16 E	04 Aug 2002 18:00	2385 m	ACM SBE37 RCM7 RCM8 RCM8 ACM/CTD	#1506 #436 #10492 #11613 #9187 #1403	51 m 52 m 211 m 712 m 1468 m 2375 m

F6-6	78° 50.03 N	06 Aug 2002	2632 m	3D ACM	#1411	49 m
	05° 00.52 E	14:00		SBE37	#438	50 m
				RCM7	#8403	239 m
				RCM8	#9997	745 m
				3D ACM	#1409	2622 m

F7-4	78° 50.00 N	06 Aug 2002	2253 m	ACM/CTD	#1404	60 m
	04° 00.01 E	22:00		SBE37	#439	61 m
				RCM8	#9195	200 m
				RCM8	#9782	706 m
				3D ACM	#1454	2243 m

F8-5	78° 50.00 N	09 Aug 2002	2415 m	ACM/CTD	#1402	54 m
	02° 48.15 E	22:00		SBE37	#440	55 m
				RCM8	#10872	115 m
				RCM8	#11888	221 m
				RCM8	#12329	722 m
				RCM8	#9786	1485 m
				3D ACM	#1400	2405 m

F9-4	78° 50.03 N	12 Aug 2002	2591 m	3D ACM	#1391	52 m
	00° 48.13 W	18:00		SBE37	#444	53 m
				RCM8	#9192	242 m
				RCM8	#5377	843 m
				RCM8	#9212	1599 m
				RCM8	#6856	2585 m
				SBE26	#259	2591 m

F10-5	78° 49.89 N	13 Aug 2002	2622 m	ACM	#1505	62 m
	01° 59.94 W	18:00		SBE37	#441	63 m
				ADCP-UP	#825	212 m
				RCM8	#9206	459 m
				RCM8	#9219	1465 m
				ACM/CTD	#1455	2612 m

F15-1	78° 49.96 N	11 Aug 2002	2489 m	RCM8	#9207	74 m
	01° 36.72 E	20:00		SBE37	#442	76 m
				RCM7	#9213	215 m
				RCM8	#12333	736 m
				RCM8	#3517	1482 m
				RCM8	#10531	2478 m

F16-1	78° 50.10 N	12 Aug 2002	2519 m	RCM8	#10002	44 m
	00° 23.99 E	10:00		SBE37	#248	46 m
				RCM7	#9403	235 m
				RCM8	#12332	736 m
				RCM8	#9185	1482 m
				RCM8	#10530	2508 m

Moorings which could not be recovered

F3-4	78° 50.33 N	-	1031 m	FSI	#1559	54 m
	07° 56.16 E			Microcat	#213	55 m
				RCM7	#8370	264 m
				RCM8	#9561	1020m

„Berichte zur Polarforschung"
Eine Titelübersicht der Hefte 1 bis 376 (1981 - 2000) erschien zuletzt im Heft 413 der nachfolgenden Reihe „Berichte zur Polar- und Meeresforschung". Ein Verzeichnis aller Hefte beider Reihen sowie eine Zusammenstellung der Abstracts in englischer Sprache finden Sie im Internet unter der Adresse: http://www.awi-bremerhaven.de/Resources/publications.html

Ab dem Heft-Nr. 377 erscheint die Reihe unter dem Namen:
„Berichte zur Polar- und Meeresforschung"

Heft-Nr. 377/2000 – „Rekrutierungsmuster ausgewählter Wattfauna nach unterschiedlich strengen Wintern" von Matthias Strasser

Heft-Nr. 378/2001 – „Der Transport von Wärme, Wasser und Salz in den Arktischen Ozean", von Boris Cisewski

Heft-Nr. 379/2001 – „Analyse hydrographischer Schnitte mit Satellitenaltimetrie", von Martin Losch

Heft-Nr. 380/2001 – „Die Expeditionen ANTARKTIS XI/1-2 des Forschungsschiffes POLARSTERN 1998/1999", herausgegeben von Eberhard Fahrbach und Saad El Naggar.

Heft-Nr. 381/2001 – „UV-Schutz- und Reparaturmechanismen bei antarktischen Diatomeen und *Phaeocystis antarctica*", von Lieselotte Riegger.

Heft-Nr. 382/2001 – „Age determination in polar Crustacea using the autofluorescent pigment lipofuscin", by Bodil Bluhm.

Heft-Nr. 383/2001 – „Zeitliche und räumliche Verteilung, Habitatspräferenzen und Populationsdynamik benthischer Copepoda Harpacticoida in der Potter Cove (King George Island, Antarktis)", von Gritta Veit-Köhler.

Heft-Nr. 384/2001 – „Beiträge aus geophysikalischen Messungen in Dronning Maud Land, Antarktis, zur Auffindung eines optimalen Bohrpunktes für eine Eiskerntiefbohrung", von Daniel Steinhage.

Heft-Nr. 385/2001 – „Actinium-227 als Tracer für Advektion und Mischung in der Tiefsee", von Walter Geibert.

Heft-Nr. 386/2001 – „Messung von optischen Eigenschaften troposphärischer Aerosole in der Arktis" von Rolf Schumacher.

Heft-Nr. 387/2001 – „Bestimmung des Ozonabbaus in der arktischen und subarktischen Stratosphäre", von Astrid Schulz.

Heft-Nr. 388/2001 – „Russian-German Cooperation SYSTEM LAPTEV SEA 2000: The Expedition LENA 2000", edited by Volker Rachold and Mikhail N. Grigoriev.

Heft-Nr. 389/2001 – „The Expeditions ARKTIS XVI/1 and ARKTIS XVI/2 of the Research Vessel 'Polarstern' in 2000", edited by Gunther Krause and Ursula Schauer.

Heft-Nr. 390/2001 – „Late Quaternary climate variations recorded in North Atlantic deep-sea ostracodes", by Claudia Didié.

Heft-Nr. 391/2001 – „The polar and subpolar North Atlantic during the last five glacial-interglacial cycles", by Jan. P. Helmke.

Heft-Nr. 392/2000 – „Geochemische Untersuchungen an hydrothermal beeinflußten Sedimenten der Bransfield Straße (Antarktis)", von Anke Dählmann.

Heft-Nr. 393/2001 – „The German-Russian Project on Siberian River Run-off (SIRRO): Scientific Cruise Report of the Kara-Sea Expedition 'SIRRO 2000' of RV 'Boris Petrov' and first results", edited by Ruediger Stein and Oleg Stepanets.

Heft-Nr. 394/2001 – „Untersuchung der Photooxidantien Wasserstoffperoxid, Methylhydroperoxid und Formaldehyd in der Troposphäre der Antarktis", von Katja Riedel.

Heft-Nr. 395/2001 – „Role of benthic cnidarians in the energy transfer processes in the Southern Ocean marine ecosystem (Antarctica)", by Covadonga Orejas Saco del Valle.

Heft-Nr. 396/2001 – „Biogeochemistry of Dissolved Carbohydrates in the Arctic", by Ralph Engbrodt.

Heft-Nr. 397/2001 – „Seasonality of marine algae and grazers of an Antarctic rocky intertidal, with emphasis on the role of the limpet *Nacilla concinna* Strebel (Gastropoda: Patellidae)", by Dohong Kim.

Heft-Nr. 398/2001 – „Polare Stratosphärenwolken und mesoskalige Dynamik am Polarwirbelrand", von Marion Müller.

Heft-Nr. 399/2001 – „North Atlantic Deep Water and Antarctic Bottom Water: Their Interaction and Influence on Modes of the Global Ocean Circulation", by Holger Brix.

Heft-Nr. 400/2001 – „The Expeditions ANTARKTIS XVIII/1-2 of the Research Vessel 'Polarstern' in 2000" edited by Victor Smetacek, Ulrich Bathmann, Saad El Naggar.

Heft-Nr. 401/2001 – „Variabilität von CH_2O (Formaldehyd) - untersucht mit Hilfe der solaren Absorptionsspektroskopie und Modellen" von Torsten Albrecht.

Heft-Nr. 402/2001 – „The Expedition ANTARKTIS XVII/3 (EASIZ III) of RV 'Polarstern' in 2000", edited by Wolf E. Arntz and Thomas Brey.

Heft-Nr. 403/2001 – „Mikrohabitatansprüche benthischer Foraminiferen in Sedimenten des Südatlantiks", von Stefanie Schumacher.

Heft-Nr. 404/2002 – „Die Expedition ANTARKTIS XVII/2 des Forschungsschiffes 'Polarstern' 2000", herausgegeben von Jörn Thiede und Hans Oerter.

Heft-Nr. 405/2002 – „Feeding Ecology of the Arctic Ice-Amphipod *Gammarus wilkitzkii*. Physiological, Morphological and Ecological Studies", by Carolin E. Arndt.

Heft-Nr. 406/2002 – „Radiolarienfauna im Ochotskischen Meer - eine aktuopaläontologische Charakterisierung der Biozönose und Taphozönose", von Anja Nimmergut.

Heft-Nr. 407/2002 – „The Expedition ANTARKTIS XVIII/5b of the Research Vessel 'Polarstern' in 2001, edited by Ulrich Bathmann.

Heft-Nr. 408/2002 – „Siedlungsmuster und Wechselbeziehungen von Seepocken (Cirripedia) auf Muschelbänken (*Mytilus edulis* L.) im Wattenmeer", von Christian Buschbaum.